EXAMINING THE ROLE OF HEDGEHOG SIGNALING IN THE PANCREATIC TUMOR MICROENVIORNMENT

by

Joseph Scott Dosch

A dissertation submitted in partial fulfillment
of the requirements for the degree of
Doctor of Philosophy
(Cellular and Molecular Biology)
in the University of Michigan
2011

Doctoral Committee:

Professor Charles Burant, Co-Chair
Professor Diane M. Simeone, Co-Chair
Professor Andrzej A. Dlugosz
Professor Eric R. Fearon
Professor Deborah L. Gumucio
Professor Sean Morrison

To Kim, Erik, and all of my friends and family,
thanks for all of your love and support.

ACKNOWLEDGEMENTS

I owe a great amount of thanks to my primary mentor Chuck Burant. Your enthusiasm for science is infectious and under your guidance I feel as if I've acquired the tools to tackle any problem in my future scientific career. I also owe a lot of thanks to my co-mentor Diane Simeone and the members of the Simeone lab who have engaged me in great discussions and are constantly challenging me to take my research to the next level. Last, but certainly not least, I want to say thanks to my wonderful wife Kimberley and my son Erik. Thanks for supporting me in good times and bad, I could not have done this without you.

PREFACE

The work described in this thesis represents both peer-reviewed and manuscript-in preparation, first author data that I have generated as a graduate student at the time of my thesis defense – April 25th, 2011. For Chapter 2, I performed all of the *in vitro* and *in vivo* experiments with the Hh pathway antagonist drugs provided by Genentech. Histology was performed by Jimmy Hogan of the Pasca lab at the University of Michigan. For Chapter 3, the Pasca lab assisted in the creation of the mouse pancreatic stellate cell (MPSC) lines. Erin Shellman processed the raw microarray data for the Shh treated MPSC lines and assisted in the data analysis by Ingenuity Pathway Analysis (IPA). In Chapter 4, Wnt2 knock-out studies were performed by Jingjiang Wu and clinical trial data was provided by Edward Kim.

Chapter 1 represents background and hypotheses that were the aim of my thesis work. Parts of this chapter were taken from excerpts of *Pancreatic cancer and hedgehog pathway signaling: new insights. Pancreatology;10(2-3):151-7* [1]. I was the first author of this review. Chapter 2 details work performed with primary human pancreatic xenografts and their treatment with HhAntag (Hh pathway antagonist), the chemotherapeutic agent gemcitabine and a combination of the two drugs. This work is currently in preparation for a manuscript submission and I will be the first author. Chapter 3 details our work in identifying the Hh pathway responsive genes in the pancreatic mesenchyme using microarray analysis and primary activated pancreatic stellate cell lines that were generated in our lab. This work is also in preparation for a

manuscript submission where I will be the first author. Chapter 4 details a comprehensive review of the data from our experiments and present on-going studies, including a clinical trial for Hh inhibitors for pancreatic cancer. All the work described in this thesis was performed under the guidance of Dr. Charles Burant and Dr. Diane Simeone.

TABLE OF CONTENTS

LIST OF FIGURES

LIST OF TABLES

ABSTRACT

EXAMINING THE ROLE OF HEDGEHOG SIGNALING IN THE PANCREATIC TUMOR MICROENVIRONMENT

by

Joseph Scott Dosch

Co-Chair: Charles Burant
Co-Chair: Diane Simeone

The Hedgehog (Hh) pathway is a conserved signaling network that plays a critical role during embryonic development as well as in the maintenance of adult tissues. Inappropriate activation of Hh signaling has been linked in the development of several tumors, including pancreatic cancer. In the context of pancreatic cancer, Hh pathway ligands secreted by the tumor cells activate this pathway in the tumor mesenchyme by a paracrine mechanism. As the role of Hh signaling in the tumor mesenchyme is not fully understood, we initiated two strategies to understand how active Hh signaling promotes pancreatic carcinogenesis. In a first approach, we used Hh pathway inhibitors to down-regulate paracrine Hh signaling in an orthotopic xenograft model of human pancreatic adenocarcinoma to test how this pathway is involved in tumor growth and progression. These experiments revealed that blocking Hh signaling in the tumor stroma leads to a significant reduction in the ability of

tumor cells to form metastases, along with affecting signals that are important in maintaining the differentiation status of the tumor cells. Second, we established a primary *in vitro* model of paracrine Hh signaling in pancreatic stellate cells. Using bioinformatics analysis we found that paracrine Hh signaling activates an invasive gene signature in pancreatic stellate cells. This was confirmed by three-dimensional invasion assays *in vitro*. Several clinical trials for Hh pathway inhibitors, including here at the University of Michigan Medical Center, have been initiated for testing the efficacy of targeting paracrine Hh signaling in the treatment of pancreatic cancer. Our studies established important *in vivo* and *in vitro* models to ask important questions about the role of paracrine Hh signaling in pancreatic cancer progression. These studies add insight to how targeting this pathway may provide important therapeutic benefit to pancreatic cancer patients.

CHAPTER 1

INTRODUCTION

Pancreatic cancer is the 4th leading cause of cancer death in the United States with a 5-year survival of less than 6% [2]. The National Cancer Institute estimates that 43,140 Americans will be diagnosed with the disease and 36,800 will succumb to it in 2010 (www.seer.cancer.gov). The age-adjusted incidence of the disease is higher in men vs. women (13.3 per 100,000 men vs. 10.5 per 100,000 women) and in African-American men vs. Caucasian men (16.7 per 100,000 men vs. 13.2 per 100,000 men). The risk factors for developing pancreatic cancer include advanced age, cigarette smoking, alcohol consumption, diabetes, obesity and a family history of the disease [3,4,5,6].

Pancreatic tumors can have a varying histological profile that includes adenosquamous carcinoma, colloid carcinoma, hepatoid carcinoma, medullary carcinoma, signet-ring cell carcinoma, undifferentiated carcinoma, and undifferentiated carcinoma with osteoclast-like giant cells [7]. Some of these histologies correspond to a poorer prognosis, for instance, adenosquamous and undifferentiated carcinoma, while others have better prognosis, such as colloid and medullary carcinoma [7]. The most common form of pancreatic cancer is infiltrating ductal adenocarcinoma. Pancreatic cancer is characterized by a glandular neoplastic epithelium surrounded by an intense desmoplastic reaction, which in many cases, the

cells in the stromal compartment greatly outnumbers the amount of tumor cells present in the tumor (**Figure 1.1**) [8]. The tumor cells express a variety of cytokeratins (cytokeratins 7, 8, 13, 18, and 19) and several serum carbohydrate antigens, such as carbohydrate antigen 19–9 (CA19–9) that are used as markers in the diagnosis and follow-up of pancreatic cancer patients [9,10,11]. Additionally, these tumors express several mucins; heavily glycosylated, high-molecular weight glycoproteins which protect the surface of epithelial tissues and have been associated with promoting the invasive and metastatic ability of several tumor types [12]. In pancreatic cancer, the aberrant expression of mucins including MUC1, MUC3, MUC4, and MUC5AC have been identified, with MUC4 expression correlating strongly with advanced pancreatic disease [10,13].

While the cell of origin of pancreatic adenocarcinoma is still a matter of debate, there is general consensus on a progression model for this disease. The most common precursor lesions of pancreatic cancer are known as PanINs (Pancreatic Intraepithelial Neoplasias) and are classified from 1A to 3 (the latter representing carcinoma *in situ*) based on defined histological characteristics [14]. Genetic alterations in PanIN lesions and pancreatic cancer have been the subject of numerous studies. The defining mutation of human pancreatic cancer which is found in greater than 80-90% of pancreatic cancers is a single amino acid change in the KRAS gene, often in codon 12 or 13 that will generate a constitutively active form of the protein [15,16]. The Ras signaling pathway includes a number of GTPases that control signaling for many important cell functions, including proliferation, cell migration, adhesion, and apoptosis.

While the KRAS mutation is considered an important early "hit" in the development of pancreatic cancer, this mutation alone is not sufficient to drive the progression of invasive pancreatic adenocarcinoma. Transgenic animals with a conditionally activated mutant $KRAS^{G12D}$ under the control of pancreas-specific promoters PDX-1 or p48 results in animals that develop high grade PanIN lesions (up to PanIN-3) at 7 to 10 months of age, but few animals spontaneously progress to invasive carcinoma [17]. Further progression of the disease requires additional mutations or loss of tumor suppressor genes such as p53, $p16^{Ink4a}$, BRCA2, and DPC4, a component of the TGFβ signaling pathway (**Figure 1.2**) [18,19,20].

The treatment options for patients diagnosed with pancreatic adenocarcinoma are relatively poor. At the time of diagnosis, more than 85% of tumors have extended beyond the organ margins, starting with invasion into the peritoneum and local lymph nodes and then commonly followed by metastases to the liver [21]. Patients with evidence of metastatic disease and/or tumor encasement of the mesenteric vasculature are not considered candidates for surgical resection and undergo largely palliative chemotherapeutic regimens that include the nucleoside analog, gemcitabine. Recent clinical trials that have utilized FOLFIRINOX, a chemotherapeutic regimen consisting of the drugs 5-FU (Fluorouracil), leucovorin (folic acid), irinotecan (topoisomerase inhibitor), and oxaliplatin extended the survival of metastatic adenocarcinoma patients for an additional 4 months compared to treatment with gemcitabine alone [22]. However, these treatments do not offer a cure, and all patients will eventually succumb to metastatic disease.

For the minority of patients with resectable disease, the complete surgical resection of the adenocarcinoma represents the only option for long-term survival. Surgical removal of the tumor is usually performed by a Whipple procedure (pancreaticoduodenectomy) for tumors arising in the head of the pancreas or by distal pancreatectomy for tumors in the body and tail of the pancreas [23]. Following surgical resection, patients are treated with a chemotherapeutic regimen that often includes platinum-based therapy along with the nucleoside analog, gemcitabine. However, adjuvant chemotherapy only affords patients with an additional survival benefit of two months compared to surgery alone [24].

Numerous clinical trials have been initiated to identify compounds that will improve patient survival that include: platinums; fluoropyrimidines; topoisomerase inhibitors; and various targeted agents including tipifarnib (farnesyltransferase inhibitor), marimastat (matrix metalloproteinase inhibitor), cetuximab (epidermal growth factor receptor (EGFR) inhibitor), erlotinib (tyrosine kinase inhibitor), and bevacizumab (anti-vascular endothelial growth factor A (VEGF-A) inhibitor) [25,26,27,28]. However, these trials have provided very limited survival benefit to pancreatic cancer patients. The failure of these trials underscores our need to better understand the biology of the disease and the important pathways involved in tumor progression.

The Hedgehog (Hh) pathway has emerged as one of the most widely studied signaling networks due to its important role in human development and disease. In the development of the normal pancreas, Hh signaling is restricted; however, in the adult organ the pathway is important for the proper function of the insulin-producing

endocrine cells [29]. Several studies have identified the abnormal expression of Hh ligands, Sonic and Indian Hedgehog, in early PanIN lesions and in invasive adenocarcinoma cells [30,31]. Importantly, these ligands have been shown not to activate Hh signaling in pancreatic cancer cells directly, but rather to activate the pathway in the tumor mesenchyme via a paracrine mechanism [32]. However, we know very little about the Hh pathway target genes that are affected in the tumor mesenchyme and how these genes may be part of a feedback loop that enhances the progression of the tumor. Recent work that parallels our own studies have suggested that currently available inhibitors of the pathway are only effective in down-regulating the paracrine Hh signaling in the tumor mesenchyme and not Hh signaling in the tumor cells [33]. These studies pose some very important questions for the field that will be detailed in this thesis: Is active Hh signaling in the tumor mesenchyme required for pancreatic tumor progression? What is the biological significance of Hh activation in the pancreatic mesenchyme? What are the Hh pathway responsive genes in the pancreatic stroma? Do these genes play a role in tumor metastasis, differentiation, or maintenance of a cancer stem cell population? Can targeting this pathway provide any therapeutic benefit to pancreatic cancer patients? These questions are at the forefront of pancreatic tumor biology and have significant implications for treatment of patients with pancreatic cancer, as Hh pathway inhibitors are entering human clinical trials.

In this thesis, I will describe how a clinically relevant Hh pathway inhibitor, HhAntag, affects primary human pancreatic tumor xenografts and how these data may give us clues to how patients may benefit from targeting paracrine Hh signaling

in pancreatic adenocarcinoma. Additionally, I will detail an *in vitro* model system that has allowed us to test how paracrine signaling from the tumor cells affects the function of primary pancreatic mesenchymal cells. Finally, I will detail experiments to identify the Hh responsive gene signature in pancreatic mesenchymal cells and describe my bioinformatics analysis approach to demonstrate how paracrine Hh signaling activates an invasive gene signature in these cells. Taken together, the data described in this thesis will present a comprehensive analysis of the role for paracrine Hh signaling in the pancreatic adenocarcinoma microenvironment.

HEDGEHOG SIGNALING PATHWAY

The Hedgehog pathway plays a critical role during development and specification of embryonic tissues and organs. Signaling occurs through autocrine and paracrine activation of cell surface receptors by peptide ligands. In the mammalian system, active signaling is stimulated by three known ligands: Sonic hedgehog (Shh), Indian hedgehog (Ihh), and Desert hedgehog (Dhh). As each ligand enters the secretory machinery, each protein is modified by addition of a palmitoyl group to its N-terminus and cholesterol to its C-terminus [34]. Shh is the most widely studied Hh pathway ligand with expression observed in the gut, nervous system, skin, and in limb bud [35,36]. Ihh is expressed in components of bone, along with the gut and pancreas, while Dhh has been found in neuronal compartments, testes and the pancreas [35]. Each ligand can equally activate the pathway and initiate expression of downstream Hh pathway target genes; however some Hh ligands may have greater potency of pathway activation in some cell types [37].

In the absence of ligand, the Hh ligand receptor Patched1 (Ptch1), which is located on the plasma membrane, represses the activity of the transmembrane protein Smoothened (Smo), through a mechanism that is still not clearly understood. To further control the activation of the pathway, protein kinases in the cytoplasm, such as Protein Kinase A (PKA) and Glycogen Synthase Kinase 3β (GSK3β), phosphorylate the Gli family transcription factors. This leads to proteosome-mediated cleavage of Gli into an N-terminal truncated form, which acts as a repressor of a subset of Hh target genes [38,39] (**Figure 1.3 A**). In the mammalian system, there are three known Gli transcription factors, Gli1, Gli2 and Gli3. Gli3 has been shown to demonstrate the role of a repressor, while Gli2 can be either an activator or repressor depending on the context, and Gli1 has been found to be an exclusive transcriptional activator [40]. Suppressor of fused (Sufu) is a conserved protein that can act as another negative regulator of the Hh pathway by binding to Gli transcription factors, both in the cytoplasm and in the nucleus, to prevent these factors from activating Hh target genes [41,42]. Conversely, ligand binding to Ptch1 releases the repression of Smo and a signaling cascade downstream of Smo leads to processing of the Gli transcription factors, predominantly Gli2, as an activator allows these proteins to translocate to the nucleus and activate the transcription of downstream target genes (**Figure 1.3 B**) [43].

It is not entirely clear how Smo leads to the activation of Gli transcription factors in mammalian cells. In *Drosophila*, ligand binding to Patched releases a Hedgehog signaling complex that is attached to microtubules and membranes and is composed of the activating transcription factor Cubitus interruptus (Ci), the kinase Fused (Fu) and the kinesin-like protein Costal2 (Cos2) [44,45]. Following the release

of this complex, Smo is stabilized by phosphorylation at its C-terminal tail by PKA and Casein Kinase I (CKI), which are bound by Cos2, along with GSK3β [46]. The three kinases are then released and can no longer process Ci into a repressor form, and the full-length Ci protein is able to translocate to the nucleus to active downstream target genes. In mammalian systems, Smo is found to be phosphorylated by the GPCR kinase GRK2 and is likely involved with other kinases in the stabilization of Smo in the context of Hh ligand stimulation [47,48]. The phosphorylation of Smo causes the receptor to traffic to the cell membrane in the primary cilium of the cell where the concentration of Gli transcription factors along with other co-factors, possibly Kif7, promotes the processing of Gli peptides into activating factors [49,50].

Recent studies have focused on the role of primary cilia in the transduction of Hh pathway signaling. In the absence of ligand, Ptch receptors are located in the primary cilia and prevent the accumulation of Smo in the cilia; however, following ligand binding to Ptch, these roles are reversed and Ptch receptors are shuttled out of the cilia while Smo receptors are concentrated in their place [51]. Gli transcription factors are also known to shuttle in and out of the primary cilia. The primary cilia appear to be able to form a signaling center that brings together Hh signaling components to coordinate the dynamic interactions among Hh signaling components that lead to the processing of Gli factors into either an activator or repressor form.

Among the best-characterized target genes associated with active Hh signaling are components of the pathway itself, including Gli1, Ptch1 and the Hh-interacting protein, Hhip. Gli1 as a target gene is specifically expressed to amplify

the initial Hh pathway signal and can be used as a reliable read-out for Hh pathway activity. Hhip, Ptch1 and the growth arrest specific protein 1, Gas1 are target genes that are expressed to regulate the negative feedback of Hh signaling by sequestering Hh ligands from stimulating Ptch receptors [52,53]. This ensures that the activity level of the Hh pathway is tightly regulated through a feedback mechanism. Depending on the cellular context, other downstream targets include cell proliferation and survival factors Cyclin D and Cyclin E, Bcl-2, angiogenesis related proteins vascular endothelial growth factor A (VEGF-A) and angiopoietins-1/2, and epithelial-to-mesenchymal transition (EMT) related factor SNAIL [54,55,56].

HEDGEHOG PATHWAY IN NORMAL PANCREATIC DEVELOPMENT

Active Hh signaling is required during the early embryonic specification of the gastrointestinal tract, with the notable exception of the pancreas, where Hh activity is repressed by activin βB and FGF2 signals released by the notochord [57]. This down-regulation of the Hh pathway is critical for pancreatic development as forced expression of Shh in the pancreatic anlage results in agenesis of the pancreas in mouse embryos [58]. Conversely, repression of Hh signaling in areas of the developing gut that normally express Hh pathway genes results in ectopic expression of pancreas-specific genes in the stomach and intestine [59]. While repressed during the early specification of cell types in the pancreatic buds, recent work using Patched1-LacZ transgenic mice, have identified expression of the Hh pathway expression via β-galactosidase (β-gal) staining as early as e10.5 in pancreatic epithelial cells along with some sporadic mesenchymal cell staining [29]. Patched1

staining increases during pancreatic development, however it later becomes restricted to the developing endocrine cells and pancreatic ducts. Other studies have shown that additional signaling components including Ihh, Dhh, and Hhip are sporadically expressed around e14.5 in the developing pancreatic epithelium [60].

In the adult pancreas, Hh pathway activity is typically very low and restricted to expression of Ihh, Dhh, Smo and Ptch1 in the islets housing the endocrine cells of the organ [60,61]; however more widespread Hh signaling can be activated under circumstances such as injury or disease [62]. Recent work has also demonstrated that Hh signaling is required for adult pancreatic function, specifically in the endocrine cells of the islet. By developing a transgenic animal carrying a pancreatic epithelium specific promoter (Pdx-1) driving cre recombinase along with a "floxed" Smoothened gene the authors produced an animal with normal pancreatic morphology, but impaired Hh signaling in the pancreatic islets. Specifically, these animals do not secrete insulin to levels comparable in wild-type animals and they developed a glucose intolerant phenotype [29]. These results provide another layer of our understanding in the role of Hh signaling in the pancreas, specifically its role in maintaining normal endocrine pancreatic function.

HEDGEHOG PATHWAY ACTIVATION IN PANCREATIC CANCER

Activation of the Hh pathway in primary human pancreatic cancer was first reported in two parallel studies [30] and [31]. The aberrant over-expression of the Hh pathway ligands, Sonic and Indian Hedgehog was identified in about 70% of human pancreatic cancer cases as well as in the majority of pancreatic cancer cell lines

(**Figure 1.4**) [31]. A similar mechanism of pathway activation has been described for prostate [63] and lung cancer [64], which differs from the mutation-driven activation of the Hh signaling pathway that has been well characterized in basal cell carcinoma (BCC) and medulloblastoma [65,66].

A deeper insight on the role of Hh signaling in pancreatic cancer, and its relationship with other oncogenic pathways, has been obtained through the study of mouse models of this disease. The most representative mouse models of pancreatic cancer are based on the expression of a mutated form of the KRAS gene, which mimics what is found in primary human cancers, specifically in the developing pancreatic epithelium [67,68]. In these transgenic animals, PanIN lesion development and progression closely resemble the human disease and interestingly Shh ligand is expressed in the majority of mouse PanINs even in very early developing lesions. Similar activation of the Hh pathway following initiation of the disease using KRAS mutation has been observed in a zebrafish model of pancreatic cancer [69].

In these disease models, Hh pathway activation is downstream of KRAS signaling. Some possible insight into the mechanism of Hh activation by oncogenic KRAS is provided by studies indicating that Shh may be a downstream target of NF-κB [70]. NF-κB is up-regulated in response to inflammatory stimuli and cellular stress, conditions found in the inflamed and fibrotic environment of early-stage tumor lesions. Detailed study of the Shh promoter and upstream region revealed multiple NF-κB binding sites that were able to activate transcriptional activity of Shh in both

in vitro and *in vivo* models [71]. This study implies that NF-κB serves as a link between oncogenic KRAS and Hh signaling.

Other mouse models have more directly addressed the role of Hh signaling in pancreatic cancer. Initial examination of the role of Hh signaling in the pancreas was examined in transgenic animals expressing Shh in the pancreatic epithelia using the PDX1 promoter that drives expression to the early developing pancreatic epithelium. These animals displayed lesions that closely resembled human PanINs and showed elevated expression of HER2/neu and mutated KRAS typically seen in pancreatic cancers [30]. However, it is not clear whether these animals would progress to a more advanced phenotype as ectopic expression of Shh ligand in the pancreatic epithelium disrupts normal pancreatic development in these animals, resulting in neonatal death of the mice due to pancreatic developmental defects.

In an alternative approach, an active form of the transcription factor Gli2 was expressed specifically in the pancreatic epithelium starting from early pancreatic development [72]. Epithelial expression of the Gli2 transgene does not disrupt pancreas development, but it does cause formation of pancreatic tumors described as undifferentiated carcinomas in adult animals. Those tumors did not progress through PanINs and bear little resemblance to human pancreatic ductal adenocarcinoma. However, simultaneous expression of active Gli2 and mutant $KRAS^{G12D}$ resulted in early onset of PanINs, indicating a synergy between activation of KRAS and the Hh pathway in PanIN progression. However, a recent study that mimicked canonical Hh signaling using transgenic animals with a constitutively active Smoothened (Rosa26-LSL-SmoM2) that was activated via a pancreatic epithelium-specific promoter

(PDX1-Cre), revealed no formation of pancreatic neoplasms up to 18 months of age [32]. Additionally, crossing these animals with $KRAS^{G12D}$ transgenic animals did not accelerate the progression of the disease nor did they observe any evidence of Hh signal transduction in pancreatic epithelial cells. Laser capture of primary human pancreatic tumor stroma and tumor stroma from these mouse models of pancreatic cancer confirmed that canonical Hh signaling was restricted to the stromal compartment.

These studies confirm additional data that suggests active Hh signaling is un-coupled from the canonical mechanism in pancreatic epithelial cells compared to the pancreatic mesenchyme [73]. In these experiments, genetic crossing of animals with a Smo loss-of-function allele (Smo^{F}) [74] into the $KRAS^{G12D}$/$Trp53^{F/+}$ (constitutively active KRAS / p53, loss-of-function allele) background did not affect the progression of PanIN to adenocarcinoma, or the long term survival of the animals in the study. In this model of pancreatic adenocarcinoma, downstream Hh target genes including Gli1 are up-regulated in the pancreatic tumor cells compared to normal pancreatic epithelium. However, Smo-depletion had no effect on the expression of Hh target genes, Gli1 and Ptch1 in micro-dissected tumor cells, suggesting that the expression of these targets is controlled by a Smo-independent mechanism. Gli1 expression, independent of active Smo, is partially explained by TGFβ signaling, which can stimulate the expression of Gli1 in the absence of Hh pathway ligands. However, while pancreatic tumor cells do not demonstrate canonical Hh signaling, the expression of down-stream target genes, including Gli1 is important for cell survival. Knockdown of Gli1 by siRNA in human pancreatic tumor cells resulted in increased

rates of apoptosis and a reduced ability to form colonies in soft agar. Importantly, these studies point to divergent mechanisms for Hh signaling in the progression of pancreatic adenocarcinoma, in which paracrine Hh signaling activates canonical target genes in the tumor stroma, while Gli transcription is driven via a Smo-independent mechanism in pancreatic tumor cells.

BIOLOGICAL ROLE OF PARACRINE HEDGEHOG SIGNALING IN PANCREATIC CANCER

Paracrine Hh signaling in the tumor stroma has been identified as an important mechanism for Hh pathway activation in pancreatic cancer. As pancreatic adenocarcinoma is characterized by a dense, desmoplastic stroma, several studies have taken aim to identify how Hh signaling may affect these cells. The fibrotic reaction in pancreatic tumors is the result of the proliferation of supporting cell types including fibroblasts and stellate cells, along with the recruitment of immune cells, and vascular-associated cells to the growing tumor [75]. This abundance of mesenchymal cells in the tumor stroma supports tumor growth and progression in multiple ways. These cells have been shown to secrete growth factors that aid in tumor proliferation by a direct feedback mechanism [76]. Additionally, these cells can support the growth and invasion of the tumor by secretion of extra-cellular matrix remodeling enzymes and expression of signaling factors that support the neovascularization of the tumor [77]. Additional evidence has suggested the desmoplastic reaction can result in the formation of a physical barrier that shields the tumor cells from responding to pharmacological treatments [78,79].

This desmoplasia also leads to a tumor architecture that is relatively avascular and poorly perfused, which limits the ability of drugs to reach the tumor cells effectively [80]. Studies using a Smo-inhibitor, IPI-926, in a mouse model of pancreatic cancer have important implications for the clinical application for targeting the tumor stroma [80]. In this study, mouse models using mutant alleles of KRAS and p53 were crossed to develop transgenic animals that develop tumors with similar desmoplasia compared to human PDA. In this model it was observed that the tumors were hypoxic, resistant to Gemcitabine, and demonstrated limited perfusion of compounds into the bulk tumor. However, treatment with IPI-926 reduced the level of stroma, increased the perfusion of the tumors, and subsequently rendered the tumors more responsive to gemcitabine treatment.

While several studies have shown robust expression of Shh ligand in pancreatic tumor cells, it is unclear how cells in the surrounding microenvironment respond to the presence of Shh. Recent studies have suggested that stromal cells in the pancreatic tissue are Hh responsive and Shh ligand signal the expansion of the stromal compartment (Figure 1.5) [81]. Transformed pancreatic epithelial cells that ectopically express Shh and transplanted orthotopically in nude mice stimulated the proliferation of stromal cells as evaluated by staining with the differentiated myofibroblast marker α-Smooth Muscle Actin (α-SMA). The proliferation of these cells was modulated with treatment of the experimental animals with a blocking antibody (5E1) that blocks the canonical ligand-receptor interaction, resulting in the inhibition of downstream Hh signaling [81]. Additionally, the expression of extra-cellular matrix (ECM) proteins collagen and fibronectin, which are characteristic of

the desmoplastic reaction in pancreatic cancer, were significantly higher in Shh expressing tumors compared to tumors lacking Shh over-expression.

It has been hypothesized that Hh-activated stroma in pancreatic cancer may provide feedback signals to the cancer cells, but the specific factors in this feedback mechanism are still relatively unknown. A recent microarray study of the mouse tumor stroma from pancreatic adenocarcinoma xenografts treated with an Hh pathway antagonist revealed that members of the Wnt and IGF pathways may be differentially regulated in response to Hh signaling [33]. Additional studies in both the intestine and prostate, which have similar mechanisms of paracrine Hh activation in the local mesenchyme, have identified pro-inflammatory and angiogenesis-related genes that are differentially regulated in response to Hh ligands [82,83].

As the tumor stroma is composed of a mixture of several different cell types, it is important to identify which cells are responsive to paracrine Hh signaling. Bone marrow mesenchymal cells have been found to migrate to the tumor microenvironment and play important roles in tumor progression and angiogenesis in several tumor models [84,85]. Recent work has identified that these cells migrate to pancreatic tumors and localize to tumor endothelial cells and participate in the neovascularization of the tumor [86]. These cells were found to express Gli2, and their migration to the tumor vasculature was blocked by treating the tumor xenografts with the Hh pathway inhibitor, cyclopamine. Importantly, it was found that IGF-1 in these cells was an important Hh target gene and that blocking this factor reduced the promotion of angiogenesis in both *in vitro* and *in vivo* models. Of note, while Hh signaling is activated in cells associated with the tumor vasculature, $CD31^+$ vascular

cells express very low levels of Gli1 and do not respond to inhibition with Hh pathway inhibitors [87].

Further evidence that paracrine Hh signaling is important for pancreatic tumor progression has emerged from experiments using knockouts of Hh signaling receptors in mesenchymal cells. Subcutaneous implantation of Shh-expressing pancreatic cancer cells with mouse embryonic fibroblasts (MEFs) that have been rendered unresponsive to Hh signaling by knockout of the Hh signaling receptor Smoothened (Smo) resulted in a marked reduction in xenograft tumor growth compared to co-implantation with wild-type MEFs [33]. These studies confirm that paracrine Hh signaling in the tumor stroma plays an important role in the development of pancreatic cancer.

HEDGEHOG PATHWAY AND CANCER STEM CELLS

A shifting paradigm in how we view cancer is the discovery that tumors are comprised of a heterogeneous mixture of cells with distinct populations that have unique tumor-initiation capability termed cancer stem cells. Much of the groundwork for identifying these cells was initiated by the application of lessons and techniques learned in identifying populations of normal, non-tumorigenic stem cells. To assess for these tumor-initiating cells, primary tumor cells from blood-borne cancers [88] along with solid tumors of the breast [89], brain [90], colon [91], along with several other solid tumor systems, are isolated and single cell suspensions from these cancers were stained with various cell surface marker combinations, sorted by fluorescent activated cell sorting (FACS) analysis and then implanted orthotopically or

subcutaneously in immune compromised animals. The resulting tumors were analyzed for their ability to recapitulate the histological and surface marker phenotype of the primary tumor as well as the ability to retain these characteristics following serial transplants into recipient animals to assay for self-renewal.

These concepts have been met with some controversy some research has challenged that these cancer stem cells are the result of artifacts of the assay and that given the proper conditions the "differentiated" cancer cell population could form tumors in animals or even that these tumor-initiating cells may not be as rare as we think [92]. Indeed, a recent study demonstrated that 1 out of 4 melanoma cells were capable of forming new tumors in xenograft experiments, suggesting that these tumorigenic cells are not a rare sub-fraction of cells in melanoma [93]. Counter to this is a limiting dilution analysis study of tumor cells isolated from pancreatic adenocarcinoma, lung cancer, and head/neck cancer which suggests that from this group of tumors the tumorigenic capacity is 1/2500 to 1/36,000 cells depending on the tumor type and individual sample [94]. While much work is still to be done to answer these questions in all tumor model systems, evidence from the identification of breast cancer stem cells in transgenic mouse models of breast cancer which bypass concerns about human/mouse xenograft models [95], along with data describing unique abilities of cancer stem cells to evade radiation [92] and chemotherapy treatments [96], make it clear that these cells represent a distinct cell population for further study in human cancers.

Evidence for a role of Hh signaling in cancer stem cells has come from both hematopoietic and solid tumor models of cancer. Specifically, in breast cancer stem

cell populations, these cells were found to have 30 fold higher level of expression of Gli1 along with significant up-regulation of Ptch1 and Gli2 compared to non-tumorigenic cells [97]. Additionally, in human glioma cancer stem cells, Hh pathway activation has been shown to be vital to the growth and survival of these cells, and down-regulation of Gli transcription factors either by chemical or molecular inhibitors leads to marked effects on cancer stem cell self-renewal and tumor initiating capacity [98].

In our own studies, we have identified a distinct population of cells within primary human pancreatic adenocarcinoma that are enriched in tumor-initiating cells and exhibit self-renewal by serial passaging in NOD/SCID animals [99]. These cells are marked by the expression of the cell surface markers CD44, CD24, and epithelial cell adhesion molecule (EpCAM) and represents a self-renewing fraction of tumorigenic cells which can establish tumors phenotypically identical to the primary patient tumor [100]. Recent limiting dilution analysis (LDA) study of tumor cells from multiple human pancreatic adenocarcinomas identified that the frequency of tumorigenic cells ranges from 1/2,500 to 1/18,000 depending on the individual patient tumor [94]. It is important to note that this study only evaluated three patient tumors, and the range of tumor-initiating cells may vary greatly depending on the phenotype and genotype of the individual patient tumors. Additionally, following our initial publication we have identified pancreatic adenocarcinomas that either lack expression of CD24 or have very high levels of expression of both CD44 and CD24, which in some patient tumors greater than 40% of the tumor cells express these markers (unpublished observations). A large scale LDA study would be ideal to compare if

tumor-initiating capacity correlates with the expression of CD44 and CD24 expression, or any of the other markers that have been attributed to cancer stem cells in pancreatic cancer including CD133, c-Met or Aldefluor positive ($ALDH^+$) cells [94,101]. This will shed more light on whether these markers are indeed informative of the cells which contain the tumorigenic activity in pancreatic adenocarcinoma.

The role of Hh signaling in pancreatic cancer stem cells is still very unclear. Direct isolation and qRT-PCR of mRNA isolated from the tumorigenic $CD44^+/CD24^+/ESA^+$ pancreatic cancer cells vs. the non-tumorigenic $CD44^-/CD24^-/ESA^-$ cells revealed higher levels of Shh expression in the tumorigenic population compared to the non-tumorigenic population [99]. We can only speculate as to what this may mean, but it is possible that this enhanced ligand expression plays an important role in regulating the expression of Hh target genes in the neighboring tumor stroma. Others have indirectly tested the importance of Hh signaling in pancreatic cancer stem cells by treatment of a metastatic cell line model of pancreatic cancer with the Smo inhibitor, cyclopamine [56]. These treatments did not significantly alter tumor size but exhibited a significant effect on preventing tumor metastasis and lead to a reduction of tumor cells with aldehyde dehydrogenase (ALDH) activity, a marker used to identify tumorigenic populations in breast cancer [102] and colon cancer [103]. However, these studies utilized xenografts generated from immortalized pancreatic cell lines and it is unclear if the cells in these lines are hierarchically organized and fit the cancer stem cell model. Additionally, while ALDH activity may represent a tumorigenic population in some solid tumors, this population of cells has not been validated by *in vivo* implantation assays for

pancreatic adenocarcinoma. Some unpublished observations in our lab suggest that while $ALDH^+$ cells have tumorigenic potential, they do not encompass all of the tumorigenic cells within the tumor as we also see tumors arising from animals implanted with $ALDH^-$ cells.

It is reasonable to hypothesize that Hh signaling in the tumor stroma may provide positive feedback signals in the form of secreted factors or changes to the tumor microenvironment that helps to maintain the pancreatic cancer stem cell population. Down-regulating Hh signaling in either the tumor cells by targeting Gli transcription factors by siRNAs or in the tumor stroma by use of Hh pathway inhibitors will help to define the importance of Hh signaling to this cell population. These will be important questions to answer in the future as we develop better *in vitro* and *in vivo* models that allow us to construct a more comprehensive picture of the role of Hh pathway signaling in the tumor microenvironment.

CLINICAL INHIBITORS OF THE HEDGEHOG PATHWAY

We have learned much about the role of Hh signaling in pancreatic tumor development from genetic manipulation of the Hh pathway in mouse models. The efficacy of targeting this pathway in xenograft models and in patients has been tested by the development of several targeted inhibitors of the Hh pathway. The discovery of an important Hh pathway inhibitor was made after newborn livestock were found with developmental defects, including cyclopia, when the female parental animals grazed in fields that contained corn lilies [104]. A specific compound isolated from these plants was named, cyclopamine, and was found to be a potent antagonist to the

Hh signaling receptor, Smoothened (Smo) [105]. Several screens of small-molecule libraries have identified more specific compounds with increased bioavailability that also antagonize Smo signaling, including: HhAntag, SANTs1-4, GDC-0449, and IPI-926 [106,107,108,109]. Additionally, other molecules that target different parts of the Hh signaling pathway, including a blocking peptide against the Hh pathway ligand, Sonic Hedgehog, and small molecules that target the Gli transcription factors, Gli1 and Gli2, have been developed for down-regulation of Hh signaling [110,111].

Several of these Hh pathway inhibitors are now in Phase I and II clinical trials to test their efficacy in patients with a variety of tumors involving the Hh pathway including: basal cell carcinoma (BCC), breast cancer, gastric cancer, medulloblastoma, small-cell lung cancer, myeloma, ovarian, and pancreatic cancer [66]. Early results from clinical trials that have been published using GDC-0449 in patients with basal cell carcinoma have been encouraging. In this report, 18 of 33 patients had distant metastatic disease, and the response rate for all 33 patients was 55% [112]. This study also demonstrated that patients were able to tolerate extended Hh pathway inhibition. The median exposure to drug was 9.8 months, with side-effects including weight-loss, fatigue, hyponatremia that did not go above grade 3 and in fewer than 10% of patients in the study. Interestingly, in a separate case report of a patient with metastatic medulloblastoma, GDC-0449 treatment resulted in a rapid decrease of tumor burden; however, within several months the patient relapsed and developed resistance to the treatment and ultimately succumbed to the disease [113]. These results underscore the limitations of targeting Hh signaling alone and why

expanding upon our knowledge of how Hh pathway is involved in tumor progression is important for designing therapeutic treatments for patients.

In contrast to treatment of tumors driven by Hh pathway mutations, it will be important to identify how targeting Hh signaling in tumor-stromal interactions will affect the progression of the disease as the dominant effect will be on the tumor microenvironment. A Phase I clinical trial is currently underway at the University of Michigan Medical Center to test the clinical response of patients with pancreatic adenocarcinoma treated with the Hedgehog pathway inhibitor, GDC-0449, in combination with gemcitabine. Additionally, we and others have initiated studies to identify the Hh responsive genes in the pancreatic tumor mesenchyme and this information will help us to understand how these inhibitors are affecting the pancreatic tumor microenvironment. These studies will provide important data to determine if targeting paracrine Hh signaling may provide a therapeutic benefit for pancreatic cancer patients

FIGURES

Figure 1.1 Pathology of Pancreatic Adenocarcinoma Progression. (A) Histological stain of normal human pancreas. **(B)** High-power magnification of a PanIN-2 lesion. **(C)** Low-power magnification of an infiltrating pancreatic adenocarcinoma. **(D)** Gomari's trichrome stain of human pancreatic adenocarcinoma. Note the large amount of connective tissue staining (blue-green stain) compared to the tumor cells (red stain) in the section.

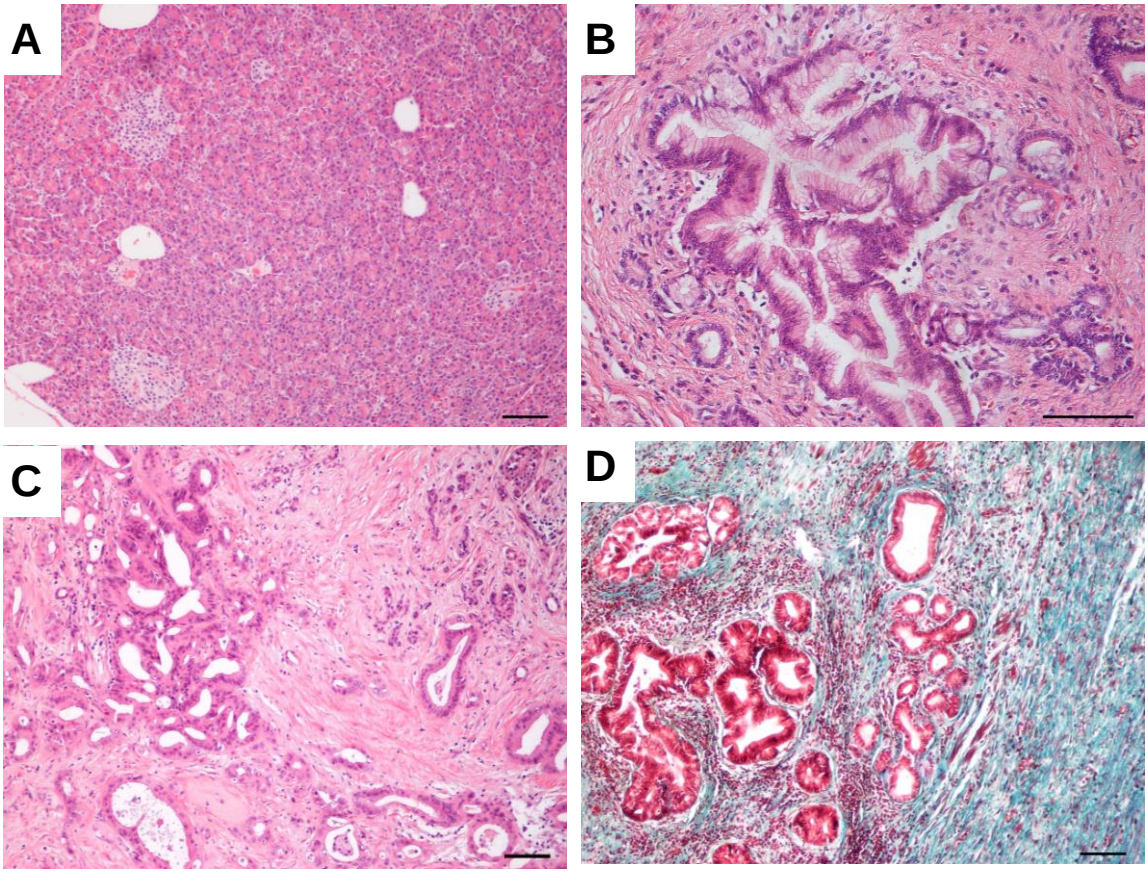

Figure 1.2 Progression Model of Pancreatic Cancer. The most common pre-cancerous lesions are termed pancreatic intraepithelial neoplasms (PanINs), graded from 1-3. Hedgehog ligands have been detected as early as PanIN1. Adapted from Bardeesy et. al Nature reviews 2002 [114].

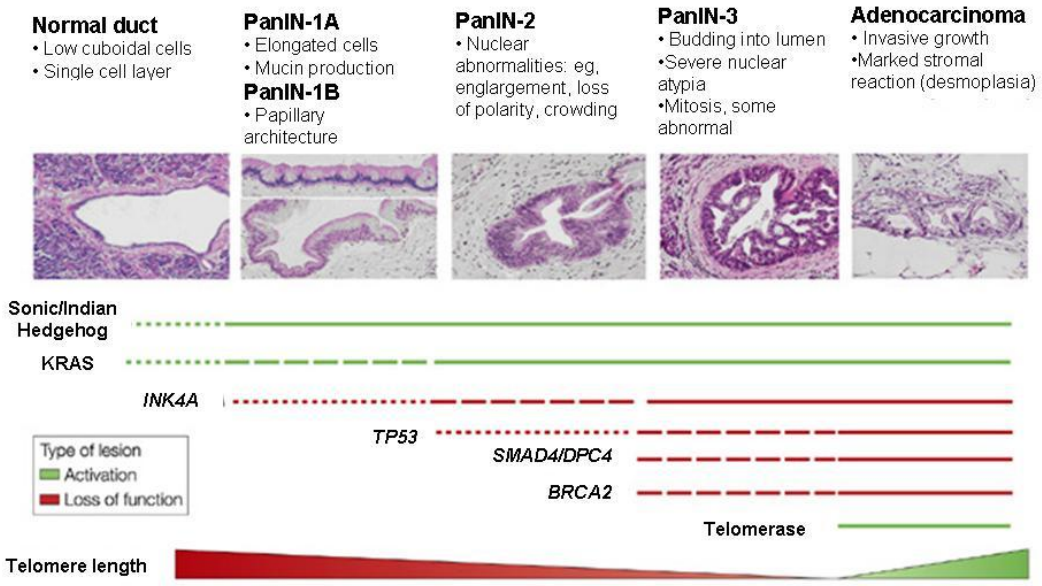

Figure 1.3 Diagram of Canonical Hh Pathway Activation. (**A**) In the absence of Hh ligand, Gli transcription factors are down-regulated or processed to a repressor form which prevents activation of downstream target genes. (**B**) Following ligand binding to Ptch, Smo is phosphorylated and stabilized at the cell membrane by a kinase complex. Gli transcription factors are not processed to a repressor form and instead translocate to the nucleus to activate downstream target genes.

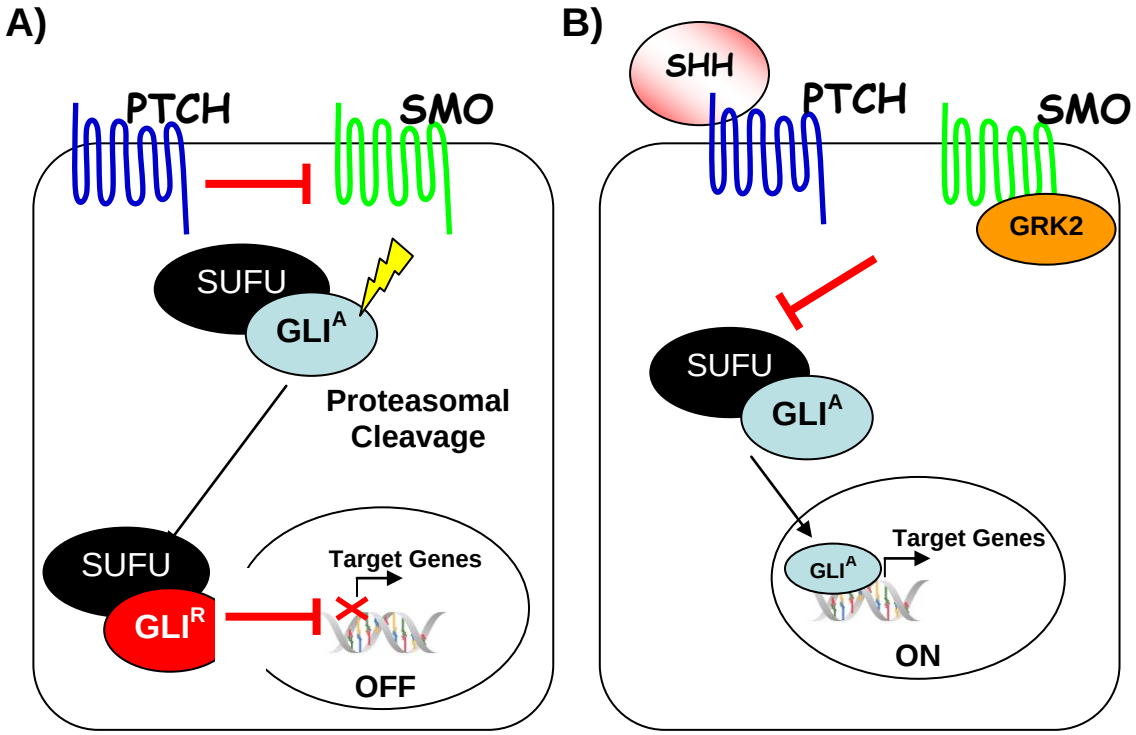

Figure 1.4 Expression of Shh in Human Pancreatic Adenocarcinoma. IHC image of normal human pancreas and a pancreatic adenocarcinoma xenograft stained for human Sonic Hedgehog (Shh, brown color). Nuclei are counterstained with hematoxylin. Staining is restricted to the neoplastic cells, while there is no Shh expression detected in the neighboring stroma.

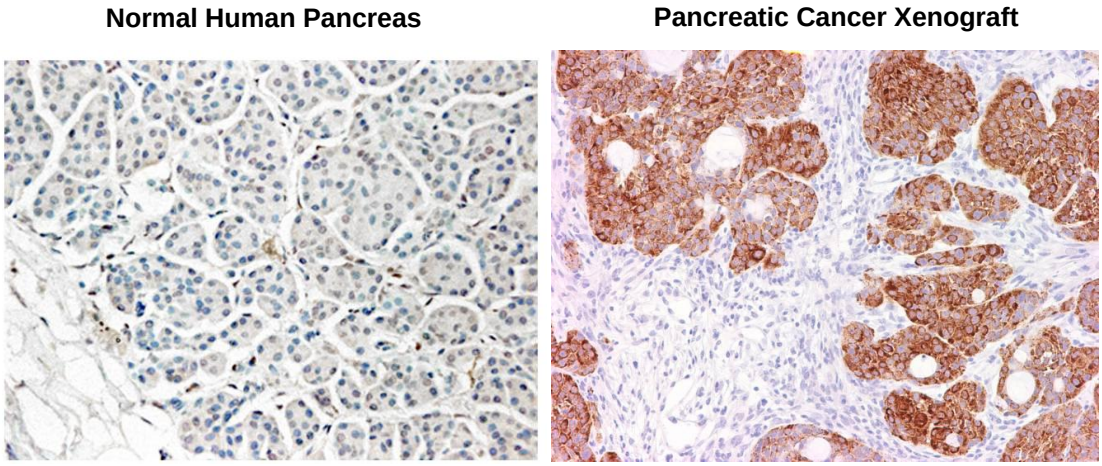

Figure 1.5 Paracrine Mechanism of Hedgehog Pathway Activation. Pancreatic tumor cells secrete Hh ligands (Shh, Ihh) into the tumor microenvironment, which activates the pathway in surrounding tumor fibroblasts. This paracrine activation, in turn, leads to the expression of a subset of yet uncharacterized Hh target genes that may play a role in fibrosis, along with neo-vascularization, recruitment of inflammatory cells, and stimulating growth factors for the tumor cells.

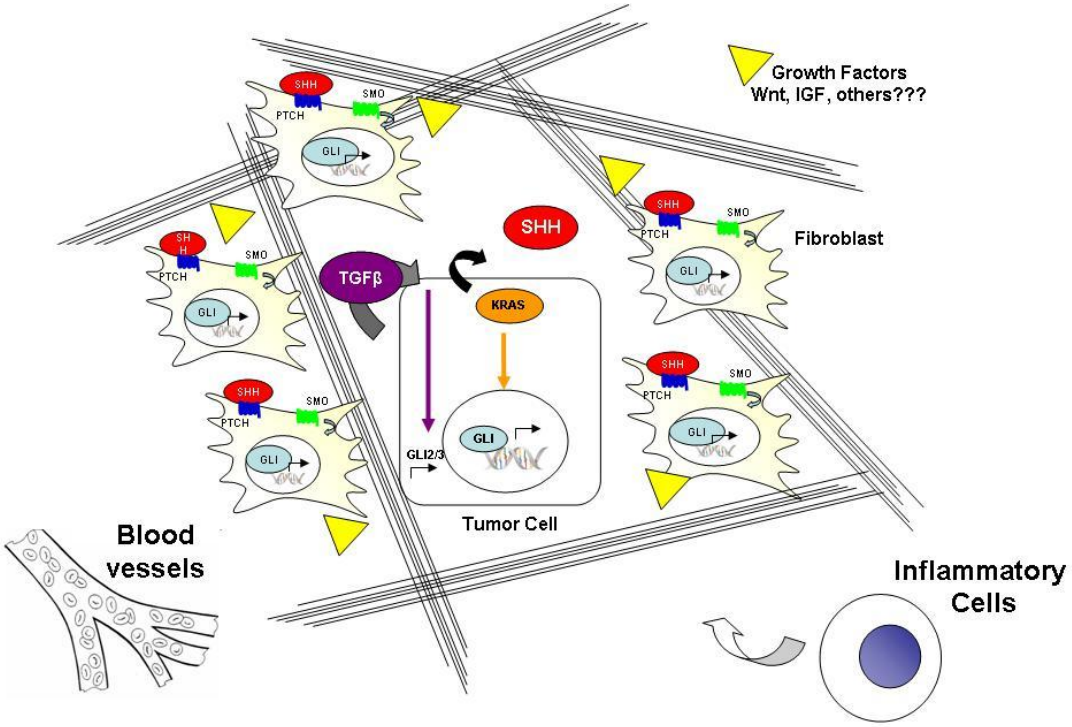

CHAPTER 2

INHIBITION OF PARACRINE HEDGEHOG SIGNALING IN HUMAN PANCREATIC ADENOCARCINOMA XENOGRAFTS

SUMMARY

Aberrant activation of the Hedgehog (Hh) pathway has been associated with the progression of several tumor types. In pancreatic cancer, a paracrine mechanism has been identified in which pancreatic tumor cells secrete Hh ligands and activate the hedgehog pathway in the surrounding tumor mesenchyme. We set out to identify the role of paracrine Hh signaling in pancreatic cancer biology utilizing an orthotopic model of human pancreatic ductal adenocarcinoma (PDA). Treatment of patient-derived PDA xenografts grown ectopically in the pancreas of mice with HhAntag alone, a potent Hh pathway inhibitor and Smoothened antagonist, did not significantly affect primary tumor volume. However, we observed a significant decrease in the number of distant metastases with HhAntag treatment. Co-treatment with the nucleoside analog, gemcitabine, a chemotherapeutic agent commonly used to treat pancreatic cancer, enhanced these affects and also resulted in differentiation of the tumor cells to a mucin producing phenotype. Finally, we observed a significant decrease in the pancreatic cancer stem cell population ($CD44^+/CD24^+/ESA^+$) in tumors treated with HhAntag. Re-implantation of tumor cells from both HhAntag-treated and HhAntag/gemcitabine co-treated animals resulted in a significant decrease in subsequent tumor growth compared to cells implanted from either control or

gemcitabine only treated animals, suggesting that HhAntag treatment decreases the tumor-initiating capacity of cancer cells. These results provide important insights into how targeting paracrine Hh signaling in pancreatic cancer may provide therapeutic benefits to patients.

INTRODUCTION

Pancreatic ductal adenocarcinoma (PDA) is a devastating disease that ranks fourth in cancer-related death in the United States, with 5-year survival rates of less than 5% [115]. Most PDA patients present clinically with non-resectable, metastatic disease. Current therapies include the cytotoxic agent gemcitabine, but a very limited therapeutic effect is observed. Even in cases where the disease is identified in its early stages, nearly all patients that undergo surgical resection of the tumor along with adjuvant chemotherapy will eventually relapse and succumb to recurrent disease [116,117]. Clinical trials that have evaluated the efficacy of targeting pancreatic adenocarcinoma with antagonists of the human epidermal growth factor receptor (EGFR) pathway, vascular endothelial growth factor (VEGF) pathway, insulin-like growth factor (IGF) pathway, and phosphoinositide 3'-kinase (PI3k)/Akt/mammalian target of rapamycin (mTOR) signaling have only demonstrated marginal clinical response in patients [27,28,118,119]. This underlines the need to develop a better understanding of pancreatic tumor biology and identify specific pathway targets which will improve clinical response.

The Hedgehog (Hh) signaling pathway has become an important area of research for pancreatic cancer following initial studies demonstrating up-regulation of

several pathway components in human cell line models and primary samples of pancreatic cancer [30,31]. In normal pancreatic development, expression of Hh signaling ligands is blocked in the developing pancreatic bud to allow for proper specification of the gland [57]. In the adult organ, Hh signaling is active at low-levels in pancreatic β-cells and is important for the regulation of insulin secretion [61]. In pancreatic tumors, Hh ligands, Sonic hedgehog (Shh) and Indian hedgehog (Ihh), are expressed in both early precursor pancreatic intraepithelial neoplasms (PanINs) and in advanced adenocarcinoma [30,120]. Desert hedgehog (Dhh), a third Hh pathway ligand that is involved in the formation of nerve sheaths and plays a role in the regulation of insulin secretion of pancreatic β-cells has not been characterized in pancreatic cancer [61].

Recent studies have demonstrated that while pancreatic tumor cells express Hh ligands, the tumor cells are not competent to transduce canonical Hh signals [32]. This suggests that Hh ligands secreted from the tumor cells initiate a paracrine mechanism in which Hh acts in the stromal compartment of the pancreatic tumor. Paracrine Hh signaling in the stroma creates a feedback loop in which downstream Hh-targets are secreted from the stroma and believed to aid in the growth and invasion of the tumor. Although it is unclear which factors are involved, members of the Wnt and IGF pathways have been shown to be differentially regulated in the stroma of PDA xenografts treated with Hh pathway inhibitors [33,86]. Additionally, over-expression of Shh by tumor cells may contribute to the intense desmoplasia that is characteristic of the disease by stimulating the proliferation of pancreatic stellate cells [81].

Hh pathway inhibitors have been shown to limit the growth of human PDA in experimental models *in vivo* [30,121,122]. Recent data has suggested that targeting paracrine Hh signaling in a mouse model of pancreatic adenocarcinoma may improve the blood flow within the tumor by ablating the tumor stroma and allowing expansion of the vasculature, thus dramatically improving the effectiveness of cytotoxic drugs, such as gemcitabine, by increasing exposure to the tumor cells to the chemotherapeutic agent [80]. Despite these studies, it is still relatively unknown how targeting paracrine Hh signaling in primary human pancreatic adenocarcinoma can affect important aspects of tumor biology that include proliferation, metastasis and cancer stem cell function. It was our aim to develop an orthotopic model of paracrine Hh-pathway inhibition, using primary human pancreatic adenocarcinoma xenografts to answer these questions.

MATERIALS AND METHODS

Treatment of Orthotopic Human PDA Xenografts

Animals used in this study were maintained in facilities approved by the American Association for the Accreditation of Laboratory Animal Care in accordance with the current regulations and standards of the US Department of Agriculture and Department of Health and Human Services. All studies were approved by the University Committee on Use and Care of Animals at the University of Michigan. Samples of human pancreatic adenocarcinomas were obtained within 30 min following surgical resection according to Institutional Review Board–approved

guidelines. Expansion of primary human pancreatic adenocarcinoma samples using NOD/SCID animals have been described previously [123].

To establish orthotopic xenografts, after administration of anesthesia, a small subcostal laparotomy was performed, and single cell suspensions of human PDA cells, transduced with a lentivirus-expressing *Renilla*-Luciferase, were then injected (5.0×10^5/ 50 μl) into the distal pancreas of NOD/SCID animals. Tumors were allowed to engraft for 2 weeks, following confirmation of a positive bioluminescence signal performed by i.p injection of luciferin and use of a Xenogen IVIS™ 200 Imager (Caliper Life Sciences; Alameda, CA). Animals were randomized into four treatment groups, seven per group, and treated for 21 days with either vehicle (0.5% methylcellulose (Sigma; St. Louis, MO) plus 0.2% Tween80 (Sigma), HhAntag 100 mg/kg by oral gavage (twice daily), gemcitabine 50 mg/kg once a week, or a combination the HhAntag and gemcitabine regimens. After 21 days of treatment, primary tumor weight was measured and metastases quantified along with harvesting of tissue for histological and FACS analysis.

Drugs

HhAntag was provided by Genentech (South San Francisco, CA) [33]. HhAntag was prepared as a 10 mg/ml solution in 0.5% methylcellulose (Sigma) plus 0.2% Tween80 (Sigma) and delivered by oral gavage 10 mg/kg twice daily. Gemcitabine (Eli Lilly; Indianapolis, IN) was re-suspended in sterile PBS and injected intraperitoneally at 50 mg/kg once a week.

RNA Extraction and Quantitative Real-Time Reverse Transcription-PCR

Tumor fragments (20 mg) were harvested from each treatment group, and the tissue was homogenized with a rotor-stator homogenizer (Polytron; Kinematica, Bohemia, NY) in RLT buffer (Qiagen; Valencia, CA). Total RNA was extracted using the RNeasy Mini kit (Qiagen). Total RNA quality and quantity was analyzed using a NanoDrop (Thermo Scientific; Rockford, IL). One microgram of total RNA was used to transcribe cDNA using the SuperScript® First-Strand Synthesis System (Invitrogen; Carlsbad, CA). From this cDNA reaction, 2 µl of RT reaction was used for qPCR using POWER SYBR Mix (Applied Biosystems; Carlsbad, CA) and the reaction was carried out on a Roto-Gene Q Real-Time Cycler (Qiagen).

Primers used for qPCR are as follows: mouse *Gli-1* forward: GGA AGT CCT ATT CAC GCC TTG A, reverse: CAA CCT TCT TGC TCA CAC ATG TAA G; mouse *Ptch-1* forward: TTG TGG AAG CCA CAG AAA ACC, reverse**:** TGT CTG GAG TCC GGA TGG A; mouse *GAPDH* forward: AGC CTC GTC CCG TAG ACA AAA T, reverse: CCG TGA GTG GAG TCA TAC TGG A, human *Gli-1* forward: GTT CAC ATG CGC AGA CAC ACT, reverse: TTC GAG GCG TGA GTA TGA CTT C; human *Ptch-1* forward: CGG CAG CCG CGA TAA G, reverse: TTA ATG ATG CCA TCT GCA TCC A, human *GAPDH* forward: CCA CAT CGC TCA GAC ACC AT, reverse: GCA ACA ATA TCC ACT TTA CCA GAG TTA A.

Histology

Paraformaldehye-fixed (4%), paraffin-embedded tissue sections were stained with H&E in the histology lab of the University of Michigan Comprehensive Cancer Center Tissue Core. For immunohistochemistry, deparaffinized and rehydrated slides

were subjected to antigen retrieval via autoclaving in a 10 mM citric acid buffer (pH 6.0). Upon cooling to room temperature for 30 min, slides were blocked with 0.3% H_2O_2 for 20 min, washed in phosphate-buffered saline (PBS), and then blocked with 1% BSA in PBS. Slides were incubated with diluted primary antibodies overnight at 4°C. The following primary antibodies were used: rabbit anti-ki67 (1:200 dilution; Novocastra), Cleaved caspase 3 was detected using a rabbit anti-cleaved caspase 3 antibody (1:100 dilution; Cell Signaling Technologies; Danvers, MA). Slides were developed using the Vectastain ABC kit (Vector Labs; Burlingame, CA). 3-3′-Diaminobenzidine tetrahydrochloride was used as a chromogen and counterstained with hematoxylin.

Flow Cytometry Analysis of Cancer Stem Cell Markers

Measurement of the $CD44^+/CD24^+/ESA^+$ cancer stem cell population after treatment with HhAntag or vehicle was carried out using FACS analysis as previously described [123]. Dissociated cells were counted and transferred to a 5-mL tube, washed twice with HBSS containing 2% heat-inactivated FBS, and re-suspended in HBSS with 2% FBS at concentration of 10^6 cells/100 μL. Sandoglobin solution (1 mg/mL) was then added to the sample at a dilution of 1:20 and the sample was incubated on ice for 20 min. The sample was then washed twice with HBSS/2% FBS and re-suspended in HBSS/2% FBS. Antibodies were added and incubated for 20 min on ice, and the sample was washed twice with HBSS/2% FBS. When needed, a secondary antibody was added by re-suspending the cells in HBSS/2%FBS followed by a 20-min incubation. After another washing, cells were re-suspended in HBSS/2%

FBS containing 4′, 6-diamidino-2-phenylindole (DAPI; 1 μg/mL final concentration). The antibodies used were: anti-CD44 phycoerythrin (PE) (BD Biosciences; San Diego, CA), anti-CD24 FITC (BD Biosciences), anti–EpCAM-allophycocyanin (APC) (Miltenyi Biotec; Auburn, CA), and biotinylated anti-H2K (Southern Biotech; Birmingham, AL) each at a dilution of 1:40. A strepavidin-APC-Cy7 (BD Biosciences) was also used. In all experiments using human pancreatic cancer primary xenograft tissue, infiltrating mouse cells were eliminated by discarding $H2K^+$ (mouse histocompatibility class I) cells during flow cytometry. Dead cells were eliminated by using the viability dye DAPI. Flow cytometry was done using a MoFlo (Beckman Coulter; Brea, CA). Side scatter and forward scatter profiles were used to eliminate cell doublets. Cells were routinely sorted twice, and the cells were reanalyzed for purity, which typically was >98%.

Statistical Analysis

To compare the incidence of metastasis in the orthotopic model, we used a Fisher's exact test to compare treatments, whereas a Mann–Whitney test was used to calculate any significant difference in the weight of the primary tumors. Fischer's exact test was performed to calculate significant differences in the number of animals with distant metastases. All statistics were compiled by using Prism version 5.01 (GraphPad Software, Inc.).

RESULTS

Paracrine Hh Signaling in Human Pancreatic Ductal Adenocarcinoma Xenografts

Paracrine Hh signaling has been detected in mouse models of pancreatic cancer and in human cell line xenografts [32,33]. To further define the role of Hh signaling in pancreatic cancer, we established xenografts from tumor fragments obtained from 13 patients that had undergone surgical resection for pancreatic ductal adenocarcinoma (**Table 2.1**). In these xenotransplantation models, as the tumor grows in the host mouse, the human tumor stroma is quickly replaced with host mouse stroma [124]. To test whether paracrine Hh signaling was active in primary human PDA xenografts, we examined the gene expression levels of several Hh pathway related genes using mouse/human species specific probe sets. Expression of Hh ligands, Sonic and Indian Hedgehog (Shh, Ihh), was found to be significantly up-regulated in our PDA xenografts compared to the expression of these genes in several samples of normal human pancreas (**Figure 2.1 A**). Additionally, using human/mouse specific probes, we observed a correlation between the levels of Shh and Ihh expression in the tumor and activation of Hh signaling, as evaluated by Gli1 and Ptch1 expression in the mouse stroma (**Figure 2.1 B**). This data supports the idea that paracrine Hh signaling in the tumor stroma is active in human PDA xenografts.

HhAntag and Gemcitabine Treatment of Orthotopic PDA Xenografts

To test how paracrine Hh signaling contributes to pancreatic ductal adenocarcinoma tumor growth and progression, we established an orthotopic model of human PDA using low passage (≤ passage 2) cells derived from patient xenograft tumors. After establishing these tumors in the pancreas of NOD/SCID animals, we treated the mice with HhAntag, an orally bioavailable Hh pathway inhibitor that

targets the Smoothened (Smo) receptor of the Hh pathway and prevent downstream activation of Hh target genes [33]. In parallel, we treated groups of animals with weekly doses of gemcitabine, a chemotherapeutic drug commonly used in the treatment of pancreatic cancer [24], or a combination of gemcitabine and HhAntag.

We selected two different patient xenografts from our initial Hh pathway analysis for our *in vivo* study. UM-PDA#1 was classified histologically as a poorly differentiated adenocarcinoma, expressed very high levels (40%) of cancer stem cell markers CD44 and CD24 [99], and subsequent follow-up with the patient revealed the disease had quickly progressed to Stage IV with metastasis to the liver (**Table 2.1**). UM-PDA#2 was classified as a moderately differentiated adenocarcinoma and had a lower percentage of the cancer stem cell population (4%) (**Table 2.1**). Quantitative expression analysis ($2^{-\wedge\Delta Ct}$) by qRT-PCR of Sonic hedgehog for UM-PDA#1 and UM-PDA#2 was found to be 0.026 and 0.020, respectively, which was just below the statistical median (0.054) for the group of xenografts analyzed in this study (**Table 2.2**).

Treatment of both tumor xenografts with HhAntag for 21 days resulted in slight reductions in primary tumor volume; however, these changes did not reach statistical significance (**Figure 2.2 A**). Treatment with gemcitabine alone did result in significant decreases compared to controls, with a 47% and 87% reduction in tumor volume for UM-PDA#1 and UM-PDA#2, respectively. Combinatorial therapy with HhAntag and gemcitabine resulted in a 77% decrease for tumor UM-PDA#1 and an 83% decrease in UM-PDA#2, compared to control treated tumors. The effect of HhAntag and gemcitabine treatment on animals with UM-PDA#1 xenografts

demonstrated synergistic activity, while the same treatment of animals with UM-PDA#2 xenografts was not statistically different from treating with gemcitabine alone. Animal weights remained the same as vehicle treated controls and no animals lost significant total body weight (>5%) which was determined by weekly weight measurements taken during treatment (data not shown).

Next, we investigated the effects of Smo-inhibition on cell proliferation and apoptosis. HhAntag treatment did not have a significant effect on the overall cellular proliferation of either UM-PDA#1 or UM-PDA#2 as evaluated by Ki67 positive cells (**Figure 2.2 B**). Additionally, treatment with gemcitabine alone did not result in significant decreases in proliferation with either tumor xenograft. We did, however, observe a significant decrease in the overall proliferation with co-treatment of HhAntag and gemcitabine in both xenografts (**Figure 2.2 B**). Similar to the results with overall proliferation, we did not observe significant changes in the number of apoptotic cells in HhAntag or gemcitabine only treated xenografts (**Figure 2.2 C**). However, we did observe a significant increase in cell death in the UM-PDA#1 animal xenografts co-treated with HhAntag and gemcitabine as evaluated by an increase in the staining for cleaved caspase 3 (CC3) (**Figure 2.2 C**). Numbers of apoptotic cells in the UM-PDA#2 animal xenografts co-treated with HhAntag and gemcitabine were not statistically different from controls. These results suggest that Smo-inhibition alone is not enough to slow the growth of the tumor by either reduction of mitotic signals or an increase in pro-apoptotic mechanisms. However, co-treatment with HhAntag and gemcitabine was able to decrease proliferation in both patient xenografts and increase the amount of apoptosis in one of the xenografts

providing evidence that these drugs may act synergistically in reducing pancreatic tumor growth.

To confirm that HhAntag treatment down-regulates the Hh pathway, we performed qRT-PCR from RNA extracted from bulk tumor tissue from each treatment group using mouse and human specific primers for Gli1 and Ptch1. We observed that mouse stromal Gli1 and Ptch1 were significantly decreased compared to controls in both HhAntag and combination treated xenografts, while Hh target gene expression levels were unchanged in the infiltrating mouse stromal component in gemcitabine treated animals (**Figure 2.2 D**). Unexpectedly, we observed increases in human Gli1 levels in UM-PDA#1 and human Ptch1 levels in UM-PDA#2 with gemcitabine and co-treatment with HhAntag (**Figure 2.2 D**). It is possible that these treatments disrupted paracrine signals in the stroma that lead to non-canonical up-regulation of these factors.

HhAntag Treatment Induces Differentiation in PDA Xenografts

Examination of histological sections from xenograft-derived tumors treated with HhAntag alone or in combination with gemcitabine revealed the appearance of vacuolated structures within the tumor cells. In tumors from UM-PDA#1 animals, we observed these structures in both the HhAntag only and combination treated group, but not in the vehicle or gemcitabine-only treated tumors (**Figure 2.3 A**). Trichrome staining, which helps to differentiate tumor cells from the connective tissue, identified a reduction in stromal cells in the regions surrounding the tumor cells with the vacuolated pattern in the tumors co-treated with HhAntag and gemcitabine. Periodic

acid-Schiff (PAS*)* staining confirmed that the vacuolated structures contained large amounts of mucin (**Figure 2.3 A**). In the UM-PDA#2 treated tumors, we only observed these structures in the combined HhAntag and gemcitabine treated animals. We also observed a significant change in the tumor architecture compared to control treated tumors with the majority of tumor cells arranged in papillary-like structures with large vacuolated spaces (**Figure 2.3 B**). Similar to UM-PDA#1 xenografts, trichrome staining of UM-PDA#2 tumors from animals treated with HhAntag and gemcitabine treated animals revealed a reduction in the stroma surrounding the differentiated tumor cells. PAS staining of sections from these HhAntag and gemcitabine treated tumors confirmed the expression of mucin in these structures (**Figure 2.3 B**). To date, this change in the apparent differentiation of PDA tumors following inhibition of paracrine Hh signaling alone, or in combination with gemcitabine treatment, has not been previously described.

HhAntag Treatment Decreases Metastasis in Orthotopic PDA Xenografts

Pancreatic ductal adenocarcinoma is a highly metastatic disease; therefore we determined whether inhibition of paracrine Hh signaling was capable of suppressing the development of distant organ metastases in our orthotopic model. We selected UM-PDA#1 for further analysis, as this tumor xenograft had demonstrated metastatic potential in previously performed studies in our laboratory. UM PDA#2 did not display metastatic potential when implanted in orthotopically in NOD/SCID mice. After 21 days of control, HhAntag or gemcitabine only treatment, along with co-treatment with both drugs we sacrificed the animals from each treatment group for pathological analysis. We observed in control treated animals, significant metastatic

spread of the disease to the peritoneal cavity, along with invasion into mesenteric lymph nodes and to the liver (**Figure 2.4 A**). Examination of these metastatic sites revealed lesions histologically identical to the primary tumor (**Figure 2.4 B**). In animals that were treated with HhAntag alone or co-treatment of HhAntag and gemcitabine, we did not detect metastases to the lymph nodes or peritoneum (**Figure 2.4 C**). Animals treated with gemcitabine also had significant reductions in metastases to the lymph nodes and peritoneum. We observed reductions in the numbers of metastases to the liver with HhAntag treatment alone and in combination with gemcitabine, although this did not reach statistical significance (**Figure 2.4 C**).

HhAntag Treatment Affects the Pancreatic Cancer Stem Cell Population

Previous work in our lab has identified a highly tumorigenic subpopulation of cells within pancreatic ductal adenocarcinoma that express CD24, CD44, and epithelial cell adhesion molecule (ESA) that we have termed cancer stem cells (CSC) due to their ability to self-renew and produce the heterogeneity of cancer cells that are present in the patient's tumor [99]. We hypothesized that knockdown of paracrine Hh signaling in the tumor stroma may alter factors that contribute to the maintenance and self-renewal of this population. To evaluate whether HhAntag or gemcitabine treatments affected this population of cells, we performed FACS analysis on single cell suspensions prepared from tumors in each treatment group. Analysis of xenograft UM-PDA#1 did not reveal any significant change in the $CD44^+/CD24^+/ESA^+$ population following any of the drug treatments compared to vehicle (**Figure 2.5 A**). However, FACS analysis of xenograft UM-PDA#2 revealed a 50% decrease in $CD44^+/CD24^+/ESA^+$ cells following HhAntag treatment alone and

in combination with gemcitabine, while the cancer stem cell population in the gemcitabine only treated animals did not change significantly from control animals (**Figure 2.5 B**). To see if the tumorigenicity of these cells had been affected by the treatment regimens, we FACS sorted and subcutaneously implanted in NOD/SCID animals, $2.5x10^4$ $DAPI^-/H2K^-$ (viable, human tumor cells) from cells dissociated from tumors in treatment group. After 6 weeks, we excised the tumors from each group and compared their final tumor weights (**Figure 2.5 C, D**). Re-implanted cells from HhAntag and co-treatment of HhAntag and gemcitabine resulted in tumors that were significantly reduced in size compared to control or gemcitabine only treated cells.

DISCUSSION

In this study, we tested the role of paracrine Hh signaling in the growth and progression of human pancreatic ductal adenocarcinoma xenografts. Our findings are consistent with other studies that have shown a significant reduction in metastases to distant organ sites, including lymph nodes and peritoneum, following inhibition of paracrine Hh signaling [122,125]. We also observed a previously unreported effect of HhAntag to enhance the apparent differentiation of cancer cells with marked increase in tumor production of mucin. In addition, the areas surrounding the differentiated structures in the animals co-treated with HhAntag and gemcitabine were mostly devoid of stroma compared to control and treatment with either drug alone. We also demonstrated that HhAntag treatment can reduce the tumorigenic capacity of human PDA cells following re-implantation of the treated cancer cells.

Our studies, along with others, have demonstrated that pancreatic tumor cells secrete Hh ligands, and this activates Hh signaling in the surrounding tumor mesenchyme [33]. However, down-regulation of paracrine Hh signaling alone in human PDA xenografts does not result in a significant reduction in primary tumor volume. This result is consistent with the finding that Smo-inhibition in a mutant KRAS/p53 transgenic animal model of pancreatic cancer does not significantly affect primary growth of the tumor [80]. However, we observed significant reductions in primary tumor volume with combination treatment of HhAntag and gemcitabine in both patient xenografts. The use of both drugs was synergistic in the treatment of UM-PDA#1, but not UM-PDA#2. This suggests that different patient tumors respond differently to Hh targeted therapy, and these differences warrant further investigation to help identify which patients may optimally benefit from this therapy.

We also observed that the PDA xenograft model was sensitive to gemcitabine treatment, raising a limitation to this model system as only 15% of patients respond to gemcitabine treatment [24]. Recent studies have demonstrated that a transgenic mouse model of human PDA, which conditionally expresses mutant KRAS and p53 alleles in pancreatic cells, generates pancreatic adenocarcinoma that is highly desmoplastic and poorly perfused [80]. Cell lines made from these tumors, and re-implanted back into immune competent animals, resulted in tumors that were well-perfused and sensitive to gemcitabine treatment, suggesting that *de novo* tumor development rather than xenotransplantation may better approximate the human PDA disease response to gemcitabine. Noticeably, in our xenograft model, the infiltrating mouse stroma that replaces the human stroma in the tumor appears reduced from the

primary patient tumor. Despite these limitations, treatment of xenotransplanted tumors provided important insight into the response of individual patient tumors, and demonstrated distinct responses to HhAntag not observed in the transgenic model of pancreatic cancer, such as the development of a more-mucin-producing epithelial component.

Our study also suggests a previously unreported role for paracrine Hh signaling in maintaining the differentiation status of the tumor epithelium. Both xenografts treated with a regimen of HhAntag alone or in combination with gemcitabine resulted in tumor regions with punctuate, vacuolated structures in the tumor cells that contained mucins. Interestingly, in the case of xenograft UM-PDA#2 co-treated with HhAntag and gemcitabine the tumor architecture was significantly altered to a papillary structure, with very prominent glandular differentiation. Typically, cell proliferation and differentiation display an inverse relationship, in that the most aggressive tumor malignancies are characterized by a high rate of proliferation and an absence of differentiation [126].

Our results suggest that paracrine Hh signaling in the tumor stroma likely provides important feedback signals to the tumor cells that maintain their differentiation status. Co-treatment with HhAntag and gemcitabine further enhances this phenotype, and suggests that the combination of these two drugs could be used to decrease the amount of stroma, enhance drug delivery, and induce a more differentiated and less aggressive tumor cell phenotype. Interestingly, this differentiated phenotype has also been observed in a patient following post-treatment biopsies in a phase I clinical trial at the University of Michigan Medical Center using

GDC-0449, an Hh pathway inhibitor and Smoothened antagonist developed by Genentech to treat naïve patients with metastatic pancreatic cancer (**Figure 2.6**). While this clinical trial is still in the early stages, and we will need to do additional studies to correlate the phenotypes seen in our xenograft studies with patients in the clinical trial, our results may help predict how inhibition of paracrine Hh signaling affects primary patient tumors and demonstrate the utility of the primary pancreatic cancer xenograft model to predict results observed in human patients.

The reduction in the development of metastases following inhibition of paracrine Hh signaling in animal models of pancreatic cancer has been reported in several recent studies [80,122,125]. Unique to our study was the use of non-immortalized patient-derived adenocarcinoma cells implanted orthotopically in NOD/SCID animals. It has been our experience in developing primary xenografts from several patient samples, that there is a range of tumor invasiveness *in vivo*, amount of infiltrating mouse stroma, the level of tumor differentiation, and the expression of signaling factors, including Hh pathway ligands. By testing a range of patient tumors we hope to better understand what treatments might work for different individual tumor phenotypes.

In our study, we utilized an invasive pancreatic ductal adenocarcinoma xenograft that under control treatment conditions, led to significant invasion of the liver, spleen, mesenteric lymph nodes, and the peritoneum. Following treatment with HhAntag alone or in combination with gemcitabine, we were unable to detect metastases in the lymph nodes or in the peritoneum. We also observed a reduction in the number of animals with metastasis to the liver in HhAntag only treated and co-

treatment with gemcitabine, but this change was not statistically significant. While we classified metastatic spread as evidence of any metastases to distant organs, HhAntag and co-treatment with gemcitabine clearly had a significant impact in limiting the tumor burden to the liver and peritoneum. Experiments are on-going to track the level of metastases by using luciferase-tagged tumor cells and whole organ imaging. This will help to establish quantitative measurement of changes in tumor burden following treatment. Additionally, it will be important to assess if inhibition of paracrine Hh signaling is able to inhibit the growth of established metastases, as many patients present clinically with late-stage, metastatic disease.

The role of cancer stem cells is also a focused area of study for solid tumor malignancies, including pancreatic cancer. In our studies, we observed a reduction in $CD44^+/CD24^+/ESA^+$ expression in one of our two treated xenografts following HhAntag treatment alone and in combination with gemcitabine compared to control. Our *in vivo* results with HhAntag suggest that this drug does not affect the tumor cells directly, therefore any change in the tumorigenic cell population is likely to be due to the differential expression of factors from the mesenchyme that maintain the cancer stem cell niche. Studies are underway to perform limiting dilution analysis (LDA) from tumor cells following each treatment regimen. This is a more robust measurement of tumor initiating capacity [93] and will clarify whether Smo-inhibition in the stroma is effective in disrupting the maintenance of the cancer stem cell population.

Targeting paracrine Hh signaling in the pancreatic tumor mesenchyme may provide an important therapeutic target for pancreatic adenocarcinoma patients.

There are still many questions to be answered about how paracrine Hh signaling affects the biology of the tumor mesenchyme and what Hh responsive genes may be differentially regulated that lead to the changes in tumor biology observed in our studies. These studies add to our understanding of how Hh signaling may be working in the pancreatic tumor microenvironment and may open up new strategies for treatment regimens for pancreatic cancer.

ACKNOWLEDGMENTS

Author Contributions: Joseph S. Dosch performed all the *in vivo* work with HhAntag. Trichrome, PAS, and Ki67 staining was done by Jimmy Hogan in Marina Pasca di Magliano's lab at the University of Michigan. FACS analysis was done with assistance by the University of Michigan Flow Cytometry Core with special thanks to Dave Adams, Ann Marie Des Lauriers, Mike Pihalja and Danielle Fasseel. Thanks to Genentech for providing the HhAntag along with suggestions for its *in vivo* use from Dr. Fred de Sauvage.

FIGURES

Figure 2.1 Paracrine Hh Signaling in Human PDA Xenografts. (A) Quantitative RT–PCR profiling of *SHH* and *IHH* mRNA in a panel of samples from normal human pancreas and low-passage (≤ 2) human PDA xenografts (normal, n=6, PDA, n=13). Gene expression normalized to species-specific GAPDH levels. **(B)** Correlation between stromal-derived Gli1 and Ptch1 mRNA levels versus tumor-derived Hh ligand (*SHH* and *IHH*) levels in human PDA xenografts (n = 13) by species-specific qRT–PCR.

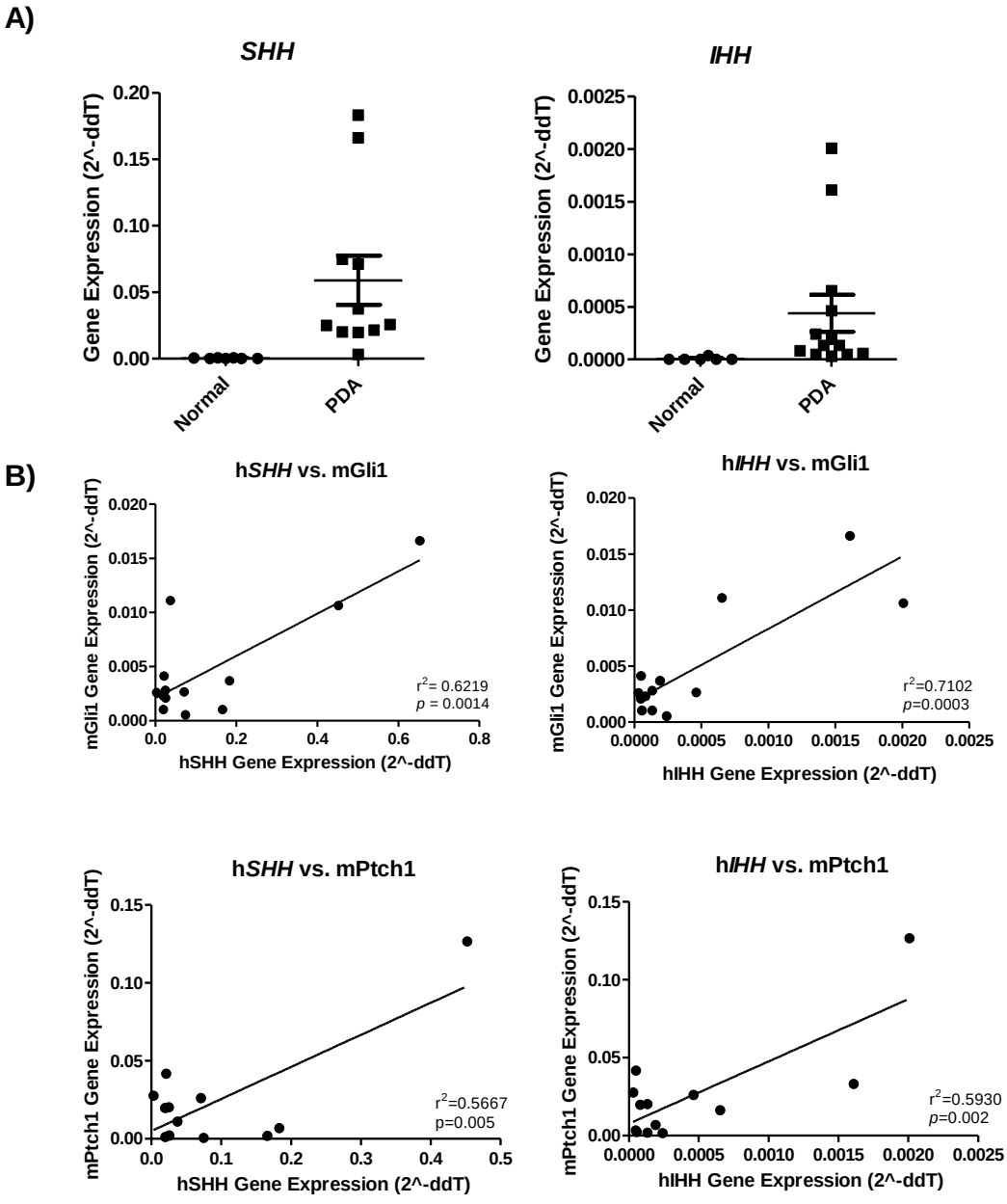

Figure 2.2 HhAntag Treatment Targets Hh Signaling in the Tumor Stroma. (A) Final tumor weights (g) of Tumor UM-PDA#1 and UM-PDA#2 following treatment (n = 6 in each group, * denotes *p*-value < 0.05. (**B**) IHC staining for Ki67 revealed a decrease in proliferation in HhAntag + Gemcitabine treated tumors for both patient tumors tested. (**C**) IHC staining for Caspase-3 revealed an increase in apoptosis in HhAntag+Gemcitabine treated tumors in UM-PDA#1 but not UM-PDA#2. **(D)** qRT-PCR analysis of each tumor following treatment using mouse/human specific Gli1 and Ptch1 primers. Gene expression was evaluated from two separate animals from each treatment group and run in triplicate. V= vehicle, G= gemcitabine, H= HhAntag, H+G= HhAntag + Gemcitabine treatment.

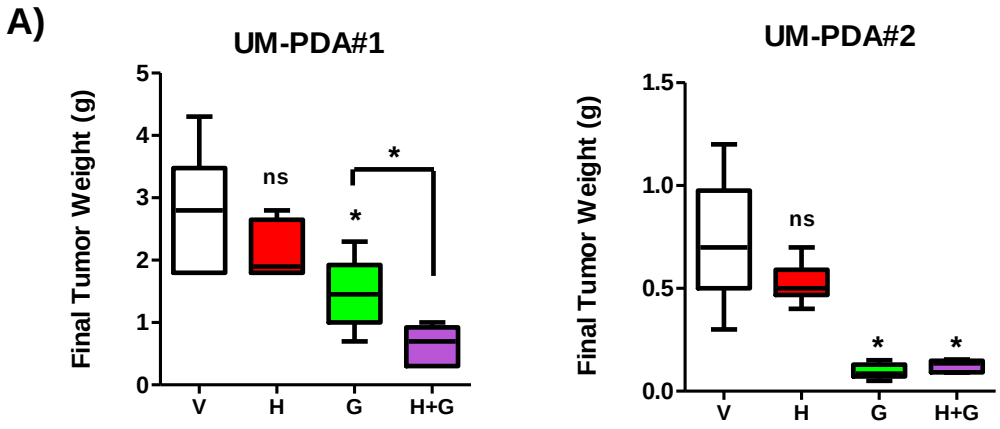

B)

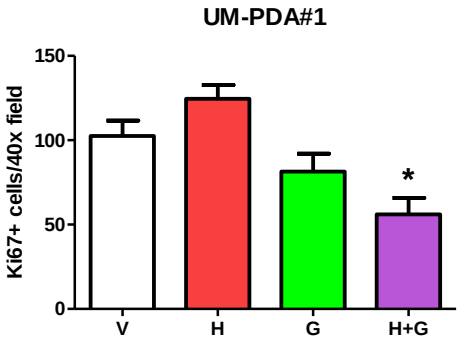
UM-PDA#1
Ki67+ cells/40x field
150
100
50
0
*
V
H
G
H+G

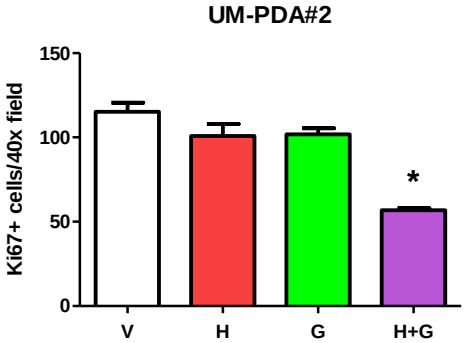
UM-PDA#2
Ki67+ cells/40x field
150
100
50
0
*
V
H
G
H+G

C)

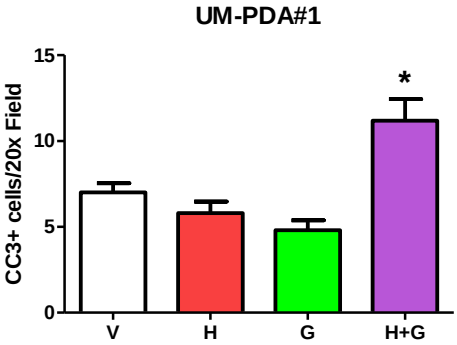
UM-PDA#1
CC3+ cells/20x Field
15
10
5
0
*
V
H
G
H+G

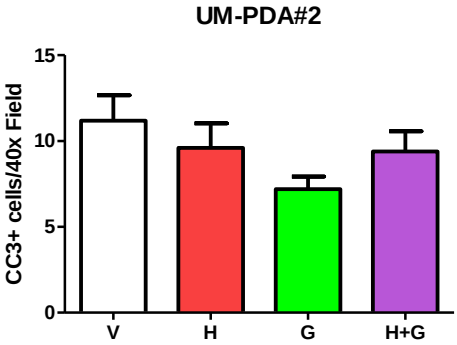
UM-PDA#2
CC3+ cells/40x Field
15
10
5
0
V
H
G
H+G

D)

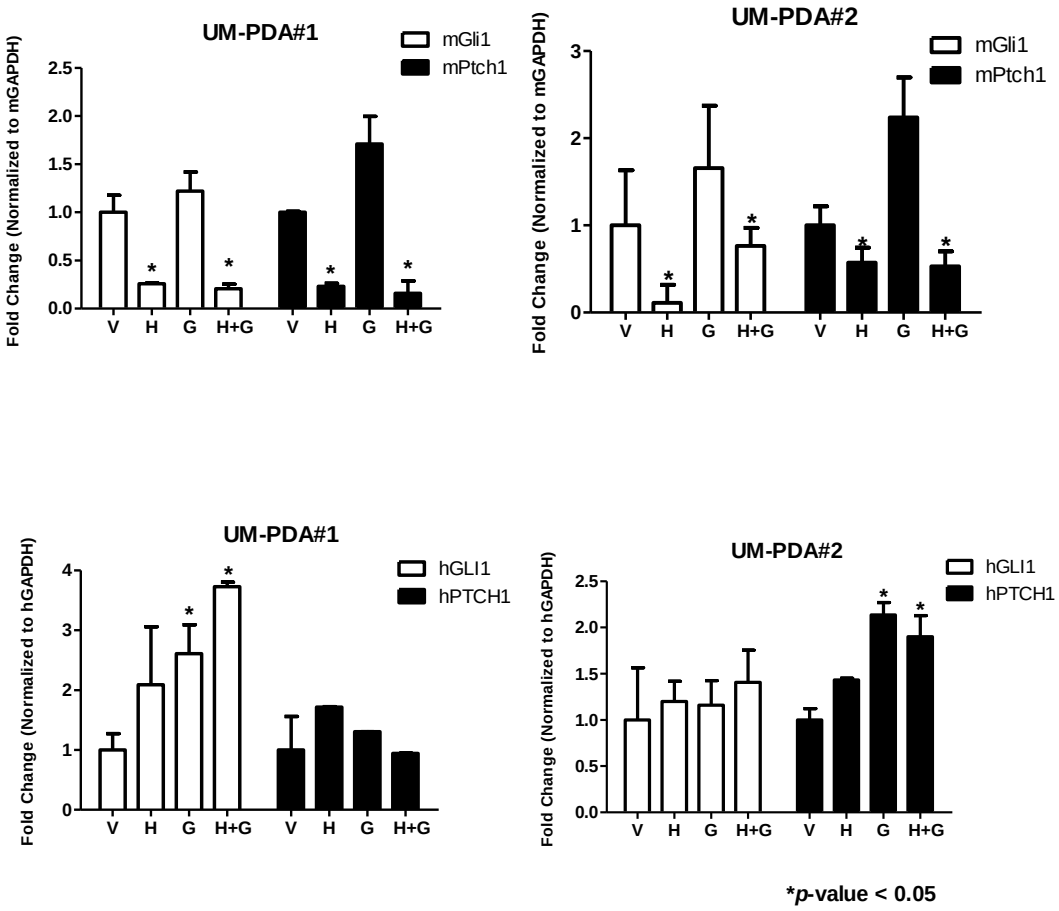
UM-PDA#1
mGli1
mPtch1
Fold Change (Normalized to mGAPDH)
2.5
2.0
1.5
1.0
0.5
0.0
V H G H+G V H G H+G
UM-PDA#2
mGli1
mPtch1
Fold Change (Normalized to mGAPDH)
3
2
1
0
V H G H+G V H G H+G
UM-PDA#1
hGLI1
hPTCH1
Fold Change (Normalized to hGAPDH)
4
3
2
1
0
V H G H+G V H G H+G
UM-PDA#2
hGLI1
hPTCH1
Fold Change (Normalized to hGAPDH)
2.5
2.0
1.5
1.0
0.5
0.0
V H G H+G V H G H+G
*p-value < 0.05

Figure 2.3 Evidence of Differentiation for Tumors UM-PDA#1 and #2 following HhAntag and Gemcitabine Treatment. (A, C) Trichrome stain of tumor UM-PDA#1 and UM-PDA#2 treatment groups. Note the cytoplasmic vesicles and intracytoplasmic lumens found in the groups treated with both HhAntag+Gemcitabine. (**B, D**) Periodic acid-Schiff (PAS) staining of tumor UM-PDA#1 and UM-PDA#2 treatment groups. Robust PAS staining for both tumor sets with HhAntag+gemcitabine treatment indicates increases in mucinous secretions.

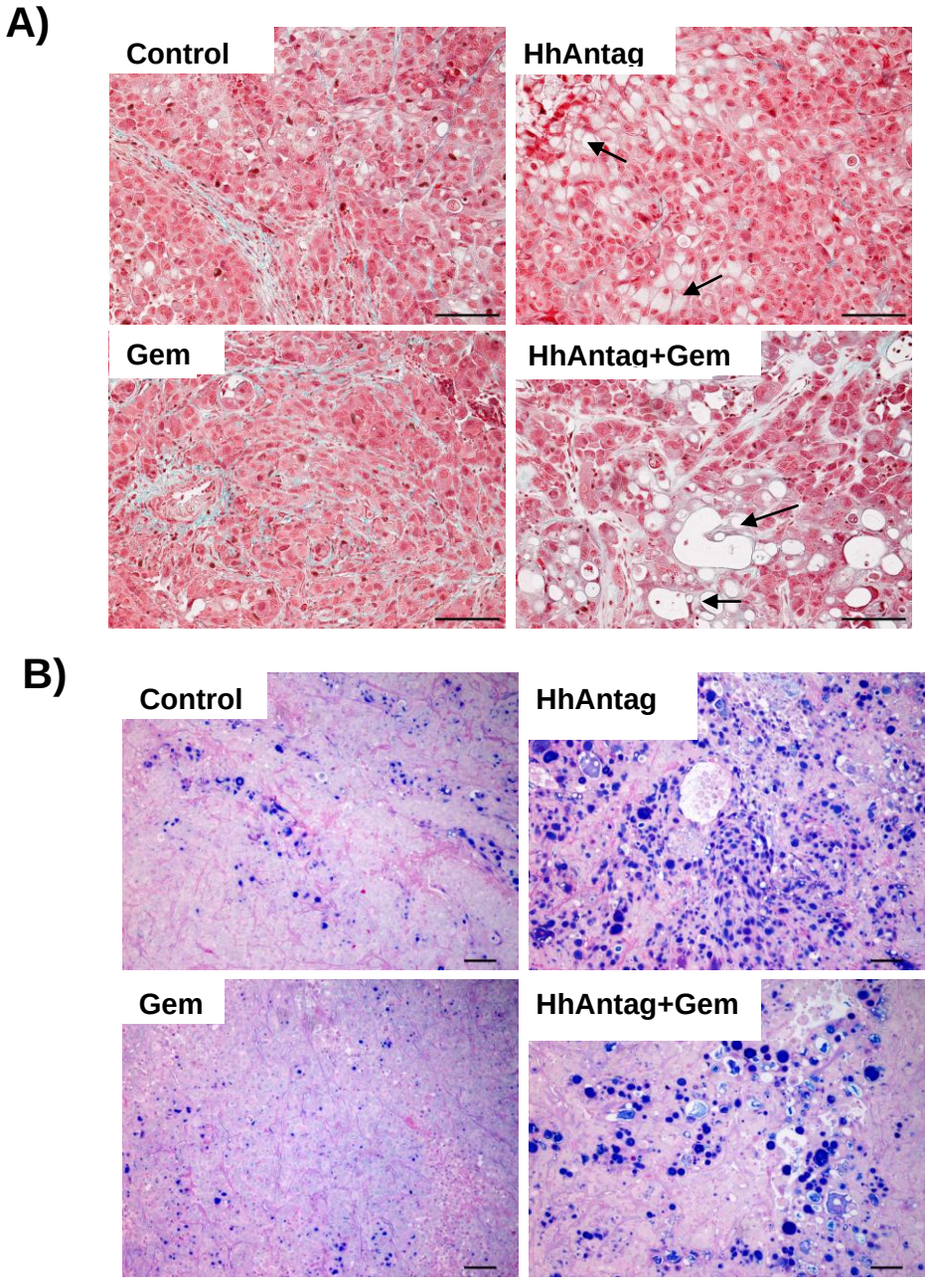

C)

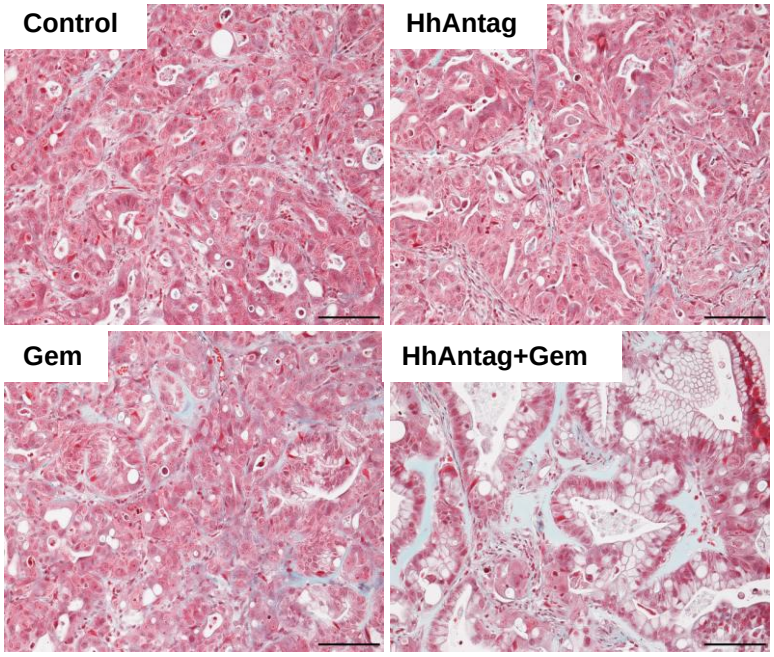
Control
HhAntag
Gem
HhAntag+Gem

D)

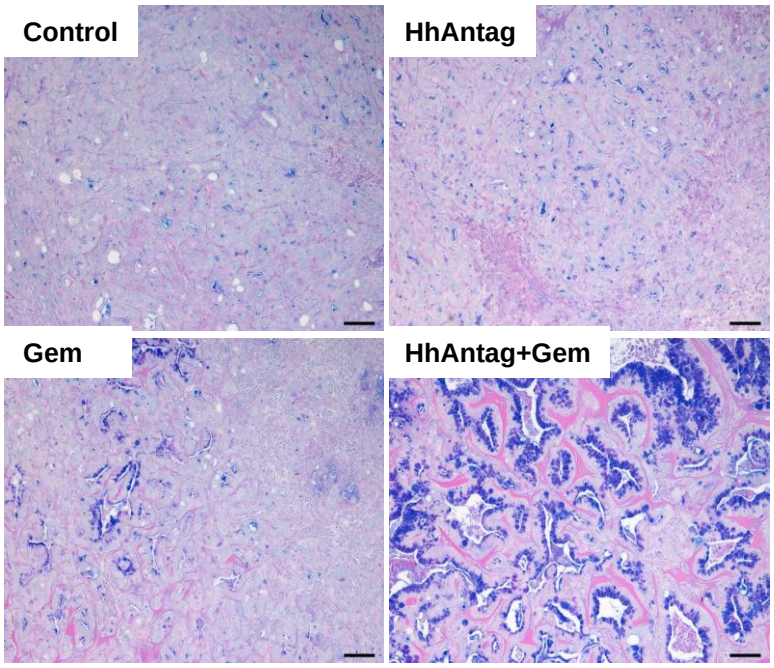
Control
HhAntag
Gem
HhAntag+Gem

Figure 2.4 HhAntag Treatment Decreases Incidence of Distant Metastases. (A) UM-PDA#1 orthotopic xenografts following 21 days of treatment. Black arrow denotes the primary tumor site. **(B)** H&E sections from metastatic lesions from the control treated xenografts (***i)*** Tumor implant in the muscle wall of the diaphragm, ***(ii)*** tumor implant superficial to the liver ***(iii)*** tumor lesion in the lymph nodes adjacent to the small intestine, ***(iv)*** tumor lesion in the spleen. **(C)** Graphical representation of the number of mice with metastasis to different organ sites. Statistical comparisons were made from each treatment group compared to controls (n = 7 each, *denotes p-value < 0.05). V= vehicle, G= gemcitabine, H= HhAntag, H+G= HhAntag + Gemcitabine treatment.

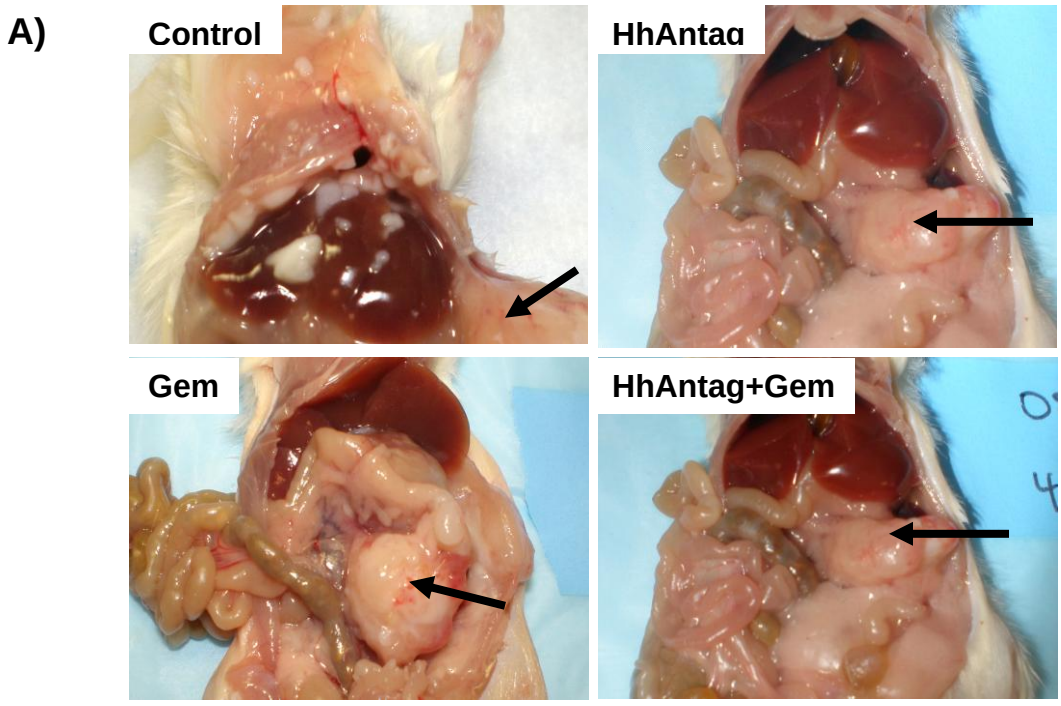

B)

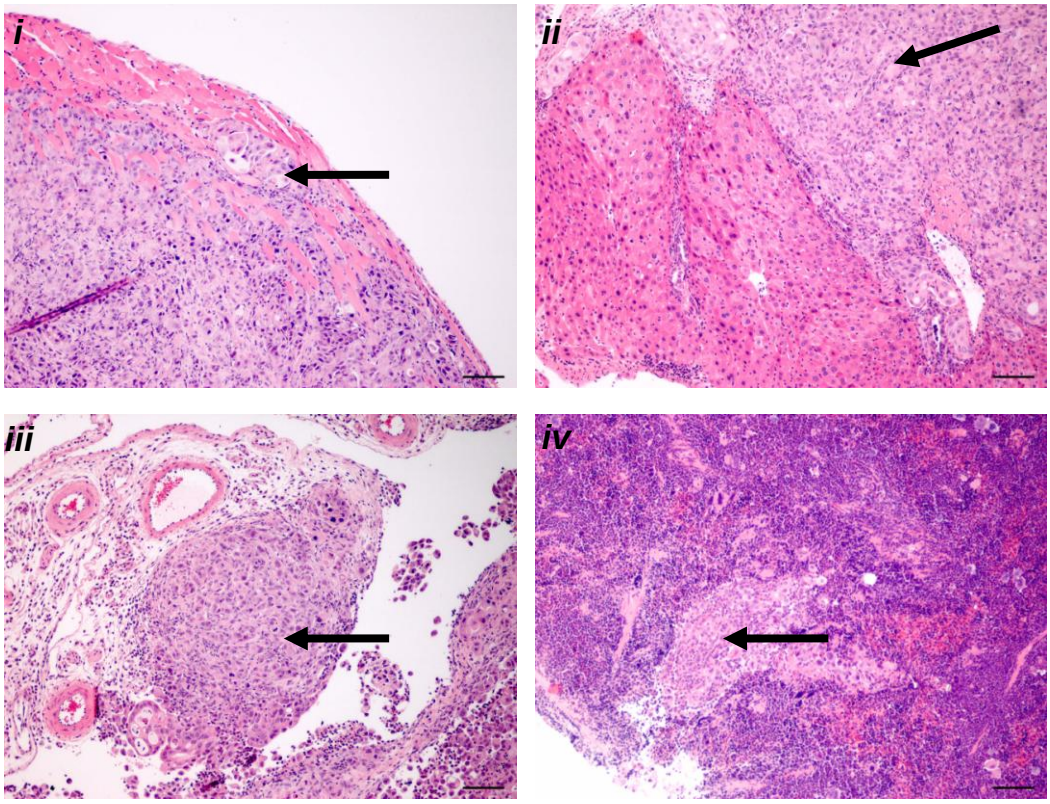
i
ii
iii
iv

C)

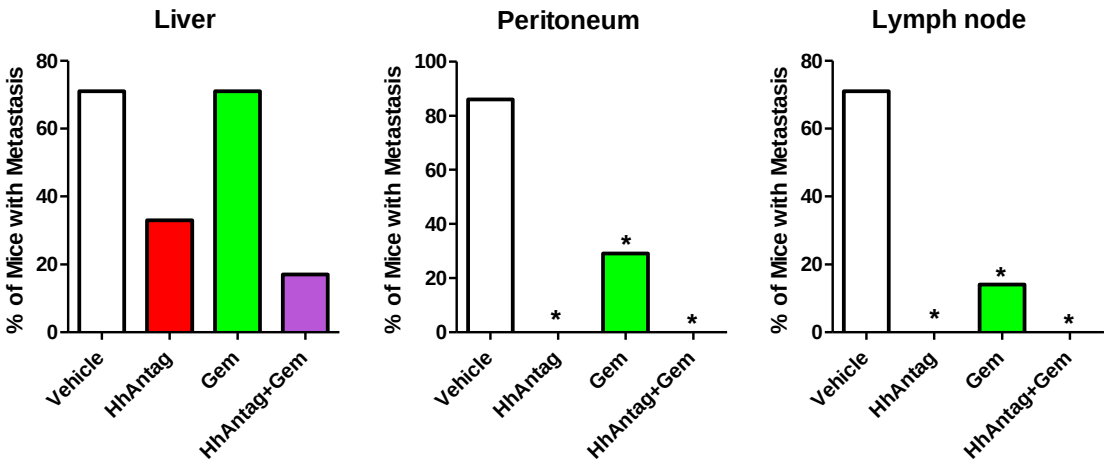
Liver
Peritoneum
Lymph node
% of Mice with Metastasis
Vehicle
HhAntag
Gem
HhAntag+Gem
n= 7 per group
* p-value < 0.05
Fisher's exact test

Figure 2.5 Analyses of $CD44^+/CD24^+/ESA^+$ Cells Following HhAntag Treatment. **(A, B)** FACS analysis of UM-PDA#1 and UM-PDA#2 xenografts following treatment. Analysis was performed in triplicate from three individually treated animals (*denotes *p*-value < 0.05). (**C**) Tumors derived from subcutaneous implantation of UM-PDA#2 cells from each treatment group. C=control, H=HhAntag only, G=Gemcitabine only, H+G=HhAntag + Gemcitabine combination (n = 3). (**D**) Graphical representation of re-implanted UM-PDA#2 tumors (*denotes *p*-value < 0.05).

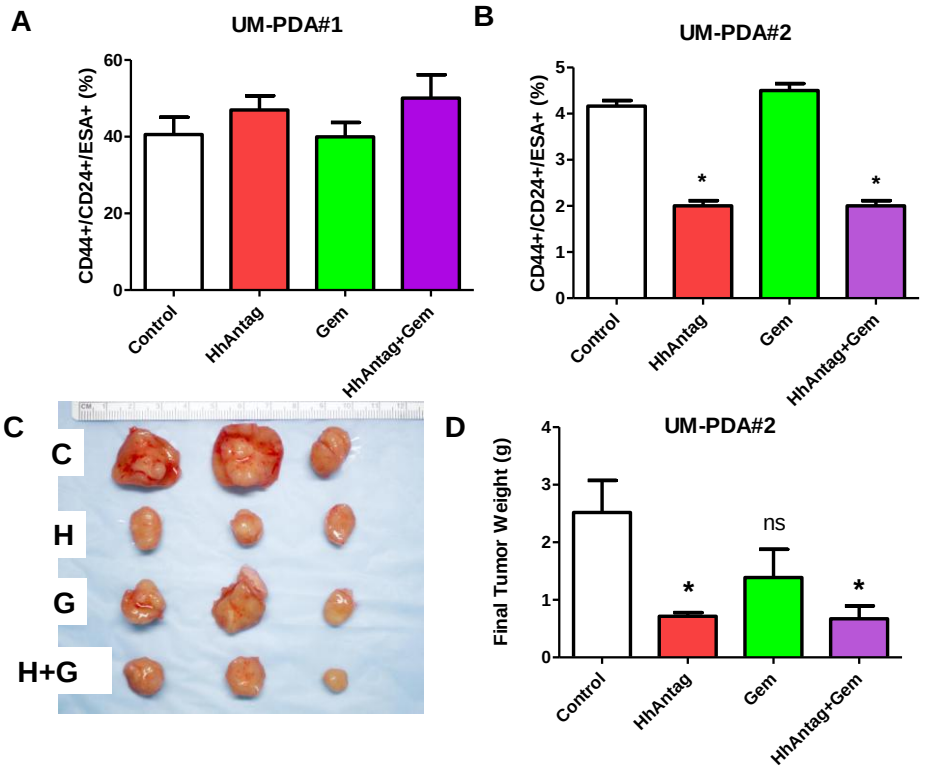

Figure 2.6 Histological Analysis of Patient PDA Biopsy Before and After treatment with GDC-0449. H&E sections of patient tumor biopsies prior and post treatment with GDC-0449. Arrows highlight the vacuolated structures observed in the tumor cells post treatment (20 x magnifications).

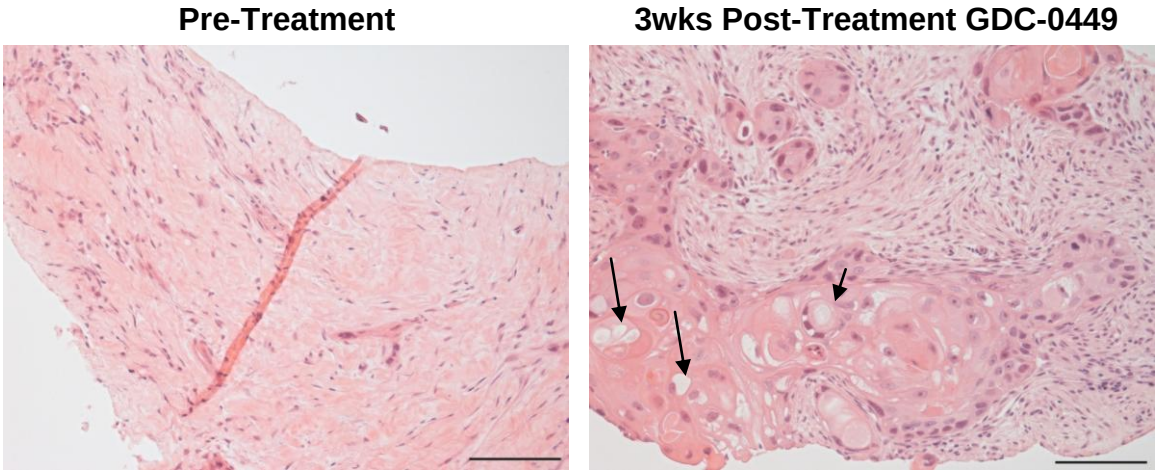

Table 2.1 Origin, stage, and pathology of human pancreatic ductal adenocarcinoma tumors included in this study.

Tumor	Origin	Patient data		Stage	Pathology	
		Sex (M/F)	Age (years)	TNM	Diagnosis	Invasive?
UM-PDA#1	Pancreatic Head, 5.0cm mass	M	74	T3 N1 M0: Stage IV	Adenocarcinoma	Liver and lymph node invasion
UM-PDA#2	n.a.	F	82	n.a.	Adenocarcinoma	n.a.
UM-PDA#3	Pancreatic Head, 2.6cm mass	M	64	T3 N1 M0: Stage IIB	Adenocarcinoma	invasion of duodenum, common bile duct, and peripancreatic soft tissue
UM-PDA#4	Pancreatic Tail 5.0cm mass	F	75	T3 N1 M0: Stage IIA	Adenocarcinoma	none
UM-PDA#5	Pancreatic Tail, 3.5cm mass	F	76	T3 N0 MX: Stage IV	Adenocarcinoma	Perineural invasion identified
UM-PDA#6	Distal Pancreas, 4.2cm mass	M	75	T3 N0 MX: Stage IIA	Adenocarcinoma	none
UM-PDA#7	Pancreatic Head, 2.5 cm mass	F	63	T3 N1 MX: Stage IIB	Adenocarcinoma	Lymph node and duodenal wall invasion detected
UM-PDA#8	Pancreatic Head, 1.8cm mass	M	81	T3 N1 MX: Stage IIB	Adenocarcinoma	Lymph node, Vascular and perineural invasion
UM-PDA#9	Pancreatic Head 2.0cm mass	M	64	T3 N1 M0: Stage IIB	Adenocarcinoma	Lymph node invasion
UM-PDA#10	Pancreatic Head 3.5cm mass	F	79	T3 N1 MX: Stage IIB	Adenocarcinoma	angiolymphatic and perineural invasion
UM-PDA#11	Pancreatic Head 3.0 cm mass	M	79	T3 N1 MX: Stage IIB	Adenocarcinoma	none
UM-PDA#12	n.a	n.a	n.a	n.a	Adenocarcinoma	n.a
UM-PDA#13	n.a	n.a	n.a	n.a	Adenocarcinoma	n.a

n.a., not available; M, male; F, female.

Table 2.2 Quantitative expression (qRT-PCR) of Hh pathway genes and cancer stem cell profiles of human PDA xenografts used in this study.

	hSHH	mGli1	mPtch1	
	$2^{-\Delta Ct}$	$2^{-\Delta Ct}$	$2^{-\Delta Ct}$	CSC%
UM-PDA#1	0.026	0.0021	0.0021	39%
UM-PDA#2	0.020	0.0023	0.0197	2.2%
UM-PDA#3	0.0032	0.0026	0.0276	1.97%
UM-PDA#4	0.1833	0.0040	0.0068	0.14%
UM-PDA#5	0.1662	0.00104	0.0018	0.1%
UM-PDA#6	0.6532	0.0166	0.0331	0.2%
UM-PDA#7	0.0374	0.0111	0.0111	0.1%
UM-PDA#8	0.0747	0.00054	0.00054	42%
UM-PDA#9	0.020	0.0010	0.00104	40%
UM-PDA#10	0.0214	0.0041	0.0417	3.04%
UM-PDA#11	0.4525	0.0106	0.1267	0.79%
UM-PDA#12	0.025	0.0028	0.0202	n.t
UM-PDA#13	0.071	0.0027	0.0261	n.t

n.t., not tested, CSC% (Cancer Stem Cell): $CD24^+/CD44^+/EpCam^+$ cells, hSHH (human Sonic Hedgehog), mGli1 (mouse Gli1), mPtch1 (mouse Patched1)

CHAPTER 3

PARACRINE HEDGEHOG SIGNALING ACTIVATES CELL MOTILITY PROGRAMS IN PANCREATIC STELLATE CELLS

SUMMARY

The Hedgehog (Hh) signaling pathway plays an important role in the development and function of the pancreas. Several studies have demonstrated aberrant Hh signaling in the progression of pancreatic cancer. Active Hh signaling in pancreatic cancer occurs through a paracrine mechanism in which pancreatic tumor cells secrete Hh ligands that activate the pathway in the surrounding stromal cells. The biological role of Hh signaling in the tumor stroma is unclear. To identify the Hh responsive genes which may be activated in the pancreatic tumor mesenchyme, we performed transcriptional profiling on a primary, immortalized mouse pancreatic stellate cell line stimulated with recombinant Sonic hedgehog (Shh) ligand. We identified 206 genes that were differentially regulated by Shh in these cells. Bioinformatic analysis of the Shh-responsive gene data set revealed a strong correlation with genes that increased the motility of mesenchymal cells in extracellular matrix. This was confirmed by 2D and 3D invasion assays that demonstrated that paracrine Hh signaling increases the invasion of pancreatic stellate cells in type I collagen. These results confirm that paracrine Hh signaling enhances the invasiveness of pancreatic stellate cells and down-regulation of this pathway may provide an important therapeutic target for treating pancreatic cancer patients.

INTRODUCTION

The aberrant activation of Hedgehog (Hh) signaling has been characterized in pancreatic cancer in several studies [30,31]. Active Hh signaling in pancreatic cancer occurs through a paracrine mechanism in which tumor cells secrete Hh ligands, Sonic and Indian hedgehog (Shh and Ihh, respectively) which activate Hh pathway target genes in the tumor mesenchyme [32,33]. It is still unclear what biological effect paracrine Hh signaling imparts on the tumor mesenchyme. However, ectopic expression of Shh by normal pancreatic epithelial cells has been shown to stimulate a desmoplastic reaction in the pancreas [81]. This expansion of stromal cells and extensive production of extracellular matrix components is a feature that defines pancreatic cancer, and appears to play a major role in the resistance of tumor cells to chemotherapeutic treatments and in mediating the invasiveness of pancreatic tumor cells [79,127].

The pancreatic tumor stroma is comprised of several different components including stellate cells, endothelial cells, nerve cells, and immune cells such as macrophages, lymphocytes, dendritic cells, along with the extracellular matrix. Pancreatic stellate cells (PSCs) have become the main focus of studies involving pancreatic tumor-stromal interactions due to their critical role in the desmoplastic response [76]. In the normal pancreas, these cells envelop the acinar structures of the exocrine pancreas and remain quiescent with vacuoles that contain large vitamin-A deposits. However, these cells can become activated by growth factors and cytokines (PDGF, IL-1, TNF-α, TGF-β, activin A) or in response to pancreatic injury or disease [128]. Activated PSCs lose the vitamin-A droplets, proliferate rapidly, and transition

to a myofibroblast-like phenotype with increased secretion of extracellular matrix components, including type I collagen, laminin, and fibronectin [129].

Several studies have demonstrated that canonical Hh signaling in pancreatic adenocarcinoma is confined to the stromal compartment [32,33]. Additionally, stromal cells which are negative for platelet endothelial cell adhesion molecule (PECAM-1 or CD31), which include pancreatic stellate cells, are responsive to inhibitors of the Hh pathway, while $CD31^{+}$ vascular cells do not show reduced levels of Hh pathway target genes in pancreatic cancer xenografts treated with an Hh pathway inhibitor (unpublished observations). This suggests that pancreatic stellate cells are the main target of Hh ligands in the pancreatic tumor microenvironment.

Paracrine Hh signaling in pancreatic cancer creates a positive feedback loop in which Hh-regulated factors are differentially expressed to promote the growth and progression of the pancreatic tumor cells. These factors are likely to include mitotic and angiogenesis-related factors, extracellular matrix remodeling enzymes, and anti-apoptotic proteins. Only a small number of factors induced by paracrine Hh signaling in the tumor stroma have been characterized. Bone marrow derived mesenchymal cells which home to the pancreatic tumor microenvironment in an Hh-regulated mechanism expresses Angiopoietin-1 (Ang-1) and Insulin-like growth factor-1 (IGF-1), which supports the neovascularization of the tumor [86]. We set out to identify the Hh responsive gene signature in pancreatic stellate cells and identify how these target genes may impact pancreatic tumor biology.

MATERIALS AND METHODS

Isolation and Cell Culture of Primary Pancreatic Fibroblasts

Primary pancreatic fibroblasts were obtained by treating either CD-1 (Charles River; Wilmington, MA) mice or Immortomouse® animals (Charles River) with caerulein, 50μg/kg every hour for 6 hours three times a week, to induce chronic pancreatitis. Following treatment, the fibrotic pancreata were excised and minced with a sterile razor blade in Media 199. The tissue fragments were digested with 200U/ml of Collagenase IV (Worthington; Lakewood, NJ) for 30 min to 1 hr. Tissue digests were washed several times with serum media and filtered through a 40 μm nylon mesh (BD Biosciences). Wild-type cells were cultured in DMEM 10% FBS media at 37°C/5% CO_2. Immortomouse-derived cells were cultured in 33°C/5% CO_2 with the addition of 10 U of mouse interferon gamma (R&D Systems; Minneapolis, MN).

Cell Culture for Array and Gene Validation

Prior to stimulation with Shh, primary and immortalized fibroblasts were incubated in DMEM low-serum (0.5% FBS) overnight. Cells were treated 24 hrs with a range of recombinant mouse Shh (R&D systems) at 100-1000ng/ml reconstituted in sterile PBS. For experiments using 5E1, a Shh blocking antibody (Iowa Hybridoma Bank), was added to the cultures at 1.0μg/ml at the same time as recombinant Shh. Total RNA from control and treated cells was prepared for Illumina array analysis by using the Illumina® TotalPrep™ RNA Amplification Kit (Ambion; Foster City, CA) according to manufacturer's instructions. Samples were checked for purity and

normalized for the Illumina MouseRef-8 v2.0 BeadChip by the University of Michigan Sequencing Core.

Gene Expression Analysis of Target Genes

Following treatment, cells were trypsinized and pelleted using serum containing media. Cells lysis was performed with buffer RLT (Qiagen) containing 2-mercaptoethanol (Sigma-Aldrich). Cell lysates were collected and homogenized with QiaShredder spin columns (Qiagen). For RNA extraction from tumor samples, the tissue was homogenized with a rotor-stator homogenizer (Polytron). Total RNA was extracted using the RNeasy Mini kit (Qiagen) according to the standard protocol provided by the manufacturer with on-column DNAase digestion.

Total RNA quality and quantity was analyzed using a NanoDrop spectrophotometer (Thermo Scientific). One microgram of Total RNA was used to transcribe cDNA using the SuperScript® First-Strand Synthesis System (Invitrogen). From this cDNA reaction, 2 µl of RT reaction was used for qPCR using POWER SYBR Mix (Applied Biosystems) and the reaction was carried out on a DNA Engine Opticon Real-Time Cycler (MJ Research). Primers used for qPCR are as follows: mouse *Gli-1* forward: GGA AGT CCT ATT CAC GCC TTG A, reverse: CAA CCT TCT TGC TCA CAC ATG TAA G; mouse *Ptch-1* forward: TTG TGG AAG CCA CAG AAA ACC, reverse**:** TGT CTG GAG TCC GGA TGG A; mouse *GAPDH* forward: AGC CTC GTC CCG TAG ACA AAA T, reverse: CCG TGA GTG GAG TCA TAC TGG A; mouse *TGFß2* forward: TCG ACA TGG ATC AGT TTA TGC G, reverse: CCC

TGG TAC TGT TGT AGA TGG A; mouse *JAM2* forward: GTG CCC ACT TCT GTT ATG ACT G, reverse: TTC CCT AGC AAA CTT GTG CCA; mouse *SFRP2* forward: CGT GGG CTC TTC CTC TTC G, reverse: ATG TTC TGG TAC TCG ATG CCG; mouse *FGF9* forward: ATG GCT CCC TTA GGT GAA GTT, reverse: TCA TTT AGC AAC ACC GGA CTG; mouse *ANGPT4* forward: AGC AGC AAC TGA CGG AGT TT, reverse: CTC TGC ACA GTC CTG GAA CA; mouse *Tiam1* forward: CCT CAC TGG GAA AGT GGA AA, reverse: TCT TCT GCT TGG AAC CGT CT; mouse *MMP13* forward: AGT TGA CAG GCT CCG AGA AA, reverse: GGC ACT CCA CAT CTT GGT TT; mouse *IL-6*, forward TAG TCC TTC CTA CCC CAA TTT CC, reverse: TTG GTC CTT AGC CAC TCC TTC; mouse *VEGFA* forward: GCA CAT AGA GAG AAT GAG CTT CC, reverse: CTC CGC TCT GAA CAA GGC T; mouse *GDF10* forward: CAG GAC ATG GTC GCT ATC CAC, reverse: ACA GGC TTT TGG TCG ATC ATT TC; mouse *Wnt-2* forward: CTC GGT GGA ATC TGG CTC TG, reverse: CAC ATT GTC ACA CAT CAC CCT.

Microarray Data Analysis

Transcriptional profiling was performed on Illumina MouseRef-8 v2.0 BeadChips (San Diego, CA) according to the manufacturer directions. All microarray data were analyzed in the statistical software R (v 2.10.1) with associated packages from the Bioconductor Suite for molecular biology. The "lumi" package was used for quality control and normalization of the chips, including background adjustment, variance stabilization and quantile normalization. Following normalization, empirical Bayes estimation of moderated t- and F-statistics was

computed to test for differential expression. Because of the relatively small number of samples, an unadjusted *p*-value of less than 0.05 was used to determine statistical significance.

Differentially regulated genes were further analyzed using Ingenuity Pathway Analysis (IPA; Ingenuity Systems, Mountain View, CA; http://www.ingenuity.com). IPA is a Java based program used to interpret the differentially expressed genes in terms of an interaction network and identify predominant canonical pathways. Canonical pathways analysis identified the pathways from the Ingenuity Pathways Analysis library of canonical pathways that were most significant to the data set. Molecules from the data set that met the statistically significant cutoff of an adjusted *p*-value <0.05 and were associated with a canonical pathway in Ingenuity's Knowledge Base were considered for the analysis.

Collagen Invasion Assays

To analyze cell invasion, 20,000 pancreatic stellate cells were embedded in 20 μl of type I collagen gel (2.0 mg/ml, BD Biosciences). After gelling, the plug was embedded in a cell-free, 300 μl collagen gel (2.0 mg/ml) cultured within a 24-well plate. After allowing the surrounding collagen to gel (1 h at 37°C), invasion was stimulated with DMEM 10% FBS or DMEM 10% FBS media conditioned for 24 hrs from L3.6pl cells, a human pancreatic cancer cell line . HhAntag was reconstituted in DMSO and replaced in the culture every 2 days. 3D invasion was evaluated after 5 days in culture. Invasion distance from the inner collagen plug into the outer collagen gel was quantified. This distance was calculated as the tip of the leading front of

stellate cells in 5 high power fields. Imaging was obtained using a Nikon Instruments Eclipse Ti-U Microscope and processed using Nikon NIS-Elements software.

RESULTS

Primary culture of Mouse Pancreatic Stellate Cells (MPSCs)

Pancreatic stellate cells are specialized pancreatic support cells that have been identified as a major source of the desmoplasia in chronic pancreatitis and in pancreatic cancer [76,130]. To determine the biological role of paracrine Hh signaling in the pancreatic mesenchyme, we developed cultures of primary mouse pancreatic stellate cells (MPSCs) from both normal CD-1 mice (designated wild-type) and from Immortomice, the latter in order to establish a primary, immortal cell line. Cells isolated from an Immortomouse express a temperature-sensitive mutant of the simian virus-40 large T-antigen (tsTAg) and allows for conditional immortalization of primary cells [131]. These cells were isolated by culturing fibrotic pancreatic tissue fragments from animals treated chronically with caerulein, a cholecystokinin (CCK) analog which induces pancreatitis and activation of pancreatic stellate cells [78,132].

The outgrowths from these tissue fragments yielded spindle-like cells that are characteristic of pancreatic stellate cells. Immunohistochemical staining of both MPSC lines confirmed the expression of stellate cell markers: α-smooth muscle actin (α-SMA) and vimentin (**Figure 3.1 A**). Flow cytometric analysis (FACS) was used to ensure that the stellate cell lines were free of cells expressing vascular, hematopoietic, or epithelial markers. MPSCs were less than 0.5% positive for both CD31 and CD45 and negative for expression of the ductal epithelial marker CD133

[133] (**Figure 3.1 B**). Studies of MPSC cultures treated with recombinant mouse Sonic hedgehog ligand showed that downstream Hh pathway target genes Gli1, Gli2, Ptch1, and Ptch2 were up-regulated in a dose-dependent manner following Shh stimulation, as evaluated by qRT-PCR analysis (**Figure 3.1 C**).

Transcriptional Profiling of Shh-Regulated Genes in MPSCs

To identify Shh-responsive genes in pancreatic stellate cell lines, we performed microarray analysis using RNA isolated from both wild-type and Immortomouse-derived pancreatic MPSCs cultured for 24 hrs in the presence or absence of recombinant Sonic hedgehog (Shh). Isolated mRNA from 4 independent cultures of both wild-type and immortomouse-derived cells were biotin-labeled and hybridized to Illumina MouseRef-8 v2.0 BeadChips. In both the wild-type pancreatic MPSC line and those derived from the Immortomouse, hierarchical clustering dendrograms showed a distinct pattern of gene expression in cells treated with recombinant Shh ligand compared with control cells (**Figure 3.2 A**).

To investigate the level of overlap between the statistically significant genes that were changed between wild-type and Immortomouse cells treated with recombinant Shh we used the R statistical software to compute an adjusted *p*-value of ($p < 0.05$), used as a cut-off for detecting significant difference in expression levels. In general, a narrow range of fold difference between the up/down Shh-regulated genes were observed compared to control. We found that for the wild-type MPSC data set this range was 2.48 to -1.69 fold change and for the Immortomouse MPSC data set the range was 2.40 to -1.98 fold change. We chose to investigate genes with

≥ 1.2 fold-changes with an adjusted *p*-value of < 0.05 for further analysis. We identified 340 genes differentially expressed in the wild-type MPSC Shh treated cells and 206 genes differentially expressed in the Immortomouse, Shh treated cells with an overlap of 51 genes between the two lines (**Figure 3.2 B**).

Bioinformatics Analysis of Hh Target Genes in MPSCs

To simplify our analysis of Hedgehog pathway target genes in subsequent experiments, we utilized the data set from the Immortomouse-derived MPSCs treated with Shh. We selected this set because the Immortomouse-derived MPSCs can be manipulated easily *in vitro* for co-culture with tumor cells or knockdown studies used for functional validation of target genes, and these cells are easily transfectable using standard techniques. Additionally, it was our experience that the wild-type (normal) pancreatic stellate cell line would senesce *in vitro* after 5 passages. Therefore, using the immortomouse-derived pancreatic stellate cells gave us the greatest flexibility in testing the role of Hh signaling in this cell type. In the immortomouse Shh-regulated gene set, 125 genes were found to be up-regulated and 81 genes were found to be down-regulated (**Figure 3.3 A**, **Table 3.1**).

Next, we compared our data set against two existing transcriptional profiles of Shh-treated mesenchyme in the intestine and prostate [82,83]. We performed this analysis to learn what genes and pathways are consistent with Hh activation in mesenchymal cells and what Hh-regulated genes may be specific to the pancreatic tumor microenvironment. Meta-analysis of all three data sets was performed by using Ingenuity Pathway Analysis (IPA), a bioinformatics program designed to

identify differentially expressed genes in terms of an interaction network and identify predominant canonical pathways. Among the top functional pathways consistent with all three Shh-responsive gene data sets were: cellular growth and proliferation, cell movement, cell cycle, cell death and immune cell tracking (**Figure 3.3 B**). Individual genes that overlapped between the pancreatic and intestinal data set include insulin-like growth factor-1 (IGF-1), growth differentiation factor 10 (GDF10), homeobox protein Nkx2-3 and leukemia inhibitory factor (LIF). Genes in overlap between our pancreatic data set and the prostate data set were identified as angiopoientin-4 (ANG-4), T-cell lymphoma invasion and metastasis 1 (TIAM1), hairy and enhancer of split 1 (HES1), and Peptidyl-prolyl cis-trans isomerase (FKBP1A). Two genes, 11β-hydroxysteroid dehydrogenase type 1 **(**HSD11B1) and Sodium-and chloride-dependent taurine transporter **(**SLC6A6) were differentially regulated in all three data sets. Additionally, we identified some factors that had not been shown to be Hh-related genes and were found only in the pancreatic stellate cell data set. These genes included Wnt2, TGFβ2, R-spondin1, and Fgf9. Our results suggest that there may be some overlap in the Hh-regulated genes in organ-specific mesenchyme, but there are subsets of Hh responsive genes that are specific to each stromal environment.

Shh-regulated Expression of Hedgehog Pathway Target Genes in MPSCs

Analysis of Shh-regulated target genes in MPSCs revealed altered regulation of genes related to secretory functions, cell movement, and angiogenesis pathways. These results are consistent with the hypothesis that paracrine Hh signaling in these

cells supports tumor growth by altering the microenvironment. To further validate these pathways, we assessed mRNA expression of representative genes identified in the microarray data set. We selected nine mRNAs that were up-regulated and three that were down-regulated for further analysis. The nine up-regulated genes we selected for validation were: Fgf9, Gdf10, Angpt4, Wnt2, Tgfβ2, Tiam1, IL6, VegfA, and Gli1. The three down-regulated genes we selected for analysis were: Sfrp2, Jam2, and Mmp13. In addition, as there is some speculation that commercially available recombinant Shh products may be contaminated with endotoxins that can affect expression of chemokines [134], we also assessed the specificity of the Shh-induced gene response by culturing MPSCs in 500 ng/ml of recombinant Shh with or without addition of 1.0 μg/ml of the Shh blocking antibody, 5E1 [135]. Of the twelve genes evaluated by qRT-PCR, ten out of the twelve genes exhibited significant Shh regulated expression consistent with our microarray data (**Figure 3.4**).

To determine if the genes identified in our Shh regulated gene profile were specific to pancreatic mesenchymal cells or general to Shh regulated gene expression in other mesenchymal cell types we performed the same gene expression analysis in primary mouse embryonic fibroblasts (MEFs). We found that only five out of the twelve genes analyzed exhibited significant Shh regulated gene expression (**Figure 3.5**). This suggests that there is a subset of Hh pathway responsive genes, including Fgf9, Tgfβ2, VegfA, IL6 and Sfrp2, that may be pancreatic specific.

Hh Pathway Regulates Motility of MPSCs in 2D and 3D Extracellular Matrix Culture

We identified several Shh-responsive genes in MPSCs that have been implicated in cell motility. To test whether paracrine Hh signaling affects cell motility, we examined how MPSCs responded to Hh pathway stimulation or inhibition in 2-dimensional (2D) and 3-dimensional (3D) invasion assays. For 2D invasion, MPSCs were seeded in the upper-well of a Boyden chamber (8 μm pores) and overlaid with a thin-layer of Matrigel. Increasing amounts of recombinant Shh ligand was added to the lower well of the chamber and the number of invading cells that had transversed to the other side of the membrane were counted after 24 hrs. Increasing amounts of recombinant Shh added to the lower chamber resulted in corresponding increases in the amount of invading MPSCs through Matrigel (**Figure 3.6 A**).

To assess how inhibition of paracrine Hh signaling affects the ability of MPSCs to invade in 3D extra-cellular matrix, we imbedded MPSCs in type I collagen plugs surrounded by a field of cell-free type I collagen. Invasion was stimulated by either standard DMEM 10% serum media, conditional media from L3.6pl cells (a high Shh expressing pancreatic cancer cell line [33]), or conditioned media with increasing doses of HhAntag, a Smoothened inhibitor and Hh pathway antagonist. We observed a significant increase in the invasion of MPSCs following addition of the L3.6pl conditioned media compared to the standard media. Following addition of HhAntag to conditioned media, we observed a decrease in invasion in a dose-dependent manner (**Figure 3.6 B**).

DISCUSSION

The tumor mesenchyme has long been implicated in playing an important role in tumor angiogenesis, metastasis, and overall growth and proliferation of cancer cells. Work in our lab and others has demonstrated that Hh signaling is activated in the pancreatic tumor stroma via a paracrine mechanism in which tumor cells secrete Hh ligands and activate the downstream Hh target genes [33]. However, very little was known about what downstream genes and biological changes may be induced in the tumor mesenchyme by paracrine Hh signaling. These studies are the first documentation of an Hh responsive gene signature in pancreatic mesenchymal cells, and the role of Hh signaling in stimulating the motility of these cells in extracellular matrix.

The lack of definitive cell-surface markers and early senescence of primary cultures prevents the direct isolation and long-term culture of pancreatic stellate cells from the normal pancreas. By using a pancreatitis-induced method to activate pancreatic stellate cells from Immortomouse animals, we were able to derive a permanent cell line to manipulate for long-term *in vitro* and *in vivo* experiments. These cells express established markers of pancreatic stellate cells, which include α-smooth muscle actin and vimentin [129] and are responsive to Sonic hedgehog ligand.

The time point selected for microarray analysis of our pancreatic stellate cell lines stimulated with Hh ligand was based on previously published studies characterizing the kinetics of Ptch1 and Gli1 induction in Shh-treated prostate and intestinal mesenchymal cells [82,83,136]. Our preliminary experiments suggested

that 24 hrs after Shh stimulation was an optimal time point to measure a strong transcriptional response of both primary and secondary Hh-responsive genes. Quantitative expression analysis of Hh target genes, Gli1 and Patched1 (Ptch1), which are indicative of active Hh signaling [43] were significantly up-regulated in MPSCs following stimulation with Sonic hedgehog.

Several previous studies have used microarrays to investigate the target genes of Shh signaling in mesenchymal cell types. Shh-stimulation of C3H/10T1/2 cells, an immortalized mouse embryonic fibroblast cell line, identified 11 induced genes (including IGF2) and 4 repressed genes (including Sfrp-1 and Sfrp-2) [137]. Recent studies with Shh-stimulation of organ specific mesenchymal cells from the prostate and intestine have also been profiled by microarray analysis [82,83]. In comparison to these studies, we identified several genes in our data set that were previously identified as potential Hh target genes in mesenchymal cells. These include Gdf10, Nkx2-3, Ang-4, Tiam1, Hes1, Sfrp-2, IGF1 and IGF2. Several of these genes have demonstrated important functions in pancreatic cancer and other malignancies. IGF-1 and Ang-2 have been shown to be up-regulated by Sonic hedgehog in bone marrow derived mesenchymal cells and these factors are involved in promoting the neovascularization of growing pancreatic tumors [86]. Additionally, aberrant regulation of Tiam1 in breast cancer associated fibroblasts has been shown to increase the invasiveness of breast cancer cells [138].

Our studies also identified several genes that had not been previously identified as Hh targets. These potential target genes included Wnt2, TGFβ2, R-spondin1, and Fgf9. The activation of pancreatic stellate cells from their normal

quiescent state to a highly proliferative state is mediated in part by TGFß signaling [139]. It is possible that paracrine Hh signals from the tumor help to perpetuate this phenotype in pancreatic stellate cells as we observed several TGFß signaling genes that were up-regulated with Shh-stimulation in pancreatic stellate cells. While there has not been a role established for Wnt signaling in pancreatic mesenchyme, the Wnt pathway is up-regulated in pancreatic cancer and micro-dissection studies of tumor stroma from patients with pancreatic adenocarcinoma has identified the up-regulation of Wnt5a and down-regulation of Sfrp-1 [140,141]. Recent studies have suggested a role for Wnt to enhance proliferation in the epithelium and stroma of chemically induced bladder cancer in mice [142]. In this work, sonic hedgehog expression in basal cells of the bladder increases upon injury and elicits increased stromal expression of Wnt protein signals, including Wnt-2 expression, which in turn stimulates the proliferation of both urothelial and stromal cells. This type of feedback mechanism may also be at work in the pancreatic tumor microenvironment.

Inhibition of paracrine Hh signaling in mouse models of pancreatic cancer and in cell line xenograft studies have demonstrated a reduction in distant metastases without dramatic changes in primary tumor volume [80,122]. This suggests that a primary role of paracrine Hh signaling in pancreatic tumor stroma is to mediate the invasion and extravasation of tumor cells. Therefore, we used Ingenuity Pathways Analysis (IPA) to determine whether Hh-responsive genes in mesenchymal cells derived from organs with known paracrine Hh signaling mechanisms correlated with an invasive gene signature. IPA meta-analysis confirmed that paracrine Hh signaling in MPSCs, along with data sets in prostate and intestinal mesenchyme, induces the

expression of genes that correspond with cell motility, inflammation, and mitotic activity. Genes that were in overlap between the pancreatic and intestinal data set include insulin-like growth factor-1 (IGF1), growth differentiation factor 10 (GDF10), homeobox protein Nkx2-3 and leukemia inhibitory factor (LIF). Expression of Nkx2-3 in gut mesenchyme has been linked to the specification and proliferation of the intestinal epithelium [143]. In overlap with the prostate data set we identified angiopoientin-4 (ANG-4), T-cell lymphoma invasion and metastasis 1 (TIAM1), hairy and enhancer of split 1 (HES1), and Peptidyl-prolyl cis-trans isomerase (FKBP1A). Two genes, 11β-hydroxysteroid dehydrogenase type 1 **(**HSD11B1) and Sodium-and chloride-dependent taurine transporter **(**SLC6A6) were differentially regulated in all three data sets, although these genes have not been linked to tumor invasion.

In order for pancreatic tumor cells to invade into the surrounding tissues, the cells have to overcome several physical barriers. These barriers include degradation of the epithelial basement membrane, navigation of the interstitial matrix, along with neovascularization of the growing tumor and extravasation of tumor cells out of the vascular network [144]. Many of these processes are normally controlled by mesenchymal cells during the development of the organ and during tissue repair following injury [75]. When we directly examined 12 genes related to these functional pathways, 10 out of 12 showed specific regulation by Hh ligand which was reversed by treatment with 5E1 blocking peptide that inhibited downstream Hh pathway activation. Interestingly, three of the genes that we analyzed including Wnt2, Gdf10, and IL6 were identified as differentially regulated in a microarray study

of tumor stroma from animals with pancreatic adenocarcinoma xenografts treated with a Hh pathway inhibitor [33]. Independent validation of these genes by a reciprocal transcriptional profiling study, suggests that these genes are indeed Hh target genes in the pancreatic tumor mesenchyme.

While we identified genes that are induced by paracrine Hh signaling, there is little known about how activation of this pathway affects the biological function of pancreatic stellate cells or cancer cells. Recent studies using an organotypic model of tumor invasion has suggested that tumor cells rely on mesenchymal cells to carve tracks in the interstitial matrix in order to invade into the surrounding tissues [145]. We observed that MPSCs stimulated with sonic hedgehog increased their transmigration through Matrigel, a pseudo-model of epithelial basement membrane. To test how paracrine Hh signaling affects the ability of MPSCs to navigate the interstitial matrix we utilized a 3D invasion assay in type I collagen. Conditioned media from an Hh ligand-expressing pancreatic cancer cell line was able to increase the invasiveness of MPSCs in type I collagen, but this was inhibited in a dose response with Smo-inhibition. These results suggest that paracrine Hh signaling in MPSCs plays an important role in the motility of these cells through the extracellular matrix.

In summary, we have developed a primary mouse pancreatic stellate cell line for use in validating Hedgehog target genes *in vitro*, and have compiled the first data set describing the Hedgehog responsive genes in pancreatic stellate cells. These studies have provided insight into how paracrine Hh signaling in the tumor mesenchyme increases the 3D migration of these cells and in turn we hypothesize that

this may lead to increased invasion of pancreatic tumor cells. Future studies will be aimed at elucidating the functional role of these Hedgehog responsive genes and how they are involved in the pancreatic tumor microenvironment. This information may help us to learn how Hedgehog pathway inhibitors may be working in the pancreatic tumor and provide insight into how we may target this pathway to improve patient responses to treatment.

ACKNOWLEDGMENTS

Author Contributions: Joseph S. Dosch performed all the *in vitro* work with the MPSCs. Special thanks to Marina Pasca di Magliano and Sabita Rakshit lab for their assistance in inducing pancreatitis in both wild-type and Immortomouse animals. Erin Shellman processed the all of the raw microarray data, performed statistical analysis and uploaded files to IPA. The University of Michigan DNA sequencing core processed the Illumina array chips with special assistance from Susan Dagenai.

FIGURES

Figure 3.1 Generation of Mouse Pancreatic Stellate Cell Lines. (A) Representative bright-field and immunofluorescence staining of MPSCs for α-SMA and vimentin. MPSCs maintained their stellate-like or spindle shape through passaging (original magnification: ×20). **(B)** FACS analysis of MPSCs for CD31, CD45, and CD133. **(C)** Shh-stimulated dose response of downstream Hh pathway genes Gli1, Gli2 and Ptch1, and Ptch2 in MPSCs as evaluated by qRT-PCR.

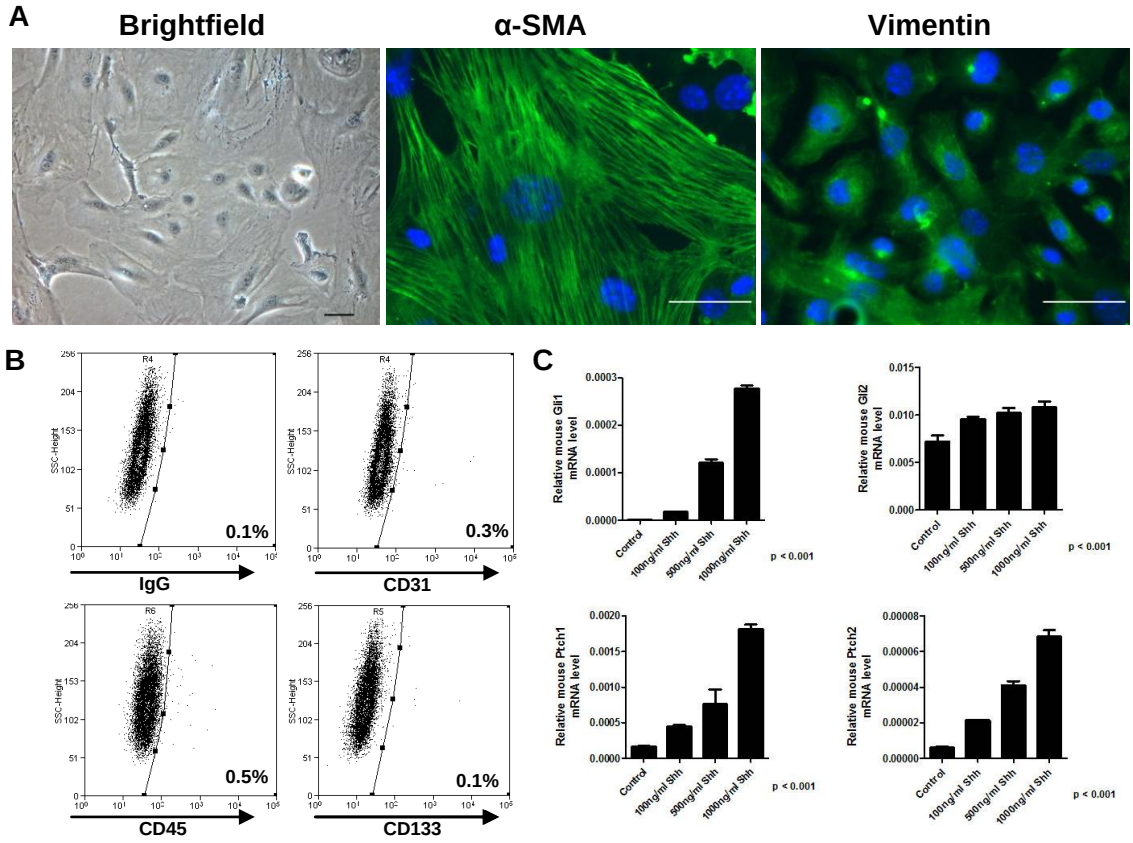

Figure 3.2 Transcriptional Profiling of Shh-Regulated Target Genes in Mouse Pancreatic Stellate Cells (MPSCs). (A) Hierarchical clustering of MPSC data sets from wild-type (WT) and immortomouse-derived (Imm) treated with recombinant Shh. The R software package was used to cluster and annotate the normalized array data. **(B)** Venn diagram and table of Shh-regulated genes in overlap between the wild-type (normal) and the immortomouse-derived MPSCs. While 51 genes were found in overlap, only 42 of these genes were differentially changing in the same positive or negative direction in both wild-type and immortomouse MPSC data sets.

A)

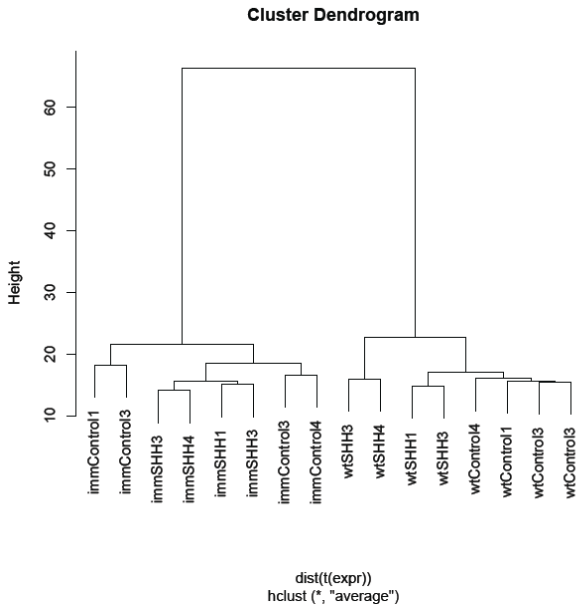

B)

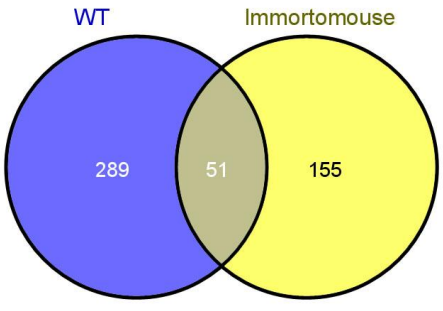

	wild-type	immorto
PPFIBP2	1.2	2.4
KRT18	1.26	2.2
LMCD1	1.56	2.15
WFDC1	1.47	1.95
FGF9	1.26	1.57
MID1IP1	1.29	1.55
GDF10	2.48	1.52
TGM2	1.4	1.5
BOK	1.87	1.5
ANGPT4	1.63	1.47
WNT2	1.32	1.46
CP	1.22	1.46
CYP2S1	1.66	1.45
ZFYVE21	1.32	1.43
CTSA	1.37	1.42
HSD11B1	1.62	1.41
DIO3	1.91	1.4
SLC6A6	1.21	1.39
PLTP	1.33	1.36
E130203B14RIK	1.33	1.35
TIAM1	1.6	1.35
ZFP521	1.29	1.32
RAP2A	1.21	1.31

	wild-type	immorto
GADD45G	1.25	1.29
HES1	1.28	1.29
OLFML3	1.49	1.29
DUSP1	1.37	1.29
IRF1	1.25	1.26
AW548124	1.58	1.25
IGFBP4	1.7	1.23
2310046K01RIK	1.65	1.21
LOC100046608	1.23	1.21
MMP13	-1.23	-1.21
AVPR1A	-1.23	-1.25
CXCL12	-1.26	-1.25
9030611O19RIK	-1.23	-1.27
MMP11	-1.3	-1.29
PTGS1	-1.22	-1.34
FLRT2	-1.23	-1.35
D0H4S114	-1.33	-1.38
GUCY1A3	-1.27	-1.43
PDLIM3	-1.33	-1.58

Figure 3.3 Pathway Analysis of Shh-regulated Target Genes in MPSCs.
(A) Heat-map of the top 50 up and down regulated Shh-regulated target genes in immortomouse-derived MPSCs. (**B**) Ingenuity Pathways Analysis (IPA) of conserved functional pathways associated with Shh-regulated target genes in MPSCs along with prostate and intestinal mesenchymal cells.

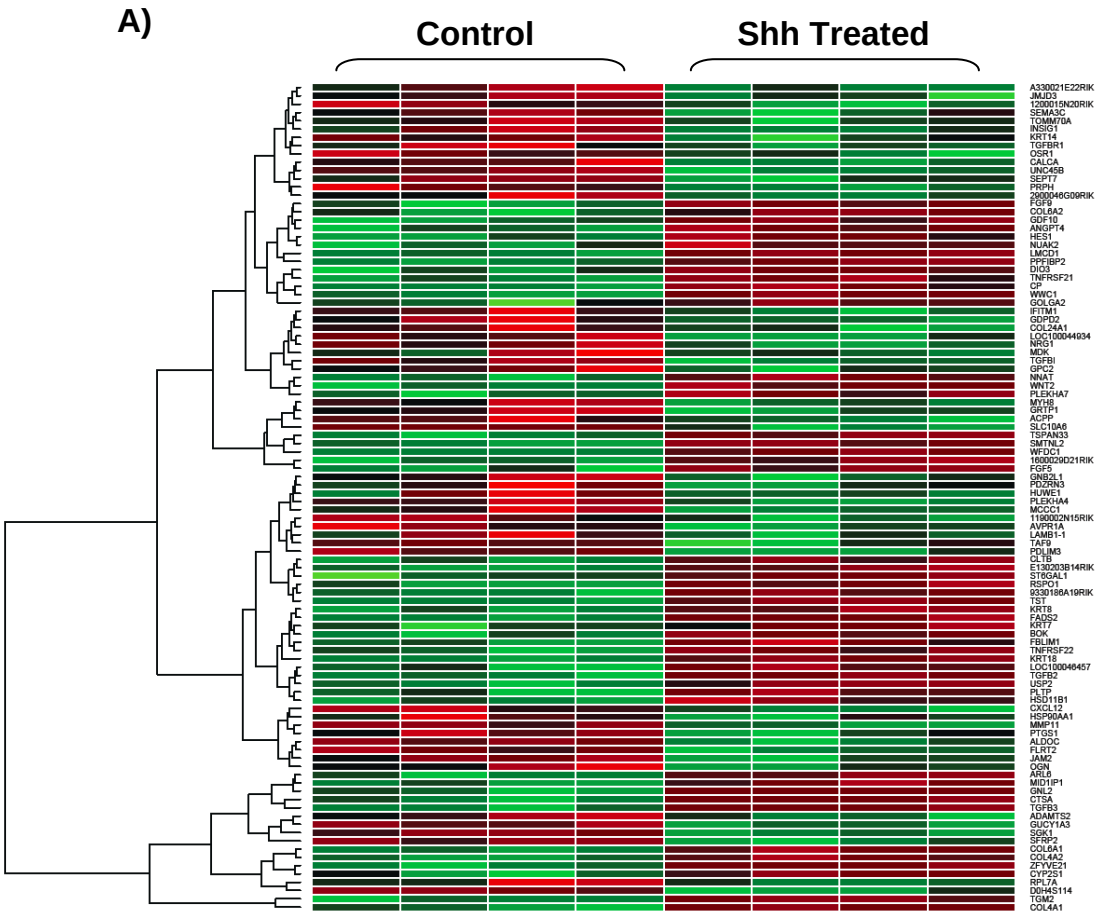

B)

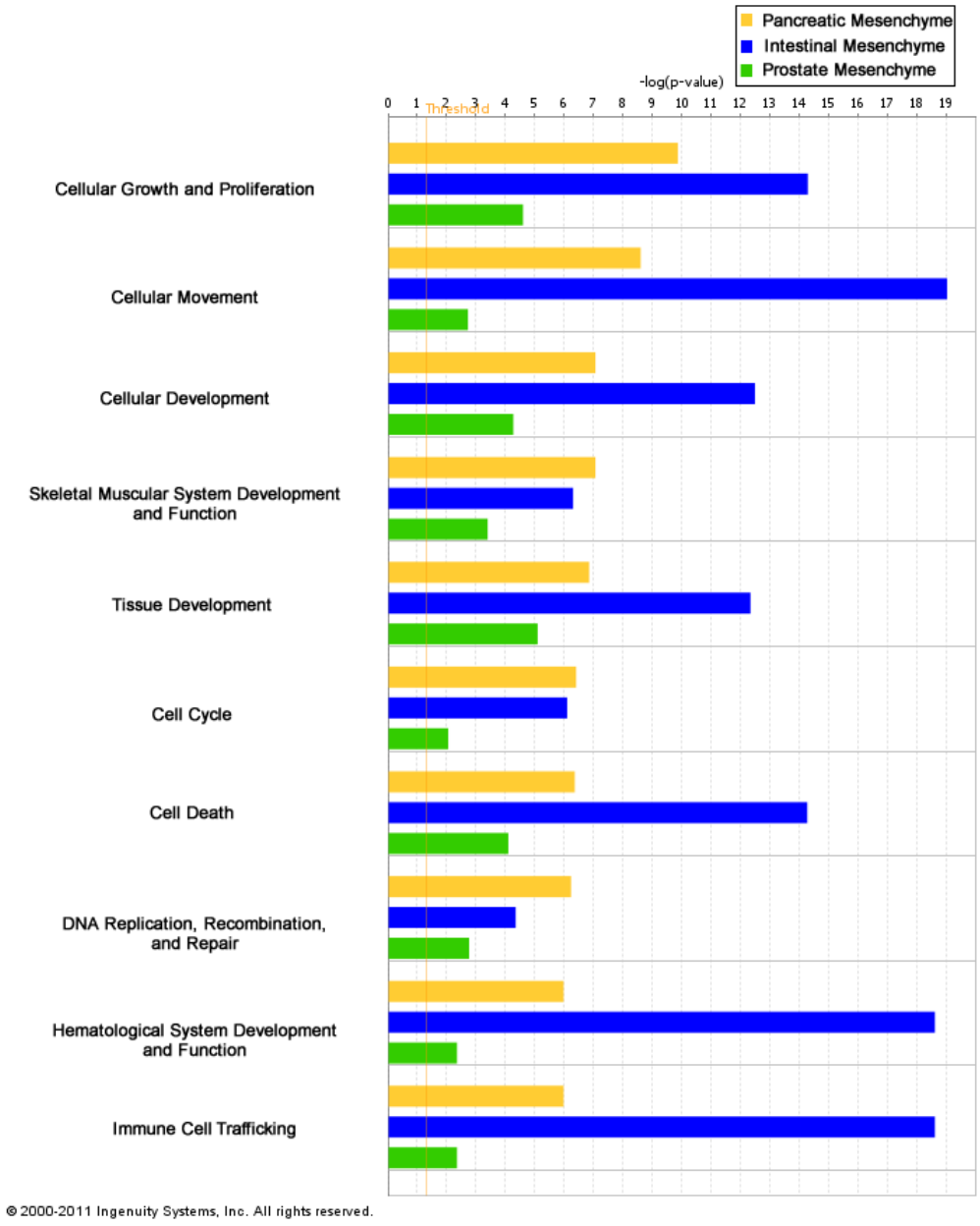
Pancreatic Mesenchyme
Intestinal Mesenchyme
Prostate Mesenchyme
-log(p-value)
0 1 2 3 4 5 6 7 8 9 10 11 12 13 14 15 16 17 18 19
Threshold
Cellular Growth and Proliferation
Cellular Movement
Cellular Development
Skeletal Muscular System Development and Function
Tissue Development
Cell Cycle
Cell Death
DNA Replication, Recombination, and Repair
Hematological System Development and Function
Immune Cell Trafficking
© 2000-2011 Ingenuity Systems, Inc. All rights reserved.

Figure 3.4 Shh-regulated Expression of Hedgehog Target Genes in MPSCs. Specific target genes related to mitotic or invasive activity were selected for further analysis. Gene expression was analyzed by qRT-PCR from MPSCs treated with either Shh alone or in combination with the Shh blocking antibody, 5E1 for 24hrs (n = 3; **, $p < 0.01$; *, $p < 0.05$).

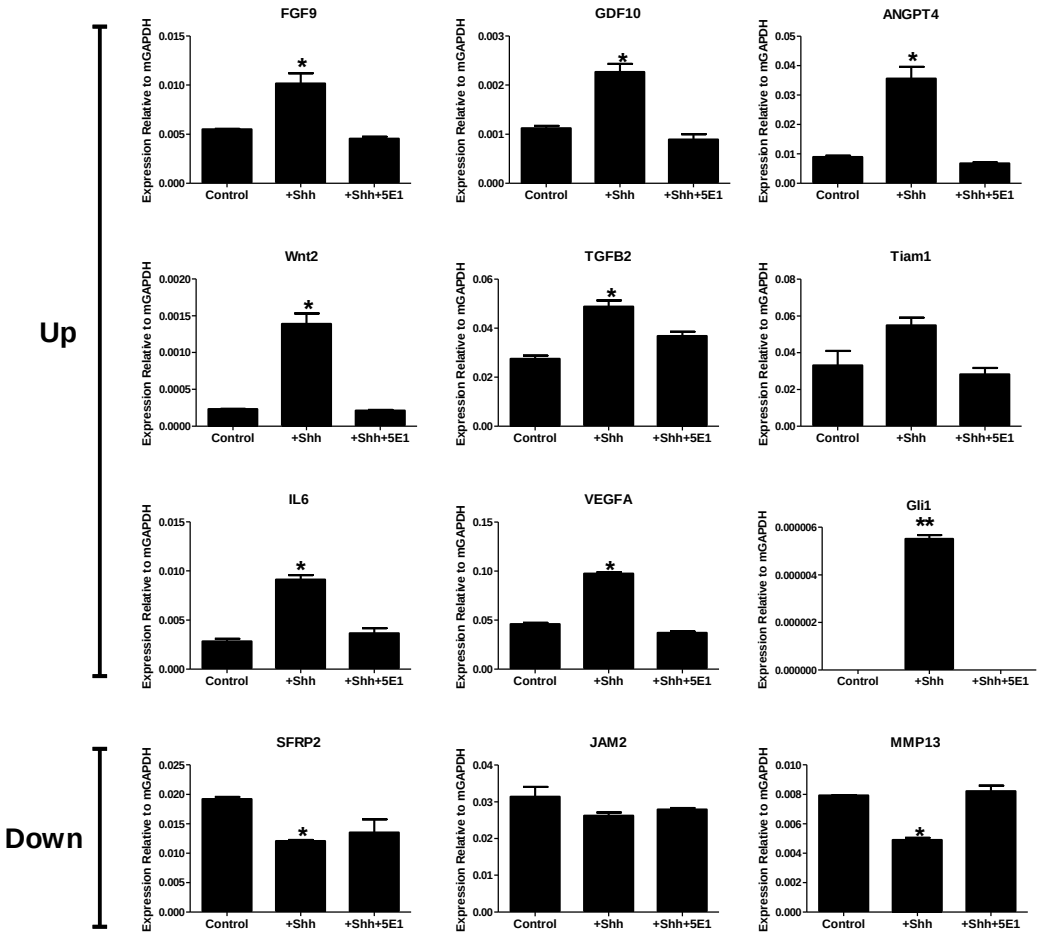

Figure 3.5 Shh-regulated Expression of Hedgehog Target Genes in Mouse Embryonic Fibroblasts (MEFs). Specific target genes related to mitotic or invasive activity were selected for further analysis. Gene expression was analyzed by qRT-PCR from MPSCs treated with either Shh alone or in combination with the Shh blocking antibody, 5E1 for 24hrs (n = 3; **, $p < 0.01$; *, $p < 0.05$).

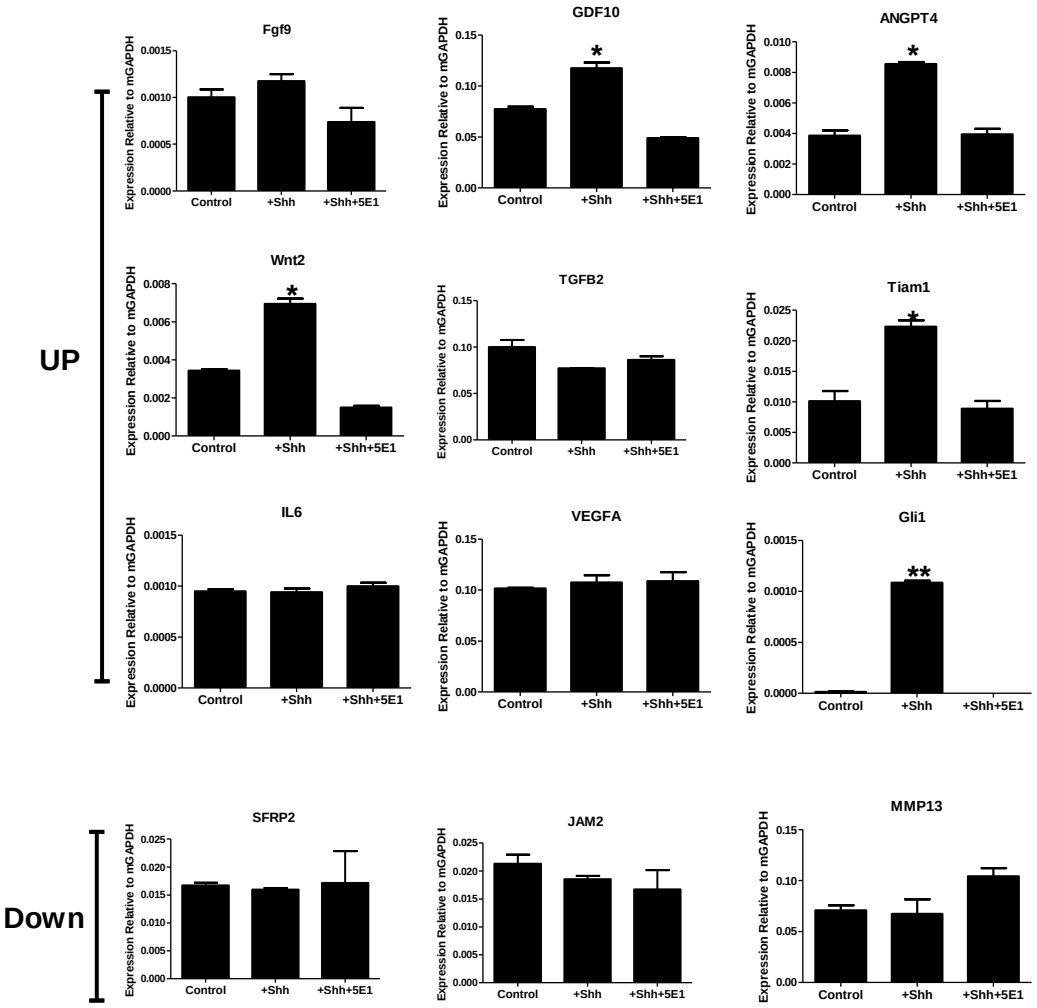

Figure 3.6 Paracrine Hh Signaling Regulates 2D and 3D invasion of MPSCs in Extracellular Matrix. (A) 2D Matrigel transmigration assay. MPSCs seed in the upper well of a Boyden chamber (8um pores) and increasing amounts of recombinant Shh added to the lower chamber. Number of invading cells counted in 5 random high-power fields ($n = 3$; **, $p < 0.01$; *, $p < 0.05$). **(B)** 3D collagen invasion assay. MPSCs seeded in a droplet of type I collagen (2mg/ml) surrounded by a field of cell free collagen. Invasion induced with standard media, conditioned media (CM) from L3.6pl cells, or CM with increasing doses of HhAntag ($n = 3$; *, $p < 0.05$, # < 0.05 (compared to conditioned media stimulated cells)

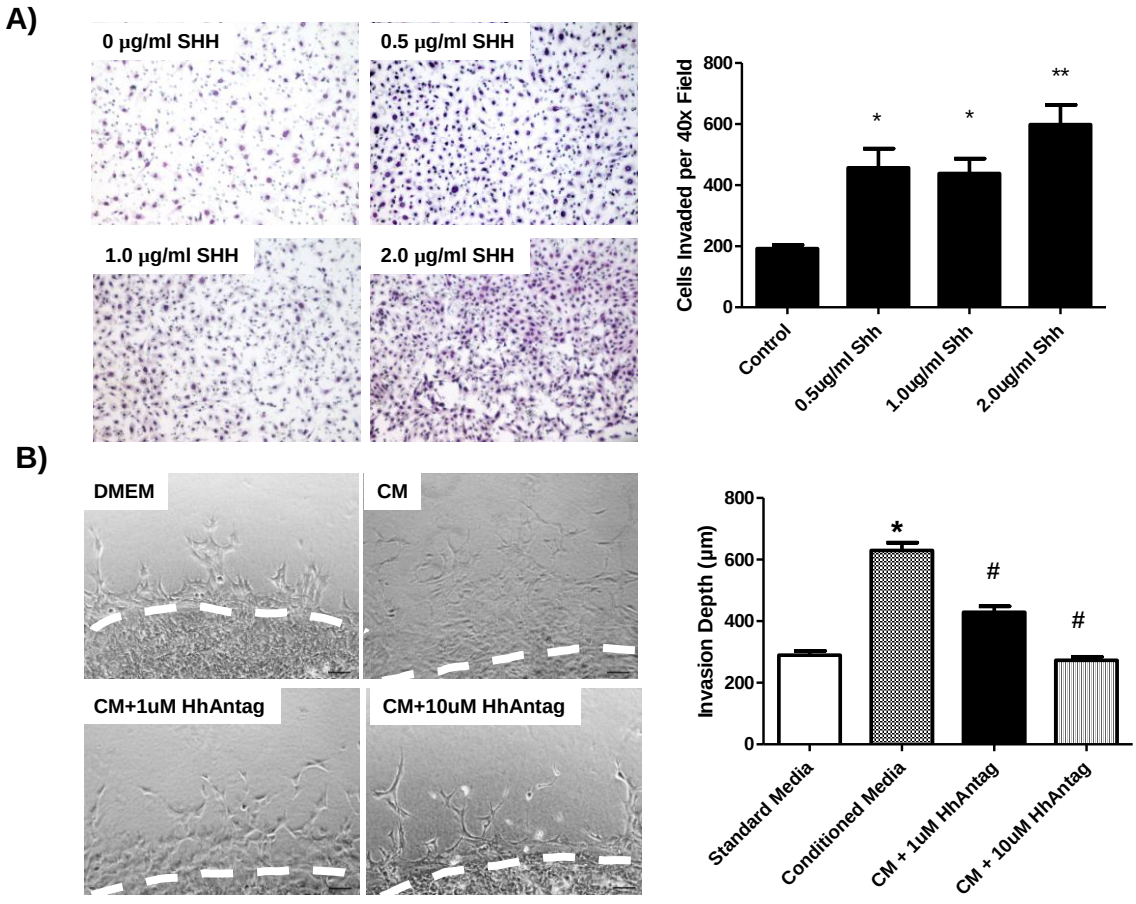

Table 3.1 Genes Differentially Regulated by Shh-treatment in Immortomouse derived MPSCs. Table generated for genes with a statistical *p*-value < 0.05 and a fold change ± 1.2.

Gene Symbol	Description	Fold Change
KRT18	Mus musculus keratin 18 (Krt18), mRNA.	2.206558
LMCD1	Mus musculus LIM and cysteine-rich domains 1 (Lmcd1), mRNA.	2.054663
PPFIBP2	Mus musculus protein tyrosine phosphatase, receptor-type, F interacting protein, binding protein 2 (Ppfibp2), mRNA.	2.045533
GOLGA2	Mus musculus golgi autoantigen, golgin subfamily a, 2 (Golga2), transcript variant 1, mRNA.	2.042706
WFDC1	Mus musculus WAP four-disulfide core domain 1, mRNA	1.959638
TGFB3	Mus musculus transforming growth factor, beta 3 (Tgfb3), mRNA.	1.851058
COL4A1	Mus musculus procollagen, type IV, alpha 1 (Col4a1), mRNA.	1.83121
TST	Mus musculus thiosulfate sulfurtransferase, mitochondrial (Tst), nuclear gene encoding mitochondrial protein, mRNA.	1.588525
KRT8	Mus musculus keratin 8 (Krt8), mRNA.	1.579524
FGF9	Mus musculus fibroblast growth factor 9	1.573808
MID1IP1	Mus musculus Mid1 interacting protein 1 (gastrulation specific G12-like (zebrafish)) (Mid1ip1), mRNA.	1.551006
FADS2	Mus musculus fatty acid desaturase 2, mRNA	1.531375
GDF10	Mus musculus growth differentiation factor 10 (Gdf10), mRNA.	1.517269
SMTNL2	Mus musculus smoothelin-like 2 (Smtnl2), mRNA.	1.512132
COL4A2	Mus musculus collagen, type IV, alpha 2 (Col4a2), mRNA.	1.508298
TGM2	Mus musculus transglutaminase 2, C polypeptide (Tgm2), mRNA.	1.503153
GAS6	Mus musculus growth arrest specific 6 (Gas6), mRNA.	1.482343
BOK	Mus musculus BCL2-related ovarian killer protein	1.47937
ANGPT4	Mus musculus angiopoietin 4 (Angpt4), mRNA.	1.472825
WNT2	Mus musculus wingless-related MMTV integration site 2	1.460694

Gene Symbol	Description			Fold Change
	(Wnt2), mRNA.			
CP	Mus musculus ceruloplasmin (Cp), transcript variant 2, mRNA.			1.457289
CYP2S1	Mus musculus cytochrome P450, family 2, subfamily s, polypeptide 1 (Cyp2s1), mRNA.			1.447383
COL6A1	Mus musculus procollagen, type VI, alpha 1 (Col6a1), mRNA.			1.440276
KRT7	Mus musculus keratin 7 (Krt7), mRNA.			1.428984
RSPO1	Mus musculus R-spondin homolog (Xenopus laevis) (Rspo1), mRNA.			1.427315
ZFYVE21	Mus musculus zinc finger, FYVE domain containing 21 (Zfyve21), mRNA.			1.426355
USP2	Mus musculus ubiquitin specific peptidase 2 (Usp2), transcript variant 2, mRNA.			1.426266
ARL6	Mus musculus ADP-ribosylation factor-like 6 (Arl6), mRNA.			1.426228
CTSA	Mus musculus cathepsin A (Ctsa), transcript variant 2, mRNA.			1.417241
HIST1H2AD	Mus musculus histone cluster 1, H2ad (Hist1h2ad), mRNA.			1.404944
HIST1H2AK	Mus musculus histone cluster 1, H2ak (Hist1h2ak), mRNA.			1.404306
DIO3	Mus musculus deiodinase, iodothyronine type III			1.401211
TNFRSF21	Mus musculus tumor necrosis factor receptor superfamily, member 21 (Tnfrsf21), mRNA.			1.400688
COL6A2	Mus musculus procollagen, type VI, alpha 2 (Col6a2), mRNA.			1.395217
TNFRSF22	Mus musculus tumor necrosis factor receptor superfamily, member 22 (Tnfrsf22), mRNA.			1.394095
BMPER	Mus musculus BMP-binding endothelial regulator (Bmper), mRNA.			1.392803
SLC6A6	Mus musculus solute carrier family 6 (neurotransmitter transporter, taurine), member 6 (Slc6a6), mRNA.			1.38631
HSD11B1	Mus musculus hydroxysteroid 11-beta dehydrogenase 1 (Hsd11b1), transcript variant 1, mRNA.			1.385022
TGFB2	Mus musculus transforming growth factor, beta 2 (Tgfb2), mRNA.			1.383533
GNL2	Mus musculus guanine nucleotide binding protein-like 2			1.370491

Gene Symbol	Description			Fold Change
	(nucleolar) (Gnl2), mRNA.			
PLTP	Mus musculus phospholipid transfer protein (Pltp), mRNA.			1.356291
FBLIM1	Mus musculus filamin binding LIM protein 1 (Fblim1), mRNA.			1.352369
TIAM1	Mus musculus T-cell lymphoma invasion and metastasis 1 (Tiam1), mRNA.			1.348358
NNAT	Mus musculus neuronatin (Nnat), transcript variant 1, mRNA.			1.344158
TSPAN33	Mus musculus tetraspanin 33 (Tspan33), mRNA.			1.338362
WWC1	Mus musculus WW, C2 and coiled-coil domain containing 1 (Wwc1), mRNA.			1.337408
PLEKHA7	Mus musculus pleckstrin homology domain containing, family A member 7 (Plekha7), mRNA.			1.331558
PMP22	Mus musculus peripheral myelin protein (Pmp22), mRNA.			1.32949
ZFP521	Mus musculus zinc finger protein 521 (Zfp521), transcript variant 2, mRNA.			1.328459
CDH3	Mus musculus cadherin 3 (Cdh3), transcript variant 1, mRNA.			1.324222
BLMH	Mus musculus bleomycin hydrolase (Blmh), mRNA.			1.321113
CLTB	Mus musculus clathrin, light polypeptide (Lcb) (Cltb), mRNA.			1.32065
RAP2A	Mus musculus RAS related protein 2a (Rap2a), mRNA.			1.314896
ST6GAL1	Mus musculus beta galactoside alpha 2,6 sialyltransferase 1 (St6gal1), mRNA.			1.312454
NKX2-3	Mus musculus NK2 transcription factor related, locus 3 (Drosophila)			1.306788
CYGB	Mus musculus cytoglobin (Cygb), mRNA.			1.300345
CCND1	Mus musculus cyclind1, mRNA			1.297539
NUAK2	Mus musculus NUAK family, SNF1-like kinase, 2 (Nuak2), mRNA.			1.296356
GADD45G	Mus musculus growth arrest and DNA-damage-inducible 45 gamma (Gadd45g), mRNA.			1.293528
HES1	Mus musculus hairy and enhancer of split 1 (Drosophila) (Hes1), mRNA.			1.292308

Gene Symbol	Description			Fold Change
OLFML3	Mus musculus olfactomedin-like 3 (Olfml3), mRNA.			1.29014
PLEKHO2	Mus musculus pleckstrin homology domain containing, family O member 2 (Plekho2), mRNA.			1.287191
DCTN6	Mus musculus dynactin 6 (Dctn6), mRNA.			1.287151
DUSP1	Mus musculus dual specificity phosphatase 1 (Dusp1), mRNA.			1.287093
ZFP36	Mus musculus zinc finger protein 36 (Zfp36), mRNA.			1.28126
RHOB	Mus musculus ras homolog gene family, member B (Rhob), mRNA.			1.279543
IGF2	Mus musculus insulin-like growth factor 2 (Igf2), mRNA.			1.274712
THY1	Mus musculus thymus cell antigen 1, theta (Thy1), mRNA.			1.271593
MGAT3	Mus musculus mannoside acetylglucosaminyltransferase 3 (Mgat3), mRNA.			1.270836
APRT	Mus musculus adenine phosphoribosyl transferase, mRNA			1.26981
SH3KBP1	Mus musculus SH3-domain kinase binding protein 1 (Sh3kbp1), mRNA.			1.265921
SERPINA3G	Mus musculus serine (or cysteine) peptidase inhibitor, clade A, member 3G (Serpina3g), mRNA.			1.263668
IRF1	Mus musculus interferon regulatory factor 1 (Irf1), mRNA.			1.262768
PALM	Mus musculus paralemmin (Palm), mRNA.			1.261623
IGF1	Mus musculus insulin-like growth factor 1 (Igf1), transcript variant 1, mRNA.			1.260723
HRBL	Mus musculus HIV-1 Rev binding protein-like (Hrbl), transcript variant 2, mRNA.			1.254217
ETS2	Mus musculus E26 avian leukemia oncogene 2, 3' domain (Ets2), mRNA.			1.251346
PLK2	Mus musculus polo-like kinase 2 (Drosophila) (Plk2), mRNA.			1.250674
HIC1	Mus musculus hypermethylated in cancer 1 (Hic1), transcript variant 1, mRNA.			1.249158
SMO	Mus musculus smoothened homolog (Drosophila) (Smo), mRNA.			1.247802
BCAM	Mus musculus basal cell adhesion molecule (Bcam), mRNA.			1.247336

Gene Symbol	Description			Fold Change
ZCCHC3	Mus musculus zinc finger, CCHC domain containing 3 (Zcchc3), mRNA.			1.246931
AW548124	Mus musculus expressed sequence AW548124 (AW548124), mRNA.			1.246607
BIRC5	Mus musculus baculoviral IAP repeat-containing 5 (Birc5), transcript variant 1, mRNA.			1.246125
IGSF9	Mus musculus immunoglobulin superfamily, member 9 (Igsf9), mRNA.			1.245336
PPP1R13B	Mus musculus protein phosphatase 1, regulatory (inhibitor) subunit 13B (Ppp1r13b), mRNA.			1.244152
H19	Mus musculus H19 fetal liver mRNA (H19) on chromosome 7.			1.241052
TOP2A	Mus musculus topoisomerase (DNA) II alpha (Top2a), mRNA.			1.237934
NDST1	Mus musculus N-deacetylase/N-sulfotransferase (heparan glucosaminyl) 1 (Ndst1), mRNA.			1.236784
SETD8	Mus musculus SET domain containing (lysine methyltransferase) 8 (Setd8), mRNA.			1.231298
IGFBP4	Mus musculus insulin-like growth factor binding protein 4, mRNA			1.230639
ACCN2	Mus musculus amiloride-sensitive cation channel 2, neuronal (Accn2), mRNA.			1.230346
DUSP6	Mus musculus dual specificity phosphatase 6 (Dusp6), mRNA.			1.229589
TNFRSF11B	Mus musculus tumor necrosis factor receptor superfamily, member 11b (osteoprotegerin) (Tnfrsf11b), mRNA.			1.227648
CHST11	Mus musculus carbohydrate sulfotransferase 11 (Chst11), mRNA.			1.225853
RPIA	Mus musculus ribose 5-phosphate isomerase A (Rpia), mRNA.			1.225795
LSM3	Mus musculus LSM3 homolog, U6 small nuclear RNA associated (S. cerevisiae) (Lsm3), mRNA.			1.223725
BMP3	Mus musculus bone morphogenetic protein 3 (Bmp3), mRNA.			1.222016
FGF5	Mus musculus fibroblast growth factor 5 (Fgf5), mRNA.			1.221948
TMEM8	Mus musculus transmembrane protein 8 (five membrane-spanning domains) (Tmem8), mRNA.			1.221207

Gene Symbol	Description			Fold Change
HMGA1	Mus musculus high mobility group AT-hook 1 (Hmga1), transcript variant 1, mRNA.			1.220418
C1QTNF1	Mus musculus C1q and tumor necrosis factor related protein 1 (C1qtnf1), mRNA.			1.220298
BBX	Mus musculus bobby sox homolog (Drosophila) (Bbx), mRNA.			1.215977
CHI3L1	Mus musculus chitinase 3-like 1 (Chi3l1), mRNA.			1.215013
MTHFD1	Mus musculus methylenetetrahydrofolate dehydrogenase (NADP+ dependent), methenyltetrahydrofolate cyclohydrolase, formyltetrahydrofolate synthase (Mthfd1), mRNA.			1.213704
E2F1	Mus musculus E2F transcription factor 1 (E2f1), mRNA.			1.212262
BANF1	Mus musculus barrier to autointegration factor 1 (Banf1), transcript variant 2, mRNA.			1.20883
BICC1	Mus musculus bicaudal C homolog 1 (Drosophila) (Bicc1), mRNA.			1.208602
GOLM1	Mus musculus golgi membrane protein 1 (Golm1), transcript variant 2, mRNA.			1.208051
AXUD1	Mus musculus AXIN1 up-regulated 1 (Axud1), mRNA.			1.205341
LIF	Mus musculus leukemia inhibitory factor (Lif), transcript variant 2, mRNA.			1.205123
NME4	Mus musculus non-metastatic cells 4, protein expressed in (Nme4), mRNA.			1.204789
FKBP1A	Mus musculus FK506 binding protein 1a (Fkbp1a), mRNA.			1.204717
ISG20L2	Mus musculus interferon stimulated exonuclease gene 20-like 2 (Isg20l2), mRNA.			1.204517
BCAR3	Mus musculus breast cancer anti-estrogen resistance 3 (Bcar3), mRNA.			1.203903
BHLHB2	Mus musculus basic helix-loop-helix domain containing, class B2 (Bhlhb2), mRNA.			1.203725
CSRP1	Mus musculus cysteine and glycine-rich protein 1 (Csrp1), mRNA.			1.202695
HS6ST1	Mus musculus heparan sulfate 6-O-sulfotransferase 1 (Hs6st1), mRNA.			1.201955
CD44	Mus musculus CD44 antigen (Cd44), transcript variant 2,			1.201885

Gene Symbol	Description			Fold Change
	mRNA.			
PEAR1	Mus musculus platelet endothelial aggregation receptor 1 (Pear1), transcript variant 1, mRNA.			1.200346
SFRP2	Mus musculus secreted frizzled-related protein 2 (Sfrp2), mRNA.			-1.98215
TGFBI	Mus musculus transforming growth factor, beta induced (Tgfbi), mRNA.			-1.49519
PDLIM3	Mus musculus PDZ and LIM domain 3 (Pdlim3), mRNA.			-1.46603
ALDOC	Mus musculus aldolase 3, C isoform (Aldoc), mRNA.			-1.45095
SGK1	Mus musculus serum/glucocorticoid regulated kinase 1 (Sgk1), mRNA.			-1.43483
INSIG1	Mus musculus insulin induced gene 1 (Insig1), mRNA.			-1.41735
UNC45B	Mus musculus unc-45 homolog B (C. elegans) (Unc45b), mRNA.			-1.36753
OSR1	Mus musculus odd-skipped related 1 (Drosophila) (Osr1), mRNA.			-1.36551
GUCY1A3	Mus musculus guanylate cyclase 1, soluble, alpha 3 (Gucy1a3), mRNA.			-1.3646
PRPH	Mus musculus peripherin (Prph), mRNA.			-1.36395
FLRT2	Mus musculus fibronectin leucine rich transmembrane protein 2 (Flrt2), mRNA.			-1.35086
THBD	Mus musculus thrombomodulin (Thbd), mRNA.			-1.34709
PTGS1	Mus musculus prostaglandin-endoperoxide synthase 1 (Ptgs1), mRNA.			-1.34438
ADAMTS2	Mus musculus a disintegrin-like and metallopeptidase (reprolysin type) with thrombospondin type 1 motif, 2 (Adamts2), mRNA.			-1.33129
JAM2	Mus musculus junction adhesion molecule 2 (Jam2), mRNA.			-1.32023
OGN	Mus musculus osteoglycin (Ogn), mRNA.			-1.31751
SEPP1	Mus musculus selenoprotein P, plasma, 1 (Sepp1), transcript variant 2, mRNA.			-1.30435

Gene Symbol	Description			Fold Change
TAF9	Mus musculus TAF9 RNA polymerase II, TATA box binding protein (TBP)-associated factor (Taf9), transcript variant 1, mRNA.			-1.30409
KRT14	Mus musculus keratin 14 (Krt14), mRNA.			-1.3036
GNB2L1	Mus musculus guanine nucleotide binding protein (G protein), beta polypeptide 2 like 1 (Gnb2l1), mRNA.			-1.29407
MMP11	Mus musculus matrix metallopeptidase 11 (Mmp11), mRNA.			-1.29144
CALCA	Mus musculus calcitonin/calcitonin-related polypeptide, alpha (Calca), transcript variant 2, mRNA.			-1.29039
SEMA3C	Mus musculus sema domain, immunoglobulin domain (Ig), short basic domain, secreted, (semaphorin) 3C, mRNA			-1.28747
IFITM1	Mus musculus interferon induced transmembrane protein 1 (Ifitm1), mRNA.			-1.28349
SNX1	Mus musculus sorting nexin 1 (Snx1), mRNA.			-1.28272
MYH8	Mus musculus myosin, heavy polypeptide 8, skeletal muscle, perinatal (Myh8), mRNA.			-1.28221
GPC2	Mus musculus glypican 2 (cerebroglycan) (Gpc2), mRNA.			-1.28021
MCCC1	Mus musculus methylcrotonoyl-Coenzyme A carboxylase 1 (alpha) (Mccc1), mRNA.			-1.27913
PDE4DIP	Mus musculus phosphodiesterase 4D interacting protein (myomegalin) (Pde4dip), transcript variant 1, mRNA.			-1.26682
PLEKHA4	Mus musculus pleckstrin homology domain containing, family A (phosphoinositide binding specific) member 4 (Plekha4), mRNA.			-1.26674
GRTP1	Mus musculus GH regulated TBC protein 1 (Grtp1), mRNA.			-1.26576
OXR1	Mus musculus oxidation resistance 1 (Oxr1), mRNA.			-1.26367
XDH	Mus musculus xanthine dehydrogenase (Xdh), mRNA.			-1.26142
NNMT	Mus musculus nicotinamide N-methyltransferase (Nnmt), mRNA.			-1.26025
SEPT7	Mus musculus septin 7 (Sept7), mRNA.			-1.26024
TUBB2B	Mus musculus tubulin, beta 2b (Tubb2b), mRNA.			-1.25523
UGT1A6A	Mus musculus UDP glucuronosyltransferase 1 family,			-1.25502

Gene Symbol	Description			Fold Change
	polypeptide A6A (Ugt1a6a), mRNA.			
CXCL12	Mus musculus chemokine (C-X-C motif) ligand 12 (Cxcl12), transcript variant 1, mRNA.			-1.25182
SLC10A6	Mus musculus solute carrier family 10 (sodium/bile acid cotransporter family), member 6 (Slc10a6), mRNA.			-1.25141
JMJD3	Mus musculus jumonji domain containing 3 (Jmjd3), mRNA.			-1.24772
CAV1	Mus musculus caveolin, caveolae protein 1 (Cav1), mRNA.			-1.24421
AVPR1A	Mus musculus arginine vasopressin receptor 1A (Avpr1a), mRNA.			-1.24165
COL24A1	Mus musculus collagen, type XXIV, alpha 1 (Col24a1), mRNA. XM_916101			-1.24155
NFKBIZ	Mus musculus nuclear factor of kappa light polypeptide gene enhancer in B-cells inhibitor, zeta (Nfkbiz), mRNA.			-1.24031
LPL	Mus musculus lipoprotein lipase (Lpl), mRNA.			-1.24002
ANTXR1	Mus musculus anthrax toxin receptor 1 (Antxr1), mRNA.			-1.23771
COL3A1	Mus musculus collagen, type III, alpha 1 (Col3a1), mRNA.			-1.23603
DDAH2	Mus musculus dimethylarginine dimethylaminohydrolase 2 (Ddah2), mRNA.			-1.23351
PKHD1L1	Mus musculus polycystic kidney and hepatic disease 1-like 1 (Pkhd1l1), mRNA.			-1.23238
PGRMC1	Mus musculus progesterone receptor membrane component 1 (Pgrmc1), mRNA.			-1.23231
ATP1B1	Mus musculus ATPase, Na+/K+ transporting, beta 1 polypeptide (Atp1b1), mRNA.			-1.23172
ANGPTL7	Mus musculus angiopoietin-like 7 (Angptl7), mRNA.			-1.23115
IFI204	Mus musculus interferon activated gene 204 (Ifi204), mRNA.			-1.22856
GDPD2	Mus musculus glycerophosphodiester phosphodiesterase domain containing 2 (Gdpd2), mRNA.			-1.22813
RASL11B	Mus musculus RAS-like, family 11, member B (Rasl11b), mRNA.			-1.22601
SEMA3A	Mus musculus sema domain, immunoglobulin domain (Ig), short basic domain, secreted, (semaphorin) 3A (Sema3a), mRNA.			-1.22415

Gene Symbol	Description			Fold Change
DHRS7	Mus musculus dehydrogenase/reductase (SDR family) member 7 (Dhrs7), mRNA.			-1.22376
ACPP	Mus musculus acid phosphatase, prostate (Acpp), transcript variant 1, mRNA.			-1.22278
SEL1L	Mus musculus sel-1 suppressor of lin-12-like (C. elegans) (Sel1l), transcript variant 1, mRNA.			-1.22089
SCYL1BP1	Mus musculus SCY1-like 1 binding protein 1 (Scyl1bp1), mRNA.			-1.22006
HNRPDL	Mus musculus heterogeneous nuclear ribonucleoprotein D-like (Hnrpdl), mRNA.			-1.21822
MMP13	Mus musculus matrix metallopeptidase 13 (Mmp13), mRNA.			-1.21802
SYTL2	Mus musculus synaptotagmin-like 2 (Sytl2), transcript variant 5, mRNA.			-1.21772
PON3	Mus musculus paraoxonase 3 (Pon3), mRNA.			-1.2172
PDGFRA	Mus musculus platelet derived growth factor receptor, alpha polypeptide (Pdgfra), transcript variant 1, mRNA.			-1.21708
CCDC109B	Mus musculus coiled-coil domain containing 109B (Ccdc109b), mRNA.			-1.21553
PALMD	Mus musculus palmdelphin, mRNA			-1.2153
NAMPT	Mus musculus nicotinamide phosphoribosyltransferase (Nampt), mRNA.			-1.21523
KRBA1	Mus musculus KRAB-A domain containing 1 (Krba1), mRNA.			-1.21488
IGFBP2	Mus musculus insulin-like growth factor binding protein 2 (Igfbp2), mRNA.			-1.21339
ATG2A	Mus musculus ATG2 autophagy related 2 homolog A (S. cerevisiae) (Atg2a), mRNA.			-1.21226
NRG1	Mus musculus neuregulin 1 (Nrg1), mRNA.			-1.21063
RGS10	Mus musculus regulator of G-protein signalling 10 (Rgs10), mRNA.			-1.20682
SULF1	Mus musculus sulfatase 1 (Sulf1), mRNA.			-1.20658
CACNA1G	Mus musculus calcium channel, voltage-dependent, T type, alpha 1G subunit (Cacna1g), mRNA.			-1.20605

Gene Symbol	Description		Fold Change
RAET1B	Mus musculus retinoic acid early transcript beta (Raet1b), mRNA.		-1.20511
ARRDC3	Mus musculus arrestin domain containing 3, mRNA		-1.20489
CLK4	Mus musculus CDC like kinase 4 (Clk4), mRNA.		-1.20106
COL4A6	Mus musculus procollagen, type IV, alpha 6 (Col4a6), mRNA.		-1.20092

CHAPTER 4

CONCLUSIONS AND FUTURE DIRECTIONS

SUMMARY

Pancreatic ductal adenocarcinoma (PDA) is a highly aggressive disease that takes the lives of the vast majority of affected patients. Our knowledge of the molecular events underlying the development and progression of PDA has steadily increased, but this has not translated into more effective therapeutic approaches for treatment of the disease. The work described in this thesis has taken a focused approach at trying to better characterize the pancreatic tumor microenvironment. A detailed understanding of the cross-talk between tumor and stromal cells may hold clues to affectively targeting pancreatic tumors in new ways. We have identified that Hedgehog (Hh) signaling is one of the important feedback mechanisms between pancreatic tumor cells and the infiltrating stroma. Targeting paracrine Hh signaling in the tumor stroma can have significant effects on tumor biology, including reduction in metastatic spread, changes in tumor cell differentiation, decreases in tumor desmoplasia, and disruption of the cancer stem cell population. Future studies will be aimed at understanding how paracrine Hh signaling and downstream Hh-target genes affect the biological function of the tumor mesenchyme and of the tumor cells themselves and how this may translate to more effective therapies for pancreatic cancer.

CONCLUSIONS

The Hedgehog pathway is widely studied for its role in the regulation of growth, development and maintenance of many different tissues within the organism. While this pathway has a clear, canonical mechanism for autocrine and paracrine signaling in normal tissues, this is not the case for pancreatic tumor cells [33]. The experiments described in this thesis confirmed a role for paracrine Hh signaling in the pancreatic tumor microenvironment. Our studies have also shown an important role of Hh signaling in mediating the invasiveness of the tumor along with maintaining the differentiation of the tumor cells which has not been previously described. Additionally, this thesis details the first transcriptional profiling analysis of Hh responsive genes in pancreatic stellate cells. Bioinformatics analysis of differentially expressed genes proposed several ways in which the Hh pathway may impact the pancreatic tumor microenvironment. One of these functional roles was related to enhancing the motility of pancreatic stellate cells in three-dimensional extracellular matrix, which was validated using an *in vitro* model system. The functional studies and model systems that are described in this thesis provide the framework for asking important questions about the role of paracrine Hh signaling in pancreatic cancer.

Role of Paracrine Hh signaling *in vivo*

In Chapter 2, we examined the effect of Hh pathway antagonist, HhAntag, alone or in combination with gemcitabine in an orthotopic model of human pancreatic ductal adenocarcinoma (PDA). Essentially all drugs that are approved for anti-cancer therapy have been tested using a subcutaneous xenograft model in immune-deficient

mice and showed promising activity before being evaluated in early clinical trials. Unfortunately, these successes have often been met by failures in a clinical trial setting, including trials for: antagonists of the human epidermal growth factor receptor (EGFR) pathway, vascular endothelial growth factor (VEGF) pathway, insulin-like growth factor (IGF) pathway, and phosphoinositide 3'-kinase (PI3k)/Akt/mammalian target of rapamycin (mTOR) signaling [27,28,118,119]. In a retrospective study performed by the National Cancer Institute (NCI), only one-third of all tested human xenograft studies had some activity in Phase II clinical trials, but even this was highly variable depending on the particular tumor histology [146]. Activity in breast cancer xenografts predicted poorly, whereas lung cancers, particularly adenocarcinomas, tend to respond better in comparison to the other diseases.

Why are subcutaneous xenograft models systems so poor at predicting therapeutic activity in the clinic? One reason may be that these pre-clinical studies often use xenografts established from immortalized cancer cell lines. These individual lines have often been established decades prior to use in pre-clinical models and after years of *in vitro* culture and selection, these cells likely do not retain the same genetic background or phenotypic characteristics as the original tumor from which the cell line was derived [147]. Our personal observation in deriving xenografts from patients with pancreatic adenocarcinoma is that there is a diverse phenotype in primary patient tumors that does not correlate with xenograft tumors from pancreatic cancer cell lines. These differences range from the amount of desmoplasia that the tumor develops, varying degrees of tumor histolopathology

which range from highly undifferentiated to mucionous neoplasms, along with differing levels of expression of important signaling ligands such as Sonic hedgehog (**Chapter 2, Figure 2.1**). Validating these observations are pre-clinical studies done from a large panel of xenografts derived from patient biopsies, instead of cancer cell lines, and activity in these xenografts was compared with clinical response. A strong prediction of clinical outcome was observed for both tumor resistance (97%) and tumor sensitivity (90%) in these studies [148].

In line with using individual patient xenografts for establishing pre-clinical models, our lab has established over 30 primary xenografts from patients with pancreatic adenocarcinoma. We utilized 13 of these tumors in our study and compared the pathology and gene expression profile of Hh signaling ligands and downstream target genes (**Chapter 2, Table 2.2**). As might be expected, we identified a range of expression of Sonic and Indian hedgehog ligands in these tumors, and the expression of these factors correlated with the expression of Hh target genes, Gli1 and Patched1, in the mouse stroma. Ectopic expression of Sonic hedgehog in a transformed, ductal-derived pancreatic epithelial cell line has correlated with a strong desmoplastic reaction that is reversible with inhibitors of the pathway [81]. An observation that we note is that two patient xenografts with the highest levels of Shh and Ihh expression also have the highest amount of infiltrating mouse stroma of the tumors that we examined in this study (**Figure 4.1**). Recent studies in transgenic animal models of pancreatic cancer have shown that the high level of desmoplastic stroma corresponds to tumors with a disorganized vasculature which limits the ability of chemotherapeutic drugs to reach their target within the

tumor [80,125]. This warrants expansion of our study to more patient xenografts to determine if there is a correlation with Hh ligand expression, tumor pathology and patient survival. This might aid in identifying patient groups which would benefit most from inhibition of paracrine Hh signaling.

Subcutaneous xenograft models of pancreatic cancer are not ideal due to their rare metastatic potential and reduced propensity to display highly invasive phenotypes. These properties are important as 85% of patients present clinically with advanced, inoperable disease [21]. For our studies, we established an orthotopic model of pancreatic adenocarcinoma by implanting tumor cells that were dissociated from individual patient xenografts (one that was spontaneously metastatic), directly in the distal pancreas of NOD/SCID mice. The advantage of this approach is that it allowed us to test the effect of inhibition of paracrine Hh signaling with or without co-treatment with gemcitabine on the progression of tumors with the genetic and histological profiles that reflected the *in vivo* characteristic found in the patient. These tumor cells were "tagged" by transducing them with a lentiviral construct that expresses *Renilla*-luciferase, and allowed us to perform non-invasive imaging of the animals to establish baseline tumor sizes prior to beginning therapy and monitor progression of the tumor growth during treatment (**Figure 4.2**) [149]. We believe that this is the first description of this platform using pancreatic adenocarcinoma cells derived from individual patients and provides a unique pre-clinical model for testing potential therapies.

To test how inhibition of paracrine Hh signaling affected the progression of pancreatic tumor growth in our system, we compared the treatment of two patient

xenografts with an inhibitor of the Hh pathway, HhAntag, and gemcitabine, the drug most commonly given to pancreatic cancer patients. HhAntag is a compound that was developed by Genentech that is 10 times more potent than the natural, Smoothened antagonist of the pathway, cyclopamine, and has been used in animal models to down-regulate Hh signaling in a wide range of malignancies [33,150]. Both PDA xenografts treated with HhAntag alone did not demonstrate a significant reduction in primary tumor size from vehicle treated animals. This is somewhat contrary to a previous report showing that blocking paracrine Hh signaling with HhAntag in a subcutaneous xenograft of pancreatic cancer led to a delay in tumor growth [33]. However, this study used a single pancreatic tumor implanted subcutaneously, which did not metastasize and the amount of desmoplasia was undocumented. These discrepancies highlight the need to expand treatment studies to a large range of tumors to be able to draw better conclusions on the effect of Hh pathway inhibition on a wide range of patient tumors. Additionally, in the analysis of the expression of Hh ligands expressed in the PDA tumors in our study we observed a wide range of Shh and Ihh expression in tumors. The xenografts chosen for our study expressed Shh and Ihh at levels slightly below the statistical median for the tumors that we analyzed. It is possible the HhAntag may be more affective at slowing the growth of pancreatic tumors with a higher level of paracrine Hh activation. Our results would suggest that testing a wide range of tumors with different Hh expression may help identify the phenotype of tumors which will respond best to inhibition of paracrine Hh signaling.

The orthotopic tumors in our studies responded significantly better to gemcitabine than the observed clinical response of patients in the clinic. There is some debate as to whether the orthotopic transplantation into SCID mice used in our study are the best model for pancreatic cancer as these animals lack important components of the immune system which may limit the desmoplastic reaction [80,151]. Indeed, *de novo* pancreatic disease arising from transgenic expression of mutant KRAS and p53 alleles in the pancreas result in tumors that have a higher desmoplastic reaction and more deficient vascular network than xenotransplanted pancreatic tumor cells [80]. While we do observe a decreased amount of infiltrating stroma in our PDA xenografts compared to patient sections from the original tumor, this is variable from tumor to tumor and indeed may be dependent on the expression of signals, including Hh ligands, from the tumor cells.

Interestingly, we have also observed evidence of decreased perfusion of tumors, and possibly chemotherapeutics in our orthotopic xenograft model. We utilize non-invasive bioluminescent imaging (BLI) to monitor the progression of tumors during treatment. Several times near the end of the 21 day treatment protocol, we encountered the complete loss of signal from a tumor that had a clear BLI signal the previous week, primarily in those animals treated with vehicle or HhAntag. The mechanism for this imaging is via intraperitoneal (IP) injection of luciferin, an oxidizable substrate that travels through the bloodstream and upon encountering the luciferase enzyme (expressed by our "tagged" tumor cells) releases a bioluminescent signal detected by a sensitive charge-couple device (CCD) camera [152]. When we recovered tumors from the animals that showed a loss of BLI signal and tested them

in culture with luciferin, these cells demonstrated competent BLI activity suggesting that the construct was not silenced. We believe this suggests that there is a point during the growth of the orthotopic xenograft tumors where there is a reduction in vascular integrity. Supportive of this contention is the observed increase in necrosis in the center of tumors, especially those recovered from animals that were treated with vehicle or HhAntag alone. It is possible that the continued sensitivity to gemcitabine treatment in our model is more about timing of the treatment: we are treating the animals during a time period where the tumor is highly vascularized and permits diffusion of compounds to the tumor. Studies are on-going to see if we can accelerate the process of desmoplasia by co-implanting tumor cells along with tumor associated fibroblasts. This may help us achieve a more clinically accurate tumor model in which the xenografts are less sensitive to gemcitabine.

Despite the limitations described above, we believe that our model is relevant to investigation of the interactions between tumor cells and the stroma. The orthotopic tumors in our model system develop a desmoplastic reaction and we have identified several patient xenografts which form spontaneous metastases that have only been seen in specially selected pancreatic cell line xenografts [153]. Additionally, transgenic animal models of pancreatic cancer generate a single genetic and histopathological profile of the disease, while use of primary PDA xenografts allows us access to test therapies against tumors with varying grades of differentiation, genetic background and stromal involvement which represents the true patient population.

The most striking result from our *in vivo* experiments was the marked inhibition of metastases in xenograft UM-PDA#1 with HhAntag treatment alone or in combination with gemcitabine while the primary tumor showed only a marginal decrease in size. These experiments show the vital dependence of the pancreatic tumor cells with its mesenchyme in the tumor microenvironment. A recent study using an organotypic assay of tumor cell invasion demonstrated how mesenchymal cells at the leading edge of the tumor carve tracks through the extracellular matrix, which the tumor cells then use to invade into surrounding tissues [145]. Additionally, presence of stromal cells in a three-dimensional model of pancreatic tumor cell invasion leads to an epithelial-to-mesenchymal transition with significant decreases in E-cadherin expression and an increase in β-catenin signaling resulting in the increased invasion of the tumor cells [154]. These studies highlight the potential importance of modulating the tumor stroma in prevention or possible treatment of metastatic disease.

While we are not exactly sure how blockage of paracrine Hh signaling in the stroma results in the reduction in metastatic spread, we have some clues from our experiments and from similar studies in the literature. The negative effect of HhAntag treatment on the metastatic seeding of pancreatic adenocarcinoma cells suggests that HhAntag does one or several things to the tumor mesenchyme. It may reduce the expression of factors in the stroma that promote the functional ability of cancer cells to invade. For example, tumor cells and mesenchymal cells are dependent on an MT1-MMP mechanism for degradation of basement membrane and invasion in type I collagen matrix [155,156]. It is possible that HhAntag treatment

disrupts signals in mesenchymal cells that localize MT1-MMP to the membrane, and this leads to a reduction in cell motility. Additionally, some of the same motility factors, including MMP-2, MT1-MMP, and TIMP-2 are involved in the extravasation of tumor cells from the bloodstream so it is possible that some tumor cells may be able to leave the tumor but cannot engraft in a new site [157]. Importantly, we find that Hh treatment of pancreas-derived fibroblasts up-regulate motility and angiogenesis pathways, indicating a mechanism that could be important for metastatic disease. Another possibility is that tumor-derived Shh is required to produce desmoplastic stroma at the site of metastasis and by blocking this with Hh inhibitors it prevents the establishment of these distant lesions.

Treatment with HhAntag alone and in combination with gemcitabine also revealed distinct changes in the tumor histological profile, with an apparent increase in differentiation of tumor cells and expression of mucins. The change observed in tumor histology with Hh inhibition has not been previously reported. Mucins comprise a large family of glycoproteins that are secreted or bound to the cellular membrane and either directly or indirectly, act to maintain the integrity of the cellular membrane, along with lubricating and protecting the epithelial surfaces in animal tissues [158]. In our studies, we observed a significant up-regulation of MUC2, a secreted mucin, with HhAntag plus gemcitabine treated tumors (not shown). It is unclear whether the change in histology alters the invasiveness of pancreatic cancer cells or simply reflects a less aggressive phenotype, but a clinical study of MUC2 expression across a panel of pancreatic adenocarcinoma tumors revealed a better prognosis with higher MUC2 expression [159].

Another hypothesis for the reduced metastatic potential of tumors following HhAntag is that the drug treatment disrupts factors that maintain the minor population of cells which are capable of new tumor initiation. However, in the case of UM-PDA#1 this population was not minor, in fact it has one of the highest levels of $CD44^+/CD24^+/EpCAM^+$ cells (greater than 40%) that we have analyzed and neither HhAntag or gemcitabine treatment affected the level of this cell population compared to vehicle treated animals. In contrast, we did observe significant reductions in markers related to the tumorigenic population of cells in UM-PDA#2 and this corresponded with delayed growth following re-implantation, but this xenograft tumor did not show evidence of metastases *in vivo*. A similar study using the Smo-inhibitor, IPI-269609 (Infinity Pharmaceuticals) to treat pancreatic cell line xenografts noted a reduction of Aldefluor positive ($ALDH^+$) cells, an activity assay for aldehyde dehydrogenase used to profile cancer stem cells in several malignancies [102,103,122]. Some preliminary experiments suggest that $ALDH^+$ cells were reduced in our HhAntag treatment groups in UM-PDA#1 xenografts (not shown). It is possible that our current markers are not as accurate at marking the true tumor initiating population and current studies in our laboratory suggest that a more accurate stem cell marker includes c-Met, also known as the hepatocyte growth factor receptor (HGFR). MET/HGFR is a receptor tyrosine kinase that binds hepatocyte growth factor (HGF) and has been implicated in cell survival and invasiveness in pancreatic cancer [160]. FACS analysis of tumor cells from HhAntag treatment groups with c-Met may reveal more accurate changes in the tumor-initiating cell population.

Pancreatic adenocarcinoma has a multi-decade long history of failed efforts in identifying an effective chemotherapeutic treatment regimen. The latest failed efforts included the use of use epidermal growth factor receptor (EGFR) inhibitors (Erbitux) in combination with radiation and treatments with vascular endothelial growth factor receptor (VEGFR) inhibitor, bevacizumab (Avastin). None showed significant effects in patient outcomes [27,161]. Gemcitabine, the currently accepted regimen for pancreatic cancer, only affords patients an average of a few weeks of increased survival [151]. These failures are likely due in part to the unique biology of the pancreatic tumor microenvironment. Pancreatic tumors are very fibrotic and recent studies suggest that these tumors have a disorganized vasculature which does not allow robust tumor perfusion [80]. Any therapy which may help to control the desmoplasia of the tumor could significantly impact the ability of chemotherapeutic agents or other secondary therapies to reach the tumor. It is clear from our studies that use of Hh antagonists in pancreatic tumors can affect the tumor mesenchyme and these effects are materialized in the inability of the tumor from invading into the local organ environment and altering the native differentiation of the epithelial cells. These are exciting results that will help us better understand how to use Hh pathway inhibition in combination with secondary agents to affect patient outcomes.

Functional Changes Induced by Hh signaling in Pancreatic Stellate Cells

In Chapter 3, we have provided the first documented transcriptional analysis of pancreatic stellate cells following Sonic Hedgehog stimulation. Our previous studies in Chapter 2 had demonstrated how pancreatic tumor cells activate Hh

signaling in the tumor mesenchyme by secretion of Hh pathway ligands but it was not clear which gene pathways were modulated by Hh signaling. The importance of these pathways were validated by targeted inhibition of paracrine Hh signaling *in vivo* that led to reduced tumor spread. The Hh pathway is well characterized for its role as a morphogen in developing epithelial tissues [162]. There is less information as to how activation of this pathway affects the mesenchyme and mediates cross-talk between epithelial and mesenchymal interactions. In the intestinal epithelium, Hh signaling mediates anti-inflammatory signals with the local mesenchyme. Inhibition of Hh signaling can lead to intestinal inflammation and death in animal models [82]. In pancreatic development, ectopic expression of Sonic hedgehog under the control of the Pdx-1 promoter in the developing epithelial anlage is incompatible with pancreas organogenesis with loss of both exocrine and endocrine tissue [58]. The pancreatic mesenchyme itself is transformed into duodenal mesoderm with functional layers of muscle that possess the ability to constrict, demonstrating that epithelial-derived Shh can impart important biological changes in the local mesenchyme. Recent studies of specialized pancreatic duct glands (PDGs) in the adult organ have been shown to express Shh in response to injury and may induce Hh-related factors in the stroma that mediate the transition of epithelial duct cells to a mucinous, metaplastic phenotype [163].

The pancreatic tumor microenvironment is dominated by infiltrating stroma and desmoplasia that surround the tumor cells. A major cause is the activation of pancreatic stellate cells (PSCs), which are specialized pancreatic fibroblast cells located at the periphery of the acini in the exocrine pancreas and are normally

quiescent [129]. Activation of PSCs can be mediated by growth factors and cytokines, such as TGF-β1, or oxidant stress which results in their transformation from a quiescent to a myofibroblast-like phenotype, which secretes excess amounts of extracellular matrix components [139]. To characterize the role of Hh signaling in these cells, we developed two cell lines to use for *in vitro* experiments. Initial attempts at culturing normal fibroblasts from human or mouse pancreas revealed that these cells often senesce in culture after only a few passages. We changed our strategy to culture pancreatic fibroblasts from mice induced with chronic pancreatitis, as correspondence with our collaborators suggested that fibroblasts from these mice have a higher proliferative capacity *in vitro*. We utilized this strategy in Immortomouse animals, which allowed us to develop a primary, conditionally immortalized cell line [131]. The development of these tools allowed us to ask important questions about the consequences of Hh signaling in pancreatic stellate cells.

Several previous studies have been performed to identify the Hh-related genes in mesenchymal cells, including embryonic fibroblasts and organ specific mesenchyme in the intestine and prostate [82,83,164]. Profiling studies of tumor-stromal interaction of prostate mesenchyme revealed that Shh-stimulation altered the transcriptional response of adult prostate mesenchyme to mimic the growth promoting actions of the fetal mesenchyme [165]. Studies analyzing the transcriptional profile of Shh and Ihh stimulated intestinal mesenchyme revealed a previous unknown function of Hh signaling in mediating anti-inflammatory signals in the tissue [82]. We performed transcriptional profiling of Shh-stimulated pancreatic

stellate cells and meta-analysis with prostate and intestinal Hh-related gene sets to learn what genes and pathways are consistent with Hh activation in mesenchymal cells and what genes may be specific to the pancreatic tumor microenvironment. Not surprisingly, we identified several genes that have been identified as Hh-related genes in Gdf10, Nkx2-3, Ang-4, Hes1, Sfrp-2, IGF1 and IGF2. Additionally, we identified some factors that had not been shown to be Hh-related genes in Wnt2, TGFβ2, R-spondin1, and Fgf9. We propose that these target genes may have roles in regulating the angiogenic-function of pancreatic stellate cells along with mediation of epithelial-to-mesenchymal transition and increased invasion of pancreatic tumor cells.

A recent study of Hh-responsive bone marrow-derived mesenchymal cells demonstrated the reliance of paracrine Hh signaling in regulating the expression of Ang-1 and IGF-1, which promoted the neovascularization of the tumor [86]. In our data set we observed the up-regulation of VEGFA, which has been shown to be the predominant vascular endothelial growth factor related protein in pancreatic tumor epithelial cells and likely plays an important role in mediating the neo-vascularization of the tumor [166]. While VEGF inhibitors have not provided significant clinical benefit to pancreatic cancer patients, this result may have more to do with drug delivery to the effective area in the tumor rather than the dependence of the tumor on these factors for tumor growth and development [27]. Alternatively, the tumors may have adapted to a relatively oxygen poor environment, rendering the reduction in vascularity by VEGF relatively ineffective. Interestingly, while we observed a number of angiogenic-related factors that were increased in pancreatic stellate cells following Shh-stimulation, study of a transgenic mouse model of pancreatic cancer

showed an increase in the vasculature following treatment of the animals with an Hh pathway inhibitor [80]. This seems counter-intuitive to successful treatment of pancreatic cancer, but the authors suggest that the more organized vascular network allows better penetrance of chemotherapeutic compounds. Closer study of angiogenesis-related genes following paracrine Hh inhibition *in vivo* may provide more answers into how these factors are manipulated by Hh signaling in the tumor microenvironment.

A striking result in our studies in Chapter 2 was the abrogation of metastases in animals treated with HhAntag alone or in combination with gemcitabine. We hypothesized that transcriptional profiling of Hh target genes in pancreatic stellate cells might provide us clues into how this pathway mediates the invasiveness of tumor cells. Interestingly, we noted a number of Wnt pathway related genes in our data set including increases in Wnt2 and R-spondin-1, and the single most down-regulated gene in our data set was Sfrp-2, an important inhibitor of Wnt pathway signaling [167]. Additional studies have shown that the pro-invasive activity of Wnt2 may go through a non-canonical mechanism involving GSK-3β and c-Jun/AP-1 signaling [168]. Canonical Wnt signaling has been shown to be active in pancreatic adenocarcinoma cells [140]. While there is a report of Wnt5a up-regulation and Sfrp-1 down-regulation in the pancreatic tumor stroma [141], to date there is not a clear mechanism of how Wnt pathway affects the biological function of pancreatic tumor mesenchyme. Recent studies have suggested a role for Wnt to enhance proliferation in the epithelium and stroma of chemically induced bladder cancer in mice [142]. In this work, Shh expression in basal cells of the bladder increases upon injury and

elicits increased stromal expression of Wnt protein signals, which in turn stimulate the proliferation of both urothelial and stromal cells. This type of feedback mechanism may also be at work in the pancreatic tumor microenvironment. Preliminary data examining the differential expression of Wnt ligands in Shh-stimulated pancreatic stellate cells revealed that only Wnt2, Wnt5b, and Wnt3a were significantly changed (**Figure 4.3**). We have also targeted the knock-down of Wnt2 in PSCs and this appears to block the ability of the cells to migrate in response to sonic hedgehog (**Figure 4.4**). Future studies will be aimed at identifying how Hedgehog/Wnt feedback may play an important role in mediating the growth and invasion of pancreatic tumor cells.

Clinical Efficacy of Paracrine Hh Inhibition in Treating Pancreatic Cancer

While we have demonstrated some exciting results in targeting paracrine Hh signaling in xenograft models of pancreatic cancer, we realize that success in animal models have rarely translated to success in the clinic. To date, the only hope for a cure from pancreatic cancer is surgical resection of the disease; however, roughly 85% of patients diagnosed with pancreatic adenocarcinoma are presented with an inoperable diagnosis. That makes identifying therapies that are effective at reducing tumor growth that convert a patient into a surgical candidate, or finding therapies that help to prevent the recurrence of pancreatic disease crucial.

Recently, a phase I clinical trial (UMCC 2010.003) has been initiated at the University of Michigan Medical Center for the treatment of patients with metastatic pancreatic ductal adenocarcinoma with GDC-0449, a Smoothened antagonist and

potent Hh pathway inhibitor developed by Genentech. The plan for this study is to include 25 patients with metastatic disease. The primary endpoint is to assess the biological effects of Hh inhibition on cancer stem cells and Hh signaling with secondary endpoints examining clinical outcome parameters. All patients in this trial will have core biopsies taken before treatment with GDC-0449 to establish a baseline of Hh pathway activity. Patients will then undergo a first cycle of GDC-0449 monotherapy for two weeks, following which another core biopsy will be taken to assess Hh-regulated changes in the tumor. Cycle 2 will then administer Gemcitabine infusion 3 times a week for 28 days. CT scans will be used to assess response at 8 week intervals.

Preliminary results of this trial have demonstrated some exiting results and important correlations with our xenograft study. Five patients have been evaluated for a response to GDC-0449 pre-treatment followed by gemcitabine treatment and have confirmed a partial response in 3 out of 5 patients. CT scans of patients following GDC-0449 treatment alone revealed very little change in the amount and size of metastases, which correlates with our xenograft study that demonstrated very little change in tumor volume with HhAntag treatment. However, following a treatment cycle with both gemcitabine and GDC-0449 a significant reduction in the metastatic liver lesions of several patients was observed (**Figure 4.5 A**). In addition, a reduction in CA-19-9 levels, a serum marker used diagnostically in pancreatic cancer, following the GDC-0449 and gemcitabine treatment cycle (**Figure 4.5 B**) has been observed. Additionally, histological changes with increased vacuolated structures in tumor cells of one patient following GDC-0449 treatment, consistent

with our findings following treatment of orthotopic tumors in mice with HhAntag (**Chapter 2, Figure 2.6**).

While this clinical trial is still in the early stages, the results are encouraging that targeting paracrine Hh signaling in pancreatic cancer patients may be a viable therapeutic strategy. As treatment has resulted in variable response in patients, it will be important to identify what parameters correlate with success, whether that may be levels of Hh ligands, expression of cancer stem cell markers, or the expression of certain Hh target genes in the tumor stroma. In the future, we hope to test inhibition of Hh signaling in a model of established liver metastases. This model may help us understand how Hh signaling of tumor cells in metastatic sites affects other organ microenvironments.

Proposed Model of Hh Signaling in Pancreatic Cancer

Based on the studies presented in this thesis, we propose an updated model for how paracrine Hh signaling in the tumor microenvironment plays critical roles in the epithelial to mesenchymal cross-talk of the tumor (**Figure 4.6**). We believe that in early neoplasms of the pancreas, where Sonic hedgehog has been shown to be expressed [30], activation of Hh signaling acts as a activator and mitogen, increasing the proliferation of pancreatic stellate cells and enhancing the desmoplastic reaction and possibly attracting bone marrow derived pro-angiogenic cells to the tumor site [86]. As the tumor progresses to more advanced stages, Hh pathway activation in stellate cells stimulates the release of factors that allow the tumor to invade into the vascular and lymphatic system. These factors are likely related to VEGFA, IGF, and

TGFβ pathways along with increased expression of ECM remodeling proteins defined in our gene profiling experiments. Additionally, Hh signaling in the mesenchyme causes the expression of factors that maintain the differentiation status of the tumor, which we proposed is mediated by Wnt pathway signals from the tumor mesenchyme.

In all, this thesis details experiments which have increased our understanding for the role of Hh pathway signaling in the pancreatic tumor microenvironment. Future work will aim to answer additional important questions about the key factors that are involved in the different aspects of pancreatic tumor biology. We hope that these studies will provide important clues in how we can use Hh pathway inhibition to provide better therapeutic options for pancreatic cancer patients.

ACKNOWLEDGMENTS

Author Contributions: Joseph S. Dosch has performed the IHC, BLI, and Wnt ligand analysis. Jingjiang Wu performed the Wnt2 knockdown experiments. Edward Kim provided the clinical trial data for patients being treated with GDC-0449 at the University of Michigan Medical Center.

FIGURES

Figure 4.1 Histological Comparison of Patient vs. Cell Line Xenografts. Representative sections from three individual patient xenografts and one xenograft generated from implantation of Panc-1 cells. Upper left and right panels represent xenografts with the highest expression of Sonic hedgehog (Shh), while the bottom left shows a xenograft with comparatively low expression of Shh. Notice the difference in tumor architecture and in the amount of infiltrating stroma. Bottom right is a Panc-1 pancreatic cancer cell line xenograft stained for sonic hedgehog. Tumor cells are very compact with little or no gland formation.

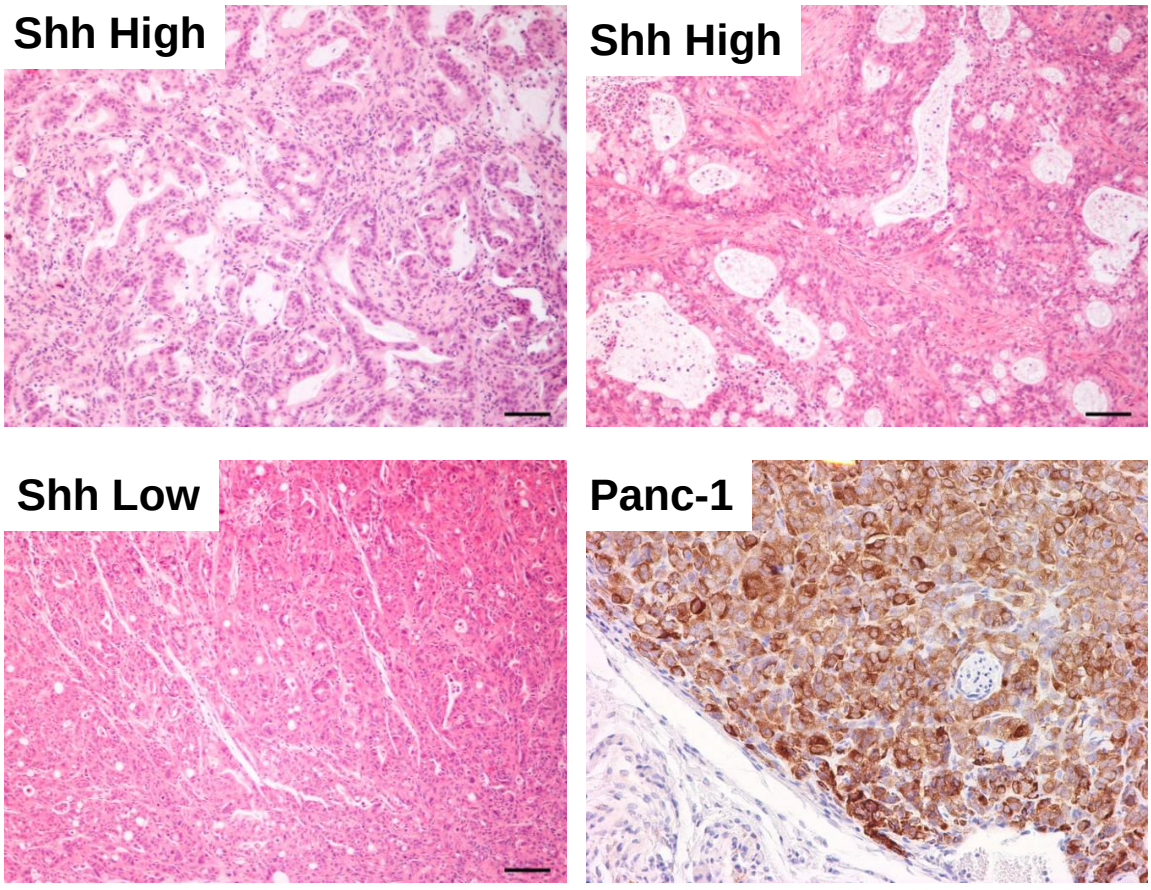

Figure 4.2 Bioluminescent Imaging (BLI) of Pancreatic Ductal Adenocarcinoma. **(A)** Animals with luciferase "tagged" patient tumor cells implanted in the pancreas, 3 weeks post-implantation **(B)** Whole organ systems; bowel, lungs, kidneys, and spleen shown here, can be imaged individually to detect both macro- and micro-metastases of pancreatic tumor cells.

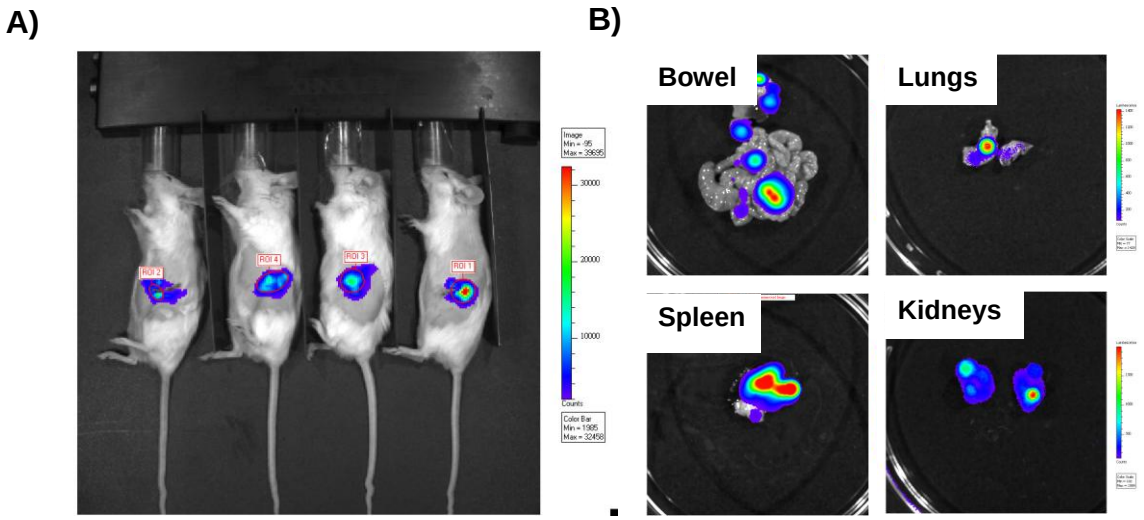

Figure 4.3 Differential Expression of Wnt ligands in Shh-treated PSCs. Quantitative expression analysis (qRT-PCR) of Wnt pathway ligands following Shh-stimulation of PSCs.

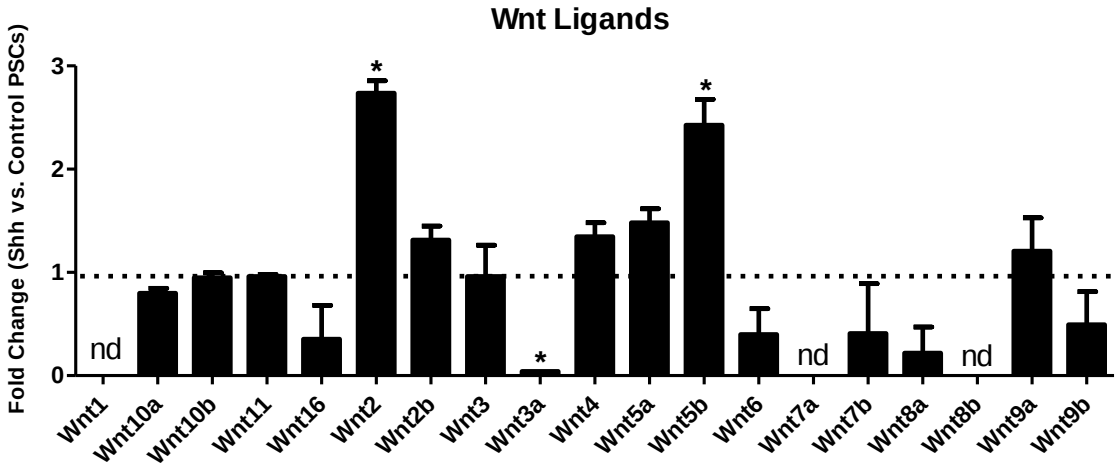

nd: not detected, *$p < 0.05$

Figure 4.4 Knockdown of Wnt2 Decreases 2D Migration of Shh-stimulated PSCs. (A) PSCs transfected with Wnt2 siRNAs decreases the amount of Wnt2 transcript by 60% after 48hrs. **(B)** PSCs with Wnt2 knockdown show a significant decrease in 2D migration following stimulation with sonic hedgehog.

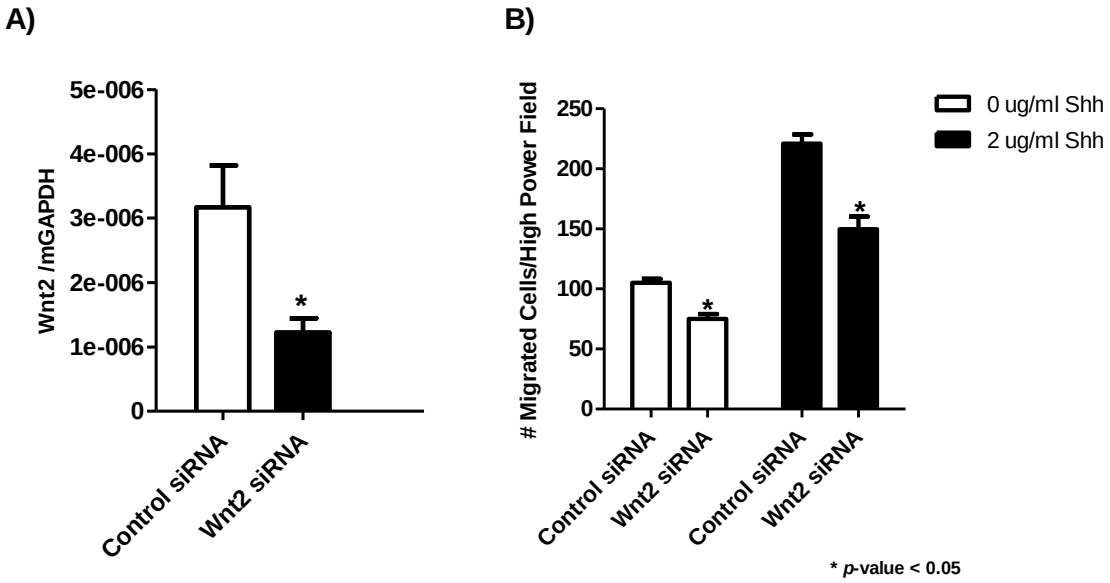

Figure 4.5 Clinical Trial of GDC-0449 in Patients with Metastatic Pancreatic Cancer. Above**,** CT scans from a patient pre and post treatment with GDC-0449 and gemcitabine. Arrows denote liver metastases found prior to treatment. Below, patient CA-19-9 serum levels (diagnostic measure of tumor burden) actually increases with GDC-0449 treatment but then drops following the GDC-0449 plus gemcitabine treatment cycles.

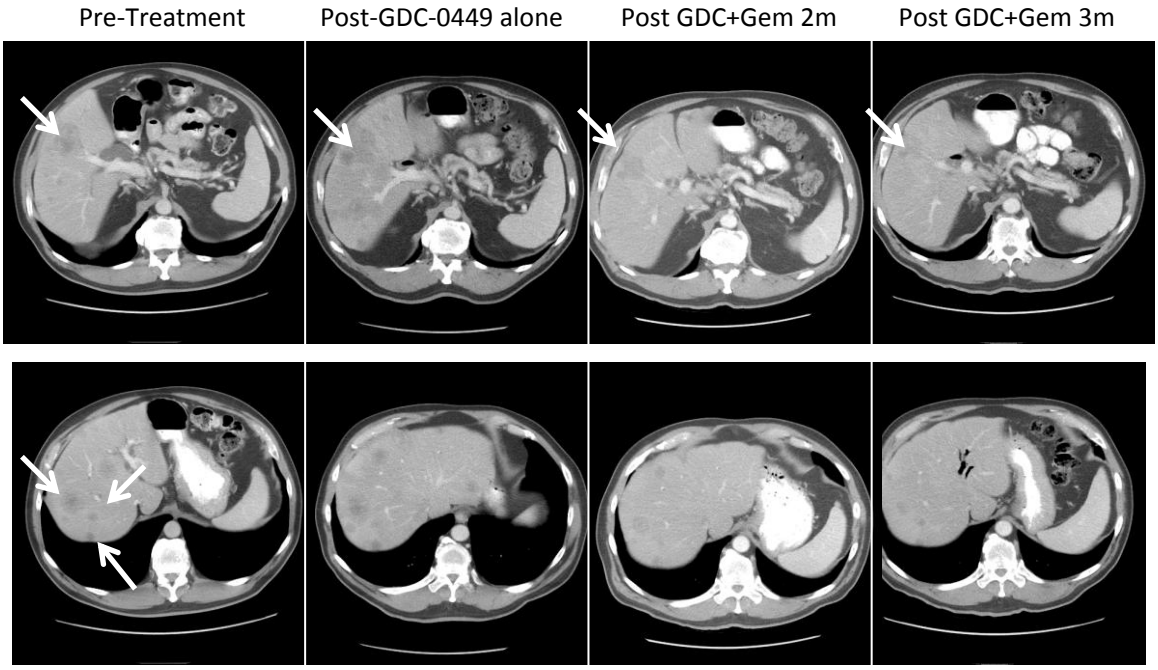

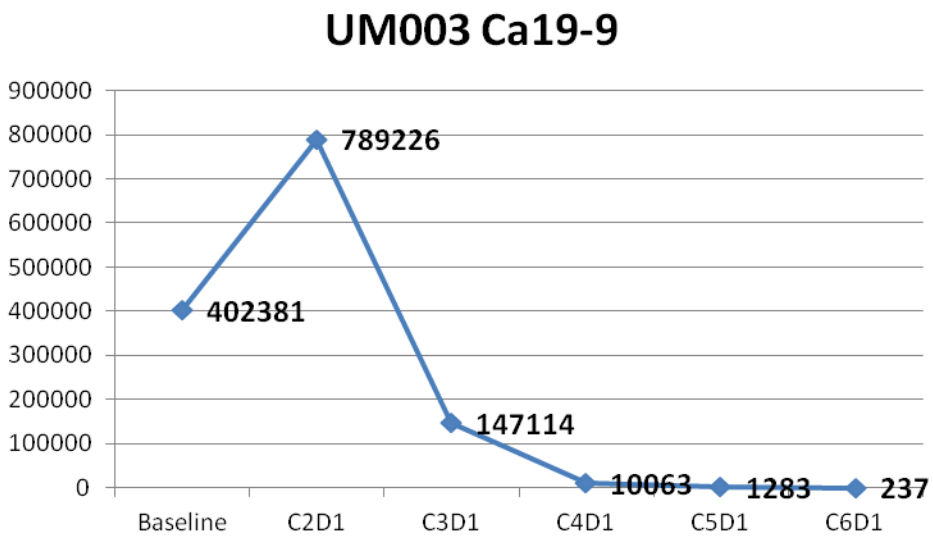

Figure 4.6 Model for Paracrine Hh Signaling in the Pancreatic Tumor Microenvironment. (A) Paracrine activation of Hh signaling in the tumor mesenchyme activates stellate cell proliferation and deposition of collagen, fibronectin and other ECM components. **(B)** Activation of Hh-target genes in the tumor stroma creates a positive feedback loop with tumor cells. These secreted factors may include Wnt, IGF and TGFβ proteins. Neo-vascularization of the tumor may be aided by IGF-1 and Angiopoietins that may be secreted by the stromal cells in response to Hh ligands.

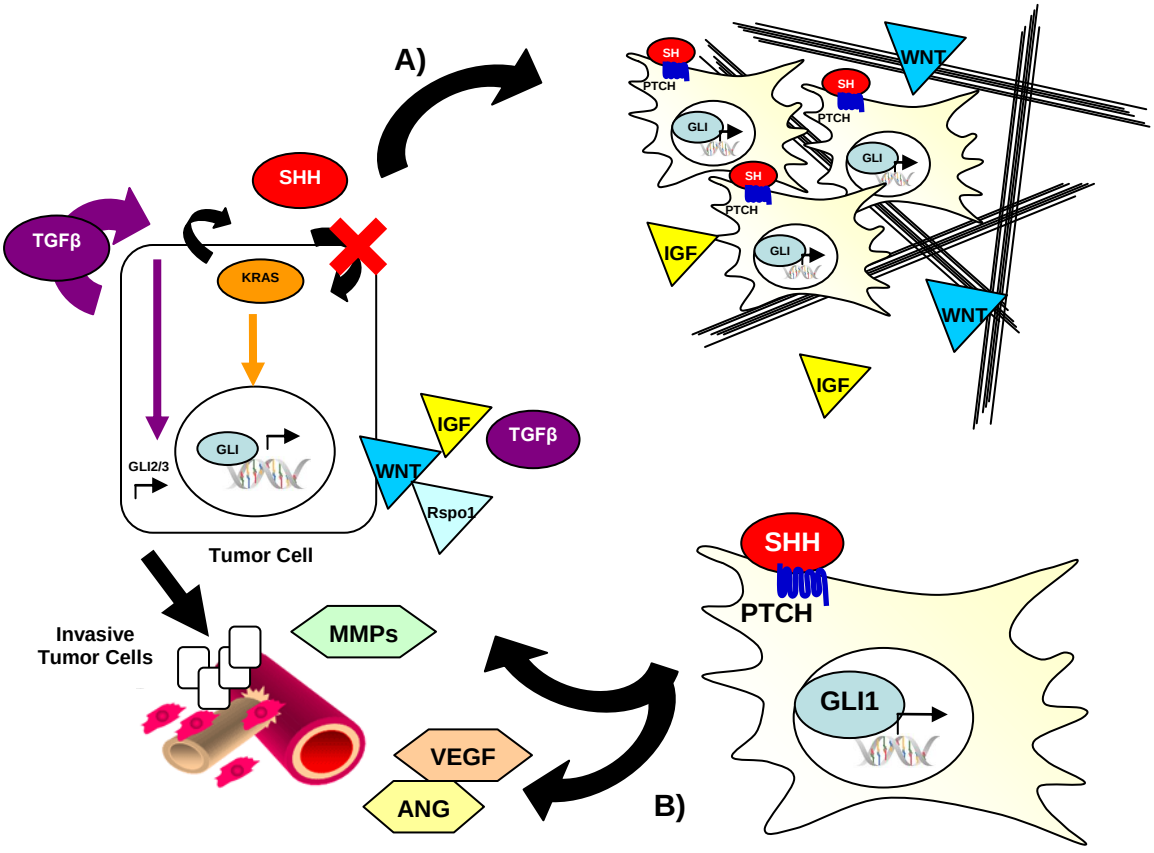

BIBLIOGRAPHY

1. Dosch JS, Pasca di Magliano M, Simeone DM Pancreatic cancer and hedgehog pathway signaling: new insights. Pancreatology 10: 151-157.

2. Jemal A, Siegel R, Xu J, Ward E Cancer statistics, 2010. CA Cancer J Clin 60: 277-300.

3. Lowenfels AB, Maisonneuve P (2006) Epidemiology and risk factors for pancreatic cancer. Best Pract Res Clin Gastroenterol 20: 197-209.

4. Michaud DS, Giovannucci E, Willett WC, Colditz GA, Stampfer MJ, et al. (2001) Physical activity, obesity, height, and the risk of pancreatic cancer. JAMA 286: 921-929.

5. Yalniz M, Pour PM (2005) Diabetes mellitus: a risk factor for pancreatic cancer? Langenbecks Arch Surg 390: 66-72.

6. Klein AP, Brune KA, Petersen GM, Goggins M, Tersmette AC, et al. (2004) Prospective risk of pancreatic cancer in familial pancreatic cancer kindreds. Cancer Res 64: 2634-2638.

7. Maitra A, Hruban RH (2008) Pancreatic cancer. Annu Rev Pathol 3: 157-188.

8. Maitra A, Kern SE, Hruban RH (2006) Molecular pathogenesis of pancreatic cancer. Best Pract Res Clin Gastroenterol 20: 211-226.

9. Fry LC, Monkemuller K, Malfertheiner P (2008) Molecular markers of pancreatic cancer: development and clinical relevance. Langenbecks Arch Surg 393: 883-890.

10. Adsay NV, Basturk O, Cheng JD, Andea AA (2005) Ductal neoplasia of the pancreas: nosologic, clinicopathologic, and biologic aspects. Semin Radiat Oncol 15: 254-264.

11. Liu MP, Guo XZ, Xu JH, Wang D, Li HY, et al. (2005) New tumor-associated antigen SC6 in pancreatic cancer. World J Gastroenterol 11: 7671-7675.

12. Bhavanandan VP (1991) Cancer-associated mucins and mucin-type glycoproteins. Glycobiology 1: 493-503.

13. Balague C, Gambus G, Carrato C, Porchet N, Aubert JP, et al. (1994) Altered expression of MUC2, MUC4, and MUC5 mucin genes in pancreas tissues and cancer cell lines. Gastroenterology 106: 1054-1061.

14. Hruban RH, Maitra A, Goggins M (2008) Update on pancreatic intraepithelial neoplasia. Int J Clin Exp Pathol 1: 306-316.

15. Smit VT, Boot AJ, Smits AM, Fleuren GJ, Cornelisse CJ, et al. (1988) KRAS codon 12 mutations occur very frequently in pancreatic adenocarcinomas. Nucleic Acids Res 16: 7773-7782.

16. Almoguera C, Shibata D, Forrester K, Martin J, Arnheim N, et al. (1988) Most human carcinomas of the exocrine pancreas contain mutant c-K-ras genes. Cell 53: 549-554.

17. Hingorani SR, Petricoin EF, Maitra A, Rajapakse V, King C, et al. (2003) Preinvasive and invasive ductal pancreatic cancer and its early detection in the mouse. Cancer Cell 4: 437-450.

18. DiGiuseppe JA, Hruban RH, Goodman SN, Polak M, van den Berg FM, et al. (1994) Overexpression of p53 protein in adenocarcinoma of the pancreas. Am J Clin Pathol 101: 684-688.

19. Hruban RH, Goggins M, Parsons J, Kern SE (2000) Progression model for pancreatic cancer. Clin Cancer Res 6: 2969-2972.

20. Goggins M, Hruban RH, Kern SE (2000) BRCA2 is inactivated late in the development of pancreatic intraepithelial neoplasia: evidence and implications. Am J Pathol 156: 1767-1771.

21. Janes RH, Jr., Niederhuber JE, Chmiel JS, Winchester DP, Ocwieja KC, et al. (1996) National patterns of care for pancreatic cancer. Results of a survey by the Commission on Cancer. Ann Surg 223: 261-272.

22. Kim R FOLFIRINOX: a new standard treatment for advanced pancreatic cancer? Lancet Oncol 12: 8-9.

23. Michalski CW, Weitz J, Buchler MW (2007) Surgery insight: surgical management of pancreatic cancer. Nat Clin Pract Oncol 4: 526-535.

24. Heinemann V, Quietzsch D, Gieseler F, Gonnermann M, Schonekas H, et al. (2006) Randomized phase III trial of gemcitabine plus cisplatin compared with gemcitabine alone in advanced pancreatic cancer. J Clin Oncol 24: 3946-3952.

25. Philip PA (2008) Improving treatment of pancreatic cancer. Lancet Oncol 9: 7-8.

26. Van Cutsem E, Verslype C, Grusenmeyer PA (2007) Lessons learned in the management of advanced pancreatic cancer. J Clin Oncol 25: 1949-1952.

27. Van Cutsem E, Vervenne WL, Bennouna J, Humblet Y, Gill S, et al. (2009) Phase III trial of bevacizumab in combination with gemcitabine and erlotinib in patients with metastatic pancreatic cancer. J Clin Oncol 27: 2231-2237.

28. Moore MJ, Goldstein D, Hamm J, Figer A, Hecht JR, et al. (2007) Erlotinib plus gemcitabine compared with gemcitabine alone in patients with advanced pancreatic cancer: a phase III trial of the National Cancer Institute of Canada Clinical Trials Group. J Clin Oncol 25: 1960-1966.

29. Lau J, Hebrok M Hedgehog signaling in pancreas epithelium regulates embryonic organ formation and adult beta-cell function. Diabetes 59: 1211-1221.

30. Thayer SP, di Magliano MP, Heiser PW, Nielsen CM, Roberts DJ, et al. (2003) Hedgehog is an early and late mediator of pancreatic cancer tumorigenesis. Nature 425: 851-856.

31. Berman DM, Karhadkar SS, Maitra A, Montes De Oca R, Gerstenblith MR, et al. (2003) Widespread requirement for Hedgehog ligand stimulation in growth of digestive tract tumours. Nature 425: 846-851.

32. Tian H, Callahan CA, DuPree KJ, Darbonne WC, Ahn CP, et al. (2009) Hedgehog signaling is restricted to the stromal compartment during pancreatic carcinogenesis. Proc Natl Acad Sci U S A 106: 4254-4259.

33. Yauch RL, Gould SE, Scales SJ, Tang T, Tian H, et al. (2008) A paracrine requirement for hedgehog signalling in cancer. Nature 455: 406-410.

34. Mann RK, Beachy PA (2004) Novel lipid modifications of secreted protein signals. Annu Rev Biochem 73: 891-923.

35. Bitgood MJ, McMahon AP (1995) Hedgehog and Bmp genes are coexpressed at many diverse sites of cell-cell interaction in the mouse embryo. Dev Biol 172: 126-138.

36. Echelard Y, Epstein DJ, St-Jacques B, Shen L, Mohler J, et al. (1993) Sonic hedgehog, a member of a family of putative signaling molecules, is implicated in the regulation of CNS polarity. Cell 75: 1417-1430.

37. Pathi S, Pagan-Westphal S, Baker DP, Garber EA, Rayhorn P, et al. (2001) Comparative biological responses to human Sonic, Indian, and Desert hedgehog. Mech Dev 106: 107-117.

38. Price MA, Kalderon D (2002) Proteolysis of the Hedgehog signaling effector Cubitus interruptus requires phosphorylation by Glycogen Synthase Kinase 3 and Casein Kinase 1. Cell 108: 823-835.

39. Jia J, Amanai K, Wang G, Tang J, Wang B, et al. (2002) Shaggy/GSK3 antagonizes Hedgehog signalling by regulating Cubitus interruptus. Nature 416: 548-552.

40. Sasaki H, Nishizaki Y, Hui C, Nakafuku M, Kondoh H (1999) Regulation of Gli2 and Gli3 activities by an amino-terminal repression domain: implication of

Gli2 and Gli3 as primary mediators of Shh signaling. Development 126: 3915-3924.

41. Cheng SY, Bishop JM (2002) Suppressor of Fused represses Gli-mediated transcription by recruiting the SAP18-mSin3 corepressor complex. Proc Natl Acad Sci U S A 99: 5442-5447.

42. Kogerman P, Grimm T, Kogerman L, Krause D, Unden AB, et al. (1999) Mammalian suppressor-of-fused modulates nuclear-cytoplasmic shuttling of Gli-1. Nat Cell Biol 1: 312-319.

43. Rubin LL, de Sauvage FJ (2006) Targeting the Hedgehog pathway in cancer. Nat Rev Drug Discov 5: 1026-1033.

44. Lum L, Zhang C, Oh S, Mann RK, von Kessler DP, et al. (2003) Hedgehog signal transduction via Smoothened association with a cytoplasmic complex scaffolded by the atypical kinesin, Costal-2. Mol Cell 12: 1261-1274.

45. Jia J, Tong C, Jiang J (2003) Smoothened transduces Hedgehog signal by physically interacting with Costal2/Fused complex through its C-terminal tail. Genes Dev 17: 2709-2720.

46. Apionishev S, Katanayeva NM, Marks SA, Kalderon D, Tomlinson A (2005) Drosophila Smoothened phosphorylation sites essential for Hedgehog signal transduction. Nat Cell Biol 7: 86-92.

47. Chen W, Ren XR, Nelson CD, Barak LS, Chen JK, et al. (2004) Activity-dependent internalization of smoothened mediated by beta-arrestin 2 and GRK2. Science 306: 2257-2260.

48. Meloni AR, Fralish GB, Kelly P, Salahpour A, Chen JK, et al. (2006) Smoothened signal transduction is promoted by G protein-coupled receptor kinase 2. Mol Cell Biol 26: 7550-7560.

49. Denef N, Neubuser D, Perez L, Cohen SM (2000) Hedgehog induces opposite changes in turnover and subcellular localization of patched and smoothened. Cell 102: 521-531.

50. Cheung HO, Zhang X, Ribeiro A, Mo R, Makino S, et al. (2009) The kinesin protein Kif7 is a critical regulator of Gli transcription factors in mammalian hedgehog signaling. Sci Signal 2: ra29.

51. Rohatgi R, Milenkovic L, Scott MP (2007) Patched1 regulates hedgehog signaling at the primary cilium. Science 317: 372-376.

52. Chuang PT, McMahon AP (1999) Vertebrate Hedgehog signalling modulated by induction of a Hedgehog-binding protein. Nature 397: 617-621.

53. Lee CS, Buttitta L, Fan CM (2001) Evidence that the WNT-inducible growth arrest-specific gene 1 encodes an antagonist of sonic hedgehog signaling in the somite. Proc Natl Acad Sci U S A 98: 11347-11352.

54. Duman-Scheel M, Weng L, Xin S, Du W (2002) Hedgehog regulates cell growth and proliferation by inducing Cyclin D and Cyclin E. Nature 417: 299-304.

55. Pola R, Ling LE, Silver M, Corbley MJ, Kearney M, et al. (2001) The morphogen Sonic hedgehog is an indirect angiogenic agent upregulating two families of angiogenic growth factors. Nat Med 7: 706-711.

56. Feldmann G, Dhara S, Fendrich V, Bedja D, Beaty R, et al. (2007) Blockade of hedgehog signaling inhibits pancreatic cancer invasion and metastases: a new paradigm for combination therapy in solid cancers. Cancer Res 67: 2187-2196.

57. Hebrok M, Kim SK, Melton DA (1998) Notochord repression of endodermal Sonic hedgehog permits pancreas development. Genes Dev 12: 1705-1713.

58. Apelqvist A, Ahlgren U, Edlund H (1997) Sonic hedgehog directs specialised mesoderm differentiation in the intestine and pancreas. Curr Biol 7: 801-804.

59. Kim SK, Melton DA (1998) Pancreas development is promoted by cyclopamine, a hedgehog signaling inhibitor. Proc Natl Acad Sci U S A 95: 13036-13041.

60. Hebrok M, Kim SK, St Jacques B, McMahon AP, Melton DA (2000) Regulation of pancreas development by hedgehog signaling. Development 127: 4905-4913.

61. Thomas MK, Rastalsky N, Lee JH, Habener JF (2000) Hedgehog signaling regulation of insulin production by pancreatic beta-cells. Diabetes 49: 2039-2047.

62. Fendrich V, Esni F, Garay MV, Feldmann G, Habbe N, et al. (2008) Hedgehog signaling is required for effective regeneration of exocrine pancreas. Gastroenterology 135: 621-631.

63. Karhadkar SS, Bova GS, Abdallah N, Dhara S, Gardner D, et al. (2004) Hedgehog signalling in prostate regeneration, neoplasia and metastasis. Nature 431: 707-712.

64. Watkins DN, Berman DM, Burkholder SG, Wang B, Beachy PA, et al. (2003) Hedgehog signalling within airway epithelial progenitors and in small-cell lung cancer. Nature 422: 313-317.

65. Li C, Chi S, Xie J Hedgehog signaling in skin cancers. Cell Signal.

66. Low JA, de Sauvage FJ Clinical Experience With Hedgehog Pathway Inhibitors. J Clin Oncol.

67. Tuveson DA, Shaw AT, Willis NA, Silver DP, Jackson EL, et al. (2004) Endogenous oncogenic K-ras(G12D) stimulates proliferation and widespread neoplastic and developmental defects. Cancer Cell 5: 375-387.

68. Aguirre AJ, Bardeesy N, Sinha M, Lopez L, Tuveson DA, et al. (2003) Activated Kras and Ink4a/Arf deficiency cooperate to produce metastatic pancreatic ductal adenocarcinoma. Genes Dev 17: 3112-3126.

69. Park SW, Davison JM, Rhee J, Hruban RH, Maitra A, et al. (2008) Oncogenic KRAS induces progenitor cell expansion and malignant transformation in zebrafish exocrine pancreas. Gastroenterology 134: 2080-2090.

70. Nakashima H, Nakamura M, Yamaguchi H, Yamanaka N, Akiyoshi T, et al. (2006) Nuclear factor-kappaB contributes to hedgehog signaling pathway activation through sonic hedgehog induction in pancreatic cancer. Cancer Res 66: 7041-7049.

71. Kasperczyk H, Baumann B, Debatin KM, Fulda S (2008) Characterization of sonic hedgehog as a novel NF-{kappa}B target gene that promotes NF-{kappa}B-mediated apoptosis resistance and tumor growth in vivo. FASEB J.

72. Pasca di Magliano M, Sekine S, Ermilov A, Ferris J, Dlugosz AA, et al. (2006) Hedgehog/Ras interactions regulate early stages of pancreatic cancer. Genes Dev 20: 3161-3173.

73. Nolan-Stevaux O, Lau J, Truitt ML, Chu GC, Hebrok M, et al. (2009) GLI1 is regulated through Smoothened-independent mechanisms in neoplastic pancreatic ducts and mediates PDAC cell survival and transformation. Genes Dev 23: 24-36.

74. Long F, Zhang XM, Karp S, Yang Y, McMahon AP (2001) Genetic manipulation of hedgehog signaling in the endochondral skeleton reveals a direct role in the regulation of chondrocyte proliferation. Development 128: 5099-5108.

75. Apte MV, Wilson JS (2007) The Desmoplastic Reaction in Pancreatic Cancer: An Increasingly Recognised Foe. Pancreatology 7: 378-379.

76. Apte MV, Park S, Phillips PA, Santucci N, Goldstein D, et al. (2004) Desmoplastic reaction in pancreatic cancer: role of pancreatic stellate cells. Pancreas 29: 179-187.

77. Phillips PA, McCarroll JA, Park S, Wu MJ, Pirola R, et al. (2003) Rat pancreatic stellate cells secrete matrix metalloproteinases: implications for extracellular matrix turnover. Gut 52: 275-282.

78. Omary MB, Lugea A, Lowe AW, Pandol SJ (2007) The pancreatic stellate cell: a star on the rise in pancreatic diseases. J Clin Invest 117: 50-59.

79. Hwang RF, Moore T, Arumugam T, Ramachandran V, Amos KD, et al. (2008) Cancer-associated stromal fibroblasts promote pancreatic tumor progression. Cancer Res 68: 918-926.

80. Olive KP, Jacobetz MA, Davidson CJ, Gopinathan A, McIntyre D, et al. (2009) Inhibition of Hedgehog signaling enhances delivery of chemotherapy in a mouse model of pancreatic cancer. Science 324: 1457-1461.

81. Bailey JM, Swanson BJ, Hamada T, Eggers JP, Singh PK, et al. (2008) Sonic hedgehog promotes desmoplasia in pancreatic cancer. Clin Cancer Res 14: 5995-6004.

82. Zacharias WJ, Li X, Madison BB, Kretovich K, Kao JY, et al. Hedgehog is an anti-inflammatory epithelial signal for the intestinal lamina propria. Gastroenterology 138: 2368-2377, 2377 e2361-2364.

83. Yu M, Gipp J, Yoon JW, Iannaccone P, Walterhouse D, et al. (2009) Sonic hedgehog-responsive genes in the fetal prostate. J Biol Chem 284: 5620-5629.

84. Gao D, Nolan DJ, Mellick AS, Bambino K, McDonnell K, et al. (2008) Endothelial progenitor cells control the angiogenic switch in mouse lung metastasis. Science 319: 195-198.

85. Joyce JA, Pollard JW (2009) Microenvironmental regulation of metastasis. Nat Rev Cancer 9: 239-252.

86. Nakamura K, Sasajima J, Mizukami Y, Sugiyama Y, Yamazaki M, et al. Hedgehog promotes neovascularization in pancreatic cancers by regulating Ang-1 and IGF-1 expression in bone-marrow derived pro-angiogenic cells. PLoS One 5: e8824.

87. Tremblay MR, Lescarbeau A, Grogan MJ, Tan E, Lin G, et al. (2009) Discovery of a potent and orally active hedgehog pathway antagonist (IPI-926). J Med Chem 52: 4400-4418.

88. Bonnet D, Dick JE (1997) Human acute myeloid leukemia is organized as a hierarchy that originates from a primitive hematopoietic cell. Nat Med 3: 730-737.

89. Al-Hajj M, Wicha MS, Benito-Hernandez A, Morrison SJ, Clarke MF (2003) Prospective identification of tumorigenic breast cancer cells. Proc Natl Acad Sci U S A 100: 3983-3988.

90. Singh SK, Hawkins C, Clarke ID, Squire JA, Bayani J, et al. (2004) Identification of human brain tumour initiating cells. Nature 432: 396-401.

91. Dalerba P, Dylla SJ, Park IK, Liu R, Wang X, et al. (2007) Phenotypic characterization of human colorectal cancer stem cells. Proc Natl Acad Sci U S A 104: 10158-10163.

92. Bao S, Wu Q, McLendon RE, Hao Y, Shi Q, et al. (2006) Glioma stem cells promote radioresistance by preferential activation of the DNA damage response. Nature 444: 756-760.

93. Quintana E, Shackleton M, Sabel MS, Fullen DR, Johnson TM, et al. (2008) Efficient tumour formation by single human melanoma cells. Nature 456: 593-598.

94. Ishizawa K, Rasheed ZA, Karisch R, Wang Q, Kowalski J, et al. Tumor-initiating cells are rare in many human tumors. Cell Stem Cell 7: 279-282.

95. Cho RW, Wang X, Diehn M, Shedden K, Chen GY, et al. (2008) Isolation and molecular characterization of cancer stem cells in MMTV-Wnt-1 murine breast tumors. Stem Cells 26: 364-371.

96. Jorgensen HG, Holyoake TL (2007) Characterization of cancer stem cells in chronic myeloid leukaemia. Biochem Soc Trans 35: 1347-1351.

97. Liu S, Dontu G, Mantle ID, Patel S, Ahn NS, et al. (2006) Hedgehog signaling and Bmi-1 regulate self-renewal of normal and malignant human mammary stem cells. Cancer Res 66: 6063-6071.

98. Clement V, Sanchez P, de Tribolet N, Radovanovic I, Ruiz i Altaba A (2007) HEDGEHOG-GLI1 signaling regulates human glioma growth, cancer stem cell self-renewal, and tumorigenicity. Curr Biol 17: 165-172.

99. Li C, Heidt DG, Dalerba P, Burant CF, Zhang L, et al. (2007) Identification of pancreatic cancer stem cells. Cancer Res 67: 1030-1037.

100. Lees CW, Zacharias WJ, Tremelling M, Noble CL, Nimmo ER, et al. (2008) Analysis of germline GLI1 variation implicates hedgehog signalling in the regulation of intestinal inflammatory pathways. PLoS Med 5: e239.

101. Hermann PC, Huber SL, Herrler T, Aicher A, Ellwart JW, et al. (2007) Distinct populations of cancer stem cells determine tumor growth and metastatic activity in human pancreatic cancer. Cell Stem Cell 1: 313-323.

102. Ginestier C, Hur MH, Charafe-Jauffret E, Monville F, Dutcher J, et al. (2007) ALDH1 is a marker of normal and malignant human mammary stem cells and a predictor of poor clinical outcome. Cell Stem Cell 1: 555-567.

103. Dylla SJ, Beviglia L, Park IK, Chartier C, Raval J, et al. (2008) Colorectal cancer stem cells are enriched in xenogeneic tumors following chemotherapy. PLoS ONE 3: e2428.

104. Bryden MM, Evans HE, Keeler RF (1971) Cyclopia in sheep caused by plant teratogens. J Anat 110: 507.

105. Chen JK, Taipale J, Cooper MK, Beachy PA (2002) Inhibition of Hedgehog signaling by direct binding of cyclopamine to Smoothened. Genes Dev 16: 2743-2748.

106. Frank-Kamenetsky M, Zhang XM, Bottega S, Guicherit O, Wichterle H, et al. (2002) Small-molecule modulators of Hedgehog signaling: identification and characterization of Smoothened agonists and antagonists. J Biol 1: 10.

107. Chen JK, Taipale J, Young KE, Maiti T, Beachy PA (2002) Small molecule modulation of Smoothened activity. Proc Natl Acad Sci U S A 99: 14071-14076.

108. Robarge KD, Brunton SA, Castanedo GM, Cui Y, Dina MS, et al. (2009) GDC-0449-a potent inhibitor of the hedgehog pathway. Bioorg Med Chem Lett 19: 5576-5581.

109. Tremblay MR, Nevalainen M, Nair SJ, Porter JR, Castro AC, et al. (2008) Semisynthetic cyclopamine analogues as potent and orally bioavailable hedgehog pathway antagonists. J Med Chem 51: 6646-6649.

110. Ericson J, Morton S, Kawakami A, Roelink H, Jessell TM (1996) Two critical periods of Sonic Hedgehog signaling required for the specification of motor neuron identity. Cell 87: 661-673.

111. Lauth M, Bergstrom A, Shimokawa T, Toftgard R (2007) Inhibition of GLI-mediated transcription and tumor cell growth by small-molecule antagonists. Proc Natl Acad Sci U S A 104: 8455-8460.

112. Von Hoff DD, LoRusso PM, Rudin CM, Reddy JC, Yauch RL, et al. (2009) Inhibition of the hedgehog pathway in advanced basal-cell carcinoma. N Engl J Med 361: 1164-1172.

113. Rudin CM, Hann CL, Laterra J, Yauch RL, Callahan CA, et al. (2009) Treatment of medulloblastoma with hedgehog pathway inhibitor GDC-0449. N Engl J Med 361: 1173-1178.

114. Bardeesy N, DePinho RA (2002) Pancreatic cancer biology and genetics. Nat Rev Cancer 2: 897-909.

115. Jemal A, Siegel R, Ward E, Hao Y, Xu J, et al. (2009) Cancer statistics, 2009. CA Cancer J Clin 59: 225-249.

116. Lohr JM (2007) Medical treatment of pancreatic cancer. Expert Rev Anticancer Ther 7: 533-544.

117. Ujiki MB, Talamonti MS (2007) Guidelines for the surgical management of pancreatic adenocarcinoma. Semin Oncol 34: 311-320.

118. Herbst RS, Kurzrock R, Hong DS, Valdivieso M, Hsu CP, et al. A first-in-human study of conatumumab in adult patients with advanced solid tumors. Clin Cancer Res 16: 5883-5891.

119. Javle MM, Shroff RT, Xiong H, Varadhachary GA, Fogelman D, et al. Inhibition of the mammalian target of rapamycin (mTOR) in advanced pancreatic cancer: results of two phase II studies. BMC Cancer 10: 368.

120. Morton JP, Mongeau ME, Klimstra DS, Morris JP, Lee YC, et al. (2007) Sonic hedgehog acts at multiple stages during pancreatic tumorigenesis. Proc Natl Acad Sci U S A 104: 5103-5108.

121. Jimeno A, Feldmann G, Suarez-Gauthier A, Rasheed Z, Solomon A, et al. (2009) A direct pancreatic cancer xenograft model as a platform for cancer stem cell therapeutic development. Mol Cancer Ther 8: 310-314.

122. Feldmann G, Fendrich V, McGovern K, Bedja D, Bisht S, et al. (2008) An orally bioavailable small-molecule inhibitor of Hedgehog signaling inhibits tumor initiation and metastasis in pancreatic cancer. Mol Cancer Ther 7: 2725-2735.

123. Dierks C, Grbic J, Zirlik K, Beigi R, Englund NP, et al. (2007) Essential role of stromally induced hedgehog signaling in B-cell malignancies. Nat Med 13: 944-951.

124. Duda DG, Fukumura D, Munn LL, Booth MF, Brown EB, et al. (2004) Differential transplantability of tumor-associated stromal cells. Cancer Res 64: 5920-5924.

125. Bailey JM, Mohr AM, Hollingsworth MA (2009) Sonic hedgehog paracrine signaling regulates metastasis and lymphangiogenesis in pancreatic cancer. Oncogene 28: 3513-3525.

126. Miyake S, Sellers WR, Safran M, Li X, Zhao W, et al. (2000) Cells degrade a novel inhibitor of differentiation with E1A-like properties upon exiting the cell cycle. Mol Cell Biol 20: 8889-8902.

127. Xu Z, Vonlaufen A, Phillips PA, Fiala-Beer E, Zhang X, et al. Role of pancreatic stellate cells in pancreatic cancer metastasis. Am J Pathol 177: 2585-2596.

128. Duner S, Lopatko Lindman J, Ansari D, Gundewar C, Andersson R Pancreatic cancer: the role of pancreatic stellate cells in tumor progression. Pancreatology 10: 673-681.

129. Apte MV, Haber PS, Applegate TL, Norton ID, McCaughan GW, et al. (1998) Periacinar stellate shaped cells in rat pancreas: identification, isolation, and culture. Gut 43: 128-133.

130. Casini A, Galli A, Pignalosa P, Frulloni L, Grappone C, et al. (2000) Collagen type I synthesized by pancreatic periacinar stellate cells (PSC) co-localizes with lipid peroxidation-derived aldehydes in chronic alcoholic pancreatitis. J Pathol 192: 81-89.

131. Whitehead RH, Joseph JL (1994) Derivation of conditionally immortalized cell lines containing the Min mutation from the normal colonic mucosa and other tissues of an "Immortomouse"/Min hybrid. Epithelial Cell Biol 3: 119-125.

132. Neuschwander-Tetri BA, Bridle KR, Wells LD, Marcu M, Ramm GA (2000) Repetitive acute pancreatic injury in the mouse induces procollagen alpha1(I) expression colocalized to pancreatic stellate cells. Lab Invest 80: 143-150.

133. Oshima Y, Suzuki A, Kawashimo K, Ishikawa M, Ohkohchi N, et al. (2007) Isolation of mouse pancreatic ductal progenitor cells expressing CD133 and c-Met by flow cytometric cell sorting. Gastroenterology 132: 720-732.

134. Wakelin SJ, Forsythe JL, Garden OJ, Howie SE (2008) Commercially available recombinant sonic hedgehog up-regulates Ptc and modulates the cytokine and chemokine expression of human macrophages: an effect mediated by endotoxin contamination? Immunobiology 213: 25-38.

135. Maun HR, Wen X, Lingel A, de Sauvage FJ, Lazarus RA, et al. Hedgehog pathway antagonist 5E1 binds hedgehog at the pseudo-active site. J Biol Chem 285: 26570-26580.

136. Lipinski RJ, Gipp JJ, Zhang J, Doles JD, Bushman W (2006) Unique and complimentary activities of the Gli transcription factors in Hedgehog signaling. Exp Cell Res 312: 1925-1938.

137. Ingram WJ, Wicking CA, Grimmond SM, Forrest AR, Wainwright BJ (2002) Novel genes regulated by Sonic Hedgehog in pluripotent mesenchymal cells. Oncogene 21: 8196-8205.

138. Xu K, Rajagopal S, Klebba I, Dong S, Ji Y, et al. The role of fibroblast Tiam1 in tumor cell invasion and metastasis. Oncogene 29: 6533-6542.

139. Apte MV, Haber PS, Darby SJ, Rodgers SC, McCaughan GW, et al. (1999) Pancreatic stellate cells are activated by proinflammatory cytokines: implications for pancreatic fibrogenesis. Gut 44: 534-541.

140. Pasca di Magliano M, Biankin AV, Heiser PW, Cano DA, Gutierrez PJ, et al. (2007) Common activation of canonical Wnt signaling in pancreatic adenocarcinoma. PLoS ONE 2: e1155.

141. Pilarsky C, Ammerpohl O, Sipos B, Dahl E, Hartmann A, et al. (2008) Activation of Wnt signalling in stroma from pancreatic cancer identified by gene expression profiling. J Cell Mol Med 12: 2823-2835.

142. Shin K, Lee J, Guo N, Kim J, Lim A, et al. Hedgehog/Wnt feedback supports regenerative proliferation of epithelial stem cells in bladder. Nature.

143. Pabst O, Zweigerdt R, Arnold HH (1999) Targeted disruption of the homeobox transcription factor Nkx2-3 in mice results in postnatal lethality and abnormal development of small intestine and spleen. Development 126: 2215-2225.

144. Schoumacher M, Goldman RD, Louvard D, Vignjevic DM Actin, microtubules, and vimentin intermediate filaments cooperate for elongation of invadopodia. J Cell Biol 189: 541-556.

145. Ridky TW, Chow JM, Wong DJ, Khavari PA Invasive three-dimensional organotypic neoplasia from multiple normal human epithelia. Nat Med 16: 1450-1455.

146. Johnson JI, Decker S, Zaharevitz D, Rubinstein LV, Venditti JM, et al. (2001) Relationships between drug activity in NCI preclinical in vitro and in vivo models and early clinical trials. Br J Cancer 84: 1424-1431.

147. Bignold LP (2007) Variation, "evolution", immortality and genetic instabilities in tumour cells. Cancer Lett 253: 155-169.

148. Fiebig HH, Maier A, Burger AM (2004) Clonogenic assay with established human tumour xenografts: correlation of in vitro to in vivo activity as a basis for anticancer drug discovery. Eur J Cancer 40: 802-820.

149. Lee CJ, Spalding AC, Ben-Josef E, Wang L, Simeone DM In vivo bioluminescent imaging of irradiated orthotopic pancreatic cancer xenografts in nonobese diabetic-severe combined immunodeficient mice: a novel method for targeting and assaying efficacy of ionizing radiation. Transl Oncol 3: 153-159.

150. Romer JT, Kimura H, Magdaleno S, Sasai K, Fuller C, et al. (2004) Suppression of the Shh pathway using a small molecule inhibitor eliminates medulloblastoma in Ptc1(+/-)p53(-/-) mice. Cancer Cell 6: 229-240.

151. Tempero M, Plunkett W, Ruiz Van Haperen V, Hainsworth J, Hochster H, et al. (2003) Randomized phase II comparison of dose-intense gemcitabine: thirty-minute infusion and fixed dose rate infusion in patients with pancreatic adenocarcinoma. J Clin Oncol 21: 3402-3408.

152. Lyons SK, Meuwissen R, Krimpenfort P, Berns A (2003) The generation of a conditional reporter that enables bioluminescence imaging of Cre/loxP-dependent tumorigenesis in mice. Cancer Res 63: 7042-7046.

153. Bruns CJ, Harbison MT, Kuniyasu H, Eue I, Fidler IJ (1999) In vivo selection and characterization of metastatic variants from human pancreatic adenocarcinoma by using orthotopic implantation in nude mice. Neoplasia 1: 50-62.

154. Froeling FE, Mirza TA, Feakins RM, Seedhar A, Elia G, et al. (2009) Organotypic culture model of pancreatic cancer demonstrates that stromal cells modulate E-cadherin, beta-catenin, and Ezrin expression in tumor cells. Am J Pathol 175: 636-648.

155. Ota I, Li XY, Hu Y, Weiss SJ (2009) Induction of a MT1-MMP and MT2-MMP-dependent basement membrane transmigration program in cancer cells by Snail1. Proc Natl Acad Sci U S A 106: 20318-20323.

156. Rowe RG, Li XY, Hu Y, Saunders TL, Virtanen I, et al. (2009) Mesenchymal cells reactivate Snail1 expression to drive three-dimensional invasion programs. J Cell Biol 184: 399-408.

157. Ries C, Egea V, Karow M, Kolb H, Jochum M, et al. (2007) MMP-2, MT1-MMP, and TIMP-2 are essential for the invasive capacity of human mesenchymal stem cells: differential regulation by inflammatory cytokines. Blood 109: 4055-4063.

158. Moniaux N, Andrianifahanana M, Brand RE, Batra SK (2004) Multiple roles of mucins in pancreatic cancer, a lethal and challenging malignancy. Br J Cancer 91: 1633-1638.

159. Pantano F, Baldi A, Santini D, Vincenzi B, Borzomati D, et al. (2009) MUC2 but not MUC5 expression correlates with prognosis in radically resected pancreatic cancer patients. Cancer Biol Ther 8: 996-999.

160. Matsushita A, Gotze T, Korc M (2007) Hepatocyte growth factor-mediated cell invasion in pancreatic cancer cells is dependent on neuropilin-1. Cancer Res 67: 10309-10316.

161. Arnoletti JP, Frolov A, Eloubeidi M, Keene K, Posey J, et al. A phase I study evaluating the role of the anti-epidermal growth factor receptor (EGFR) antibody cetuximab as a radiosensitizer with chemoradiation for locally advanced pancreatic cancer. Cancer Chemother Pharmacol.

162. Dessaud E, McMahon AP, Briscoe J (2008) Pattern formation in the vertebrate neural tube: a sonic hedgehog morphogen-regulated transcriptional network. Development 135: 2489-2503.

163. Strobel O, Rosow DE, Rakhlin EY, Lauwers GY, Trainor AG, et al. Pancreatic duct glands are distinct ductal compartments that react to chronic injury and mediate Shh-induced metaplasia. Gastroenterology 138: 1166-1177.

164. Yoon JW, Kita Y, Frank DJ, Majewski RR, Konicek BA, et al. (2002) Gene expression profiling leads to identification of GLI1-binding elements in target genes and a role for multiple downstream pathways in GLI1-induced cell transformation. J Biol Chem 277: 5548-5555.

165. Shaw A, Gipp J, Bushman W (2009) The Sonic Hedgehog pathway stimulates prostate tumor growth by paracrine signaling and recapitulates embryonic gene expression in tumor myofibroblasts. Oncogene 28: 4480-4490.

166. Fukasawa M, Korc M (2004) Vascular endothelial growth factor-trap suppresses tumorigenicity of multiple pancreatic cancer cell lines. Clin Cancer Res 10: 3327-3332.

167. Esteve P, Bovolenta P The advantages and disadvantages of sfrp1 and sfrp2 expression in pathological events. Tohoku J Exp Med 221: 11-17.

168. Le Floch N, Rivat C, De Wever O, Bruyneel E, Mareel M, et al. (2005) The proinvasive activity of Wnt-2 is mediated through a noncanonical Wnt pathway coupled to GSK-3beta and c-Jun/AP-1 signaling. FASEB J 19: 144-146.